

INVESTIGATION OF ADAPTIVE AUTO-RECLOSING FOR RADIAL DISTRIBUTION
SYSTEM WITH DISTRIBUTED ENERGY RESOURCES

A Thesis

by

AMMAR FAYEZ A ALEITHAN

Submitted to the Office of Graduate and Professional Studies of
Texas A&M University
in partial fulfillment of the requirements for the degree of

MASTER OF SCIENCE

Chair of Committee,	Karen L. Butler-Purry
Committee Members,	Chanan Singh
	Shankar P. Bhattacharyya
	Sergiy Butenko
Head of Department,	Miroslav M. Begovic

May 2018

Major Subject: Electrical Engineering

Copyright 2018 Ammar Al-Eithan

ABSTRACT

DERs (distributed energy resources) recently have gained popularity in electrical distribution systems. The interconnection of DERs to RDS (radial distribution systems) introduces challenges to the protection and control system of the RDS. Bidirectional current flow is introduced to the RDS due to the interconnection of DERs at load side. In this case, the conventional protection scheme might fail to maintain the proper level of security and dependability. The majority of faults in RDS are temporary in nature and require the auto-reclosing scheme to reduce the impact of such faults. Connecting two live electrical systems requires proper synchronization to avoid mechanical damage to generators. This thesis investigates an approach to have adaptive auto-reclosing in RDS with interconnected DERs. The approach is based on zonal directional overcurrent protection, which utilizes the overcurrent condition with the current directions to determine the faulty zone. The approach suggests tripping DERs connected to the faulty zone and limiting the auto-reclosing to the zonal breaker closer to the grid substation. Doing this, the synchronization requirements are avoided as reclosing is performed to a de-energized zone. Also, the adaptive approach adjusts the TDS (time dial setting) of the recloser fast curve to re-establish coordination with fuses in the zone. Due to the interconnection of DERs, fuse and recloser might see different fault currents, which might cause miscoordination. The adaptive approach allows the implementation of “Fuse Saving” scheme, which is usually desired in RDS.

The suggested approach in this thesis was implemented on PSCADTM/EMTDCTM applied to a test system. The test system is a modified dual IEEE 34 node distribution test feeder with interconnected DERs. The behavior of the approach was investigated by simulating various faults types at different locations on the test system. The approach for the zonal breaker was successful in identifying the right breaker to perform the auto-reclosing following the right sequence. The

adaptive approach was also successful in restoring the fuse-recloser sequence of operation. The fuse saving scheme operation sequence was sustained as well. However, the minimum coordination margin between the fuse and the recloser was not maintained properly for most of the case studies.

DEDICATION

Dedicated proudly to my father, the memory of my mother, my wife, and my children. I would never have accomplished this much without their support.

ACKNOWLEDGEMENTS

I would like to thank my advisor, Dr. Butler-Purry, for her guidance and support throughout the course of this research. Also, I would like to thank my committee members, Dr. Sing, Dr. Bhattacharyya, Dr. Butenko, and Dr. Bukkapatnam for their valuable time.

Sincere thanks to my sponsor, Saudi Aramco, for the valuable chance to pursue my higher education degree. They made my dream come true.

Thanks also go to my friends and colleagues in Power System Automation Lab for their help and great companionship. Also, thanks to the department faculty and staff for making my time at Texas A&M University a great experience. Finally, thanks to my father and family for their encouragement, and to my wife for her great patience and love.

CONTRIBUTORS AND FUNDING SOURCES

This work was supervised by a thesis committee consisting of my advisor, Professor Karen L. Butler-Purry, Professor Chanan Singh, and Professor Shankar P. Bhattacharyya of the Department of Electrical and Computer Engineering, and Professor Sergiy Butenko of the Department of Industrial and Systems Engineering.

All work for the thesis was completed by the student, under the advisement of Professor Karen L. Butler-Purry of the Department of Electrical and Computer Engineering.

Graduate study was supported by a scholarship from Saudi Aramco.

NOMENCLATURE

DER	Distributed Energy Resources
RDS	Radial Distribution System
DG	Distributed Generation
IEEE	Institute of Electrical and Electronics Engineers
IEC	International Electrotechnical Commission
FCL	Fault Current Limiter
CTI	Coordinating Time Interval
TDS	Time-Dial Setting
TCC	Time-Current Curve
MMT	Minimum MeltingTime
TCT	Total Clearing Time
ANSI	American National Standards Institute
CT	Current Transformer
VT	Voltage Transformer
IED	Intelligent Electronic Device
CB	Circuit Breaker
ZB	Zonal Breaker

TABLE OF CONTENTS

	Page
ABSTRACT	ii
DEDICATION	iv
ACKNOWLEDGEMENTS	v
CONTRIBUTORS AND FUNDING SOURCES	vi
NOMENCLATURE	vii
LIST OF FIGURES	x
LIST OF TABLES	xii
1 INTRODUCTION	1
1.1 Power System Is Evolving	1
1.2 Challenges to Protection System	2
1.3 Problem Definition.....	4
1.4 Research Objective and Approach.....	5
2 DISTRIBUTION SYSTEM PROTECTION REVIEW	6
2.1 Overview.....	6
2.2 Protection Schemes of RDS.....	10
2.2.1 Relays.....	14
2.2.2 Auto-Recloser	18
2.2.3 Fuse	19
2.2.4 Directional Element	21
2.2.4.1 Sequence-Quantities Power Directional Elements (32).....	25
2.2.4.2 Positive-Sequence Power Directional Element (32P).....	26
2.2.4.3 Negative-Sequence Power Directional Element (32Q)	27
2.2.4.4 Zero-Sequence Power Directional Element (32V)	29
2.2.4.5 Zero-Sequence Power Directional Element (32I).....	29
2.2.4.6 Negative-Sequence Impedance Directional Element (67 _{NEG})	31
2.3 Review of RDS with DER Protection Schemes	31
3 PROBLEM FORMULATION FOR AUTO-RECLOSING SCHEME IN RDS WITH DER	45

3.1 DER Interconnection in RDS Protection Challenges	45
3.1.1 Protection Blinding	45
3.1.2 Miscoordination	46
3.1.3 Sympathetic Tripping.....	48
3.1.4 Synchronization	49
3.2 Problem Formulation	49
4 SOLUTION METHODOLOGY	51
4.1 Zoning.....	52
4.2 Communication-Assisted Directional Overcurrent.....	54
4.3 Zonal Reclosing	55
4.4 Zonal Breaker Logic	57
4.5 Adaptive Reclosing.....	59
5 CASE STUDIES AND FINDINGS.....	65
5.1 Test System.....	65
5.2 PSCAD Model	78
5.2.1 Fuse Model.....	83
5.3 Case Studies	85
5.3.1 Case 1: Feeder A Zone 1 lateral at 808-810	88
5.3.2 Case 2: Feeder A Zone 3 lateral at 832-Transformer	93
5.3.3 Case 3: Feeder B Zone 4 lateral at 862-838.....	98
5.4 Results.....	104
5.5 Summary	117
6 CONCLUSIONS AND FUTURE WORK	118
6.1 Study Work	118
6.2 Summary of Findings and Conclusions	119
6.3 Future Work	120
REFERENCES	122
APPENDIX A.....	129

LIST OF FIGURES

	Page
Figure 1 Smart grid RDS with DER Interconnection, adapted from [14]	3
Figure 2 Protective Device Coordination Principles, reprinted from [8].....	12
Figure 3 Coordination of Inverse Time-Overcurrent Protective Devices, reprinted from [8].....	13
Figure 4 U4 IEEE (US) Extremely Inverse Time-Overcurrent Curves, reprinted from [10]	16
Figure 5 C3 IEC Extremely Inverse Time-Overcurrent Curves, reprinted from [10]	17
Figure 6 Fuse Speed Ratio Comparison, reprinted from [13].....	21
Figure 7 Typical Directional Element Characteristics, reprinted from [4]	24
Figure 8 Operating/Polarizing Quantities Plane for Negative-Sequence Directional Element, reprinted from [17]	28
Figure 9 Protection Blinding Due to DG Interconnection	46
Figure 10 Recloser-Fuse Miscoordination with DG Interconnection, reprinted from [31]	47
Figure 11 Sympathetic Tripping due to DG, adapted from [26].....	48
Figure 12 Illustration of Zoning Scheme for RDS with DG Interconnection, reprinted from [25]	53
Figure 13 Fault Current Direction.....	55
Figure 14 Zonal Auto-Reclosing on the RDS, adapted from [50]	56
Figure 15 CB Logic Concept	58
Figure 16 Simple RDS Illustrating Recloser-Fuse Currents, reprinted from [26]	61
Figure 17 Recloser-Fuse Coordination Curves, reprinted from [26]	62
Figure 18 Adaptive Recloser Algorithm for Restoring Fuse Coordination, , reprinted from [26]	64
Figure 19 Test System Overall Diagram, adapted from [51].....	65

Figure 20 IEEE 34 Node Test Feeder Standard Distribution Feeder, reprinted from [50].....	68
Figure 21 Test System Divided into Zones with DGs.....	73
Figure 22 Sequence of Breaker Operation.....	82
Figure 23 Synchronous Machine Model for DGs.....	83
Figure 24 Fuse Custom Model in PSCAD.....	85
Figure 25 Fault Locations on Test System	87
Figure 26 Time Diagram for Case 1 Scenario 1	89
Figure 27 Time Diagram for Case 1 Scenario 2	90
Figure 28 Time Diagram for Case 1 Scenario 3	92
Figure 29 Time Diagram for Case 1 Scenario 4	93
Figure 30 Time Diagram for Case 2 Scenario 1	95
Figure 31 Time Diagram for Case 2 Scenario 2	96
Figure 32 Time Diagram for Case 2 Scenario 3	97
Figure 33 Time Diagram for Case 2 Scenario 4	98
Figure 34 Time Diagram for Case 3 Scenario 1	100
Figure 35 Time Diagram for Case 3 Scenario 2	101
Figure 36 Time Diagram for Case 3 Scenario 3	102
Figure 37 Time Diagram for Case 3 Scenario 4	103

LIST OF TABLES

	Page
Table 1 Distribution System Configuration Types, adapted from [2]	9
Table 2 IEEE C37.112 (US) Inverse Time-Overcurrent Curve Equations, reprinted from [9].....	15
Table 3 IEC Inverse Time-Overcurrent Curve Equations, reprinted from [10]	15
Table 4 Quantities for 90° Connected Phase Directional Element, reprinted from [15]	25
Table 5 Quantities for Positive-Sequence Directional Element, reprinted from [15].....	26
Table 6 Quantities for Traditional Negative-Sequence Directional Element, reprinted from [15].....	27
Table 7 Review of Protection Methods to Mitigate DG Interconnection Impact on RDS	37
Table 8 Zonal Breaker Logic	59
Table 9 IEEE 34 Node Test Feeder Transformer Data, reprinted from [51]	66
Table 10 Regulating Transformers Data, reprinted from [51]	67
Table 11 Test System Load Flow Output	69
Table 12 DGs Capacity with Connection Node.....	74
Table 13 Laterals' Fuses.....	75
Table 14 Available Short Circuit Currents at Nodes Where Fuses were installed	75
Table 15 Overcurrent Protection Settings.....	78
Table 16 Grid Parameters	79
Table 17 Directional Element Settings	81
Table 18 Study System Simulation Operating Point	86
Table 19 Laterals Permanent Fault Simulation Results	105
Table 20 Laterals Temporary Fault Simulation Results	108

Table 21 Main Line Fault Simulation Results112

1 INTRODUCTION

1.1 Power System Is Evolving

Since the early development of electrical power grids, their design and structure have not had major changes. In recent decades, the industry has faced challenges that conventional grids cannot keep up with. Existing grids are ageing and demand huge renovation investments while technologies in use are becoming outdated as well. Recently, the concept of smart grid has gained popularity in the industry as a response to revolutionize the grid. The electrical power grid is an expensive investment but vital to the development of countries and the wellbeing of nations. Furthermore, concerns about global warming and environmental protection issues must be considered in any engineering solution.

Driven by the need to increase the efficiency of the electrical grid, provide a cost-effective and environmentally friendly solution, the smart grid enterprise was developed and adopted by the power industry. The development of the smart grid was based on utilization of advanced communication technologies, integration of renewables, de-regulation of the market, the formation of Micro Grids and the use of smart and interactive management algorithms. DER are gaining popularity as an important attribute of the smart grid. DER, which are mainly enabled by renewables, supply power at load side achieving a considerable saving on grid infrastructure investment. DER increase the generation capacity of the grid to respond to the rapidly increasing load growth. Being installed at load side, the DER interconnection to the distribution system saves the investment cost on transmission and distribution of the infrastructure expansion. When DER are enable by renewables (e.g. wind and solar), they provide clean and environmentally friendly energy.

The interconnection of DER on an electrical distribution system mandates changes in the way the system is controlled. The vast majority of distribution systems are built with radial topology, referred to as Radial Distribution System (RDS). Radial topology is characterized by one direction power flow, from the substation to the load. Protection schemes are the main controller and first line of defense against faults. Traditionally, protection schemes for RDS are designed and configured based on the assumption of unidirectional power flow. The interconnection of DER at load side causes power to flow bidirectionally and negates the validity of this assumption. Therefore, protection schemes are expected to malfunction and have to be revised whenever DER are added to RDS.

1.2 Challenges to Protection System

RDS topology is characterized by one-path power supply, opposite to loop or network topology where power supply may be possible through different paths. This fact is used to design the protection system of RDS. Power can only flow in one direction, from supply (or substation in this case) to load. Accordingly, different protection devices are coordinated using time delay. The device closest to load receives instantaneous trip characteristics while time delay is introduced for devices upstream. The Time delay increases the closer a protective device is to the substation and further from RDS end. However, once DER are added to RDS, this fact is no longer valid. DER introduce bi-directional power flow in RDS; as shown in Figure 1. The current can flow upward or downward based on the location of DER, the power output of DER, and the power consumption of the load. To reduce the impact of DER interconnection, IEEE 1547 standard mandates disconnection of all DER in the electrical distribution area for every fault in the system [1].

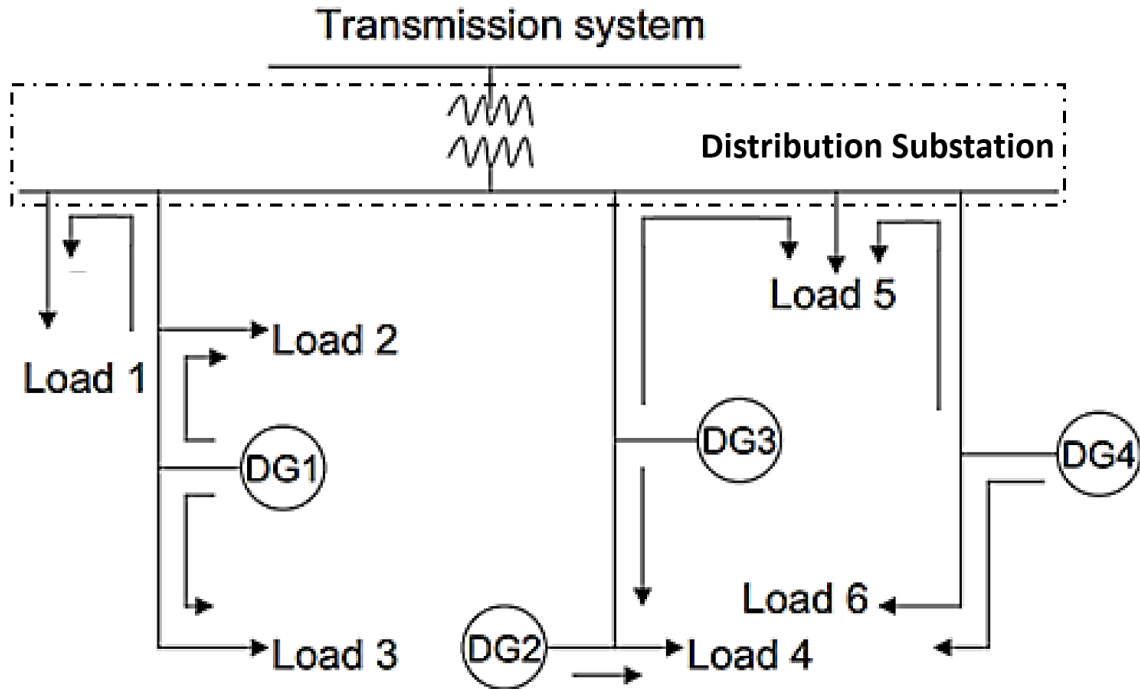


Figure 1 Smart grid RDS with DER Interconnection, adapted from [14]

The requirements of protection systems are based on the anticipated hazards, the level of acceptable protection against those hazards, and the relative cost of the protection system. The hazards that protection system aims to reduce are:

- a) Overcurrent such as faults or overload
- b) Electric shock
- c) Fire
- d) Loss of discrimination
- e) Interruption of power supply

Protection must be effective and responsive to a disturbance with the minimum effect on normal operation. [2]. Hence the revised design of protection schemes for RDS with DER interconnection must account for all of the above considerations. Researchers and engineers have identified the

need to revise existing protection schemes or develop new philosophies to overcome DER interconnection challenges. Aside from adaptive protection schemes, the literature details several methods to mitigate the impact of DER interconnection on distribution system conventional protection. These methods can be classified into 1) finding the limit of DER penetration on distribution system that does not have any effect on protection operation; 2) revising existing protection schemes or settings based on the new configuration; 3) limiting DER contribution to fault current using Fault Current Limiters (FCLs) [3].

1.3 Problem Definition

The vast majority of medium voltage RDS consists of overhead lines. Overhead lines are known for being highly susceptible to momentary faults. Overhead lines are bare conductors where the air is used as an insulation medium. Air can be easily interrupted creating a current path and consequently a fault. It is estimated that 80% - 95% of overhead line trips are caused by temporary faults [4]. Such interruptions are caused by weather conditions such as lightning or temporary contact with objects such as trees or animals. If given sufficient time, such faults will clear out by themselves without any need for human intervention. Based on this fact, protection systems for overhead lines have auto-reclosing capabilities to eliminate the impact of such interruption. Reclosers are a packaged device that has control as well as a circuit interrupting mechanism [4]. Likewise, multi-function relays may have a reclosing function that can perform the same service.

The auto-reclosing reach is extended to cover for temporary faults within fuse reach. This feature, referred to as a fuse-saving scheme, improves the reliability of power supply. To achieve this, the recloser acts on “fast-curve” that is faster than a fuse. If the fault persists, reclosers move to “slow-curve” to allow the fuse to act if the fault is in the fuse protected zone. On the other hand,

a fuse-blowing scheme is used if loads, such as electronic equipment, are sensitive to the impact of momentary trips [4].

Once DER are added to RDS, auto-reclosing is no longer straightforward. Reclosing scheme is a type of overcurrent protection. It depends on sensing overcurrent caused by a fault. Therefore, reclosers must correctly sense the fault through an overcurrent element then act based on the sequence of operations considering appropriate curve, fast or slow. The interconnection of DER in RDS causes bi-directional power flow and multi-sourcing of fault. These facts might cause blinding, miscoordination, sympathetic tripping which ultimately leads to protection malfunctions. On top of that, proper synchronization is required for the auto-reclosing operation with the presence of DER. The auto-reclosing scheme requires a very fast operation which could connect two live systems in case DER are not disconnected in response to a fault. Proper synchronization is a must to connect any two live systems together to avoid generator damages and stability issues [5].

1.4 Research Objective and Approach

This work investigates an adaptive auto-reclosing scheme in RDS with high penetration of DER. The effectiveness and performance of the scheme to mitigate temporary faults are examined. The adaptive scheme is implemented in parallel with a zonal protection scheme in RDS. The RDS is divided into zones separated by circuit breakers. Coordination of the auto-recloser operation with fuses and application of fuse saving are investigated as well. The scheme is applied to a modified dual IEEE 34 node test feeder and simulated using PSCADTM/EMTDCTM software. The results of the simulation show the performance of the scheme considering various scenarios.

2 DISTRIBUTION SYSTEM PROTECTION REVIEW

2.1 Overview

An electrical power distribution system is the portion of an electrical system that connects individual customers to the source of bulk power. It is the electrical network between a consumer's connection point and the larger overall transmission network [6]. The emphases of a distribution system design are accessibility, safety, and continuity of service. Unlike a transmission network, maximizing efficiency is not a priority, but it is still important. The shift in priority focus is due to the fact that distribution systems have shorter distances and lower power per line [6]. Distribution voltage levels are basically standardized around 12 kV. They vary between 11.6 and 13.2 kV, depending on the preference of the utility and history of installations. Electric utilities are adopting higher voltages (34.5/19.9 kV) for distribution systems to enhance their efficiency. This is made possible because of better and more economical insulating materials [6].

The distribution system is the last segment of the electrical network before connecting to the load. Loads vary significantly in power consumption level, demand consistency, and power factor, making it important for utilities to know the nature of the loads connected to the network to ensure proper design and operations. However, the number of loads (or consumers) is very large. Therefore, utilities have load classifications based on structure occupancy. These load types are indicative of operation and connection requirements. Classifications are as follows:

- a) **Residential loads:** This refers to combined loads of single-family dwellings and apartment complexes. Mostly, such loads are single-phase, but apartment complexes have a three-phase service connection. In general, this type of load comprises about 80 to 85% of loads connected at a distribution system.

- b) **Commercial loads:** This refers to stores, shopping malls, schools, office buildings, and complexes. They represent about 15% of load customers.
- c) **Industrial loads:** This refers to factories, plants, and manufacturing facilities. Although this type of load represents at maximum 5% of utility customers, power consumption is 25 to 30% of total power supplied by utilities [6].

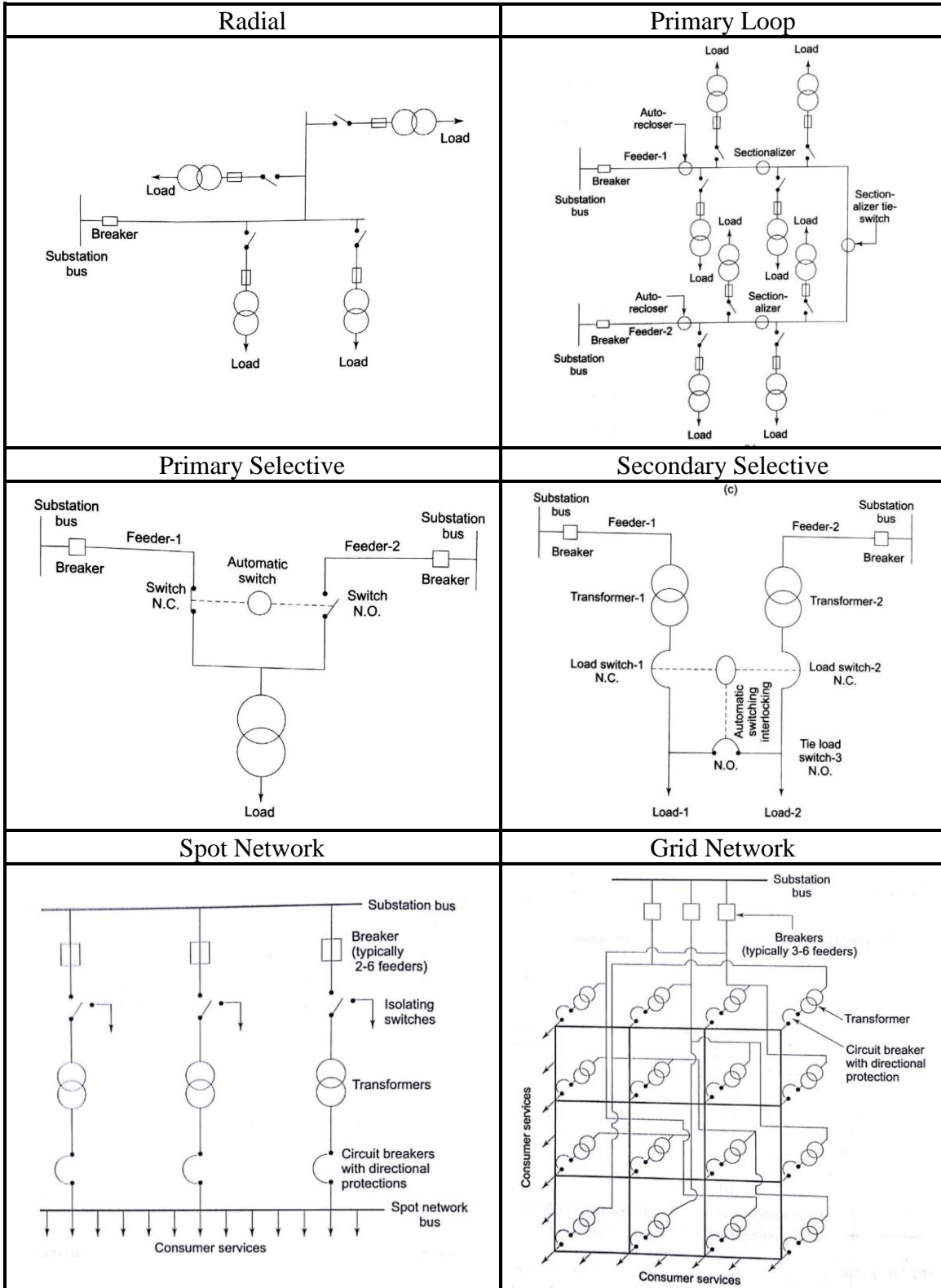
Electrical distribution systems are configured based on operation and load connection requirements. Configurations or layouts of a distribution system can be categorized into six different types. These types vary by power supply reliability, operation flexibility, and cost. Following is a brief summary of each type, along with illustrated diagrams in Table 1:

- i. **Radial:** The main characteristic of this configuration is that power is supplied to load by one source and through one path only. This configuration is the most common and is the least expensive compared to other configurations. However, the reliability of power supply is relatively low due to exposure to many interruption possibilities. Failure at any point in the system (overhead line, underground cable, or transformer) leads to a power outage at the load. This configuration is suitable for small and non-critical loads such as rural loads.
- ii. **Primary loop:** Another name for this configuration is open ring system. Power is supplied to the load by two power sources. The main line is connected through a tie switch that is usually operated at normal position. Reliability in this configuration is enhanced compared to the radial configuration.
- iii. **Primary selective:** This configuration has two power sources as well. High-voltage switches are used ahead of the load transformers. These switches automatically switch in

the case of a fault at the main feeder to restore power to the load rapidly. This configuration is suitable for large, essential, or continuous-process industrial consumers.

- iv. **Secondary selective:** Another name for this configuration is open ring main system. Power is supplied through two power sources. Two primary feeders are each connected to a transformer. On the secondary side, a normally open tie switch is used to automatically switch to the healthy feeder in the case of a fault. Power supply reliability is significantly enhanced in this configuration. The availability of dual transformers eliminates the possibility of long interruptions. Therefore, this configuration is used for industrial plants and critical institutions like hospitals.
- v. **Spot network:** Another name of this configuration is closed ring system. Two or more parallel transformers work to supply load, providing maximum service reliability with operating flexibility and eliminating momentary or long-duration outages. However, the protection system becomes more complicated. Directional power relay is used for protection in this configuration. It is used in metropolitan areas or high-density loads.
- vi. **Grid network:** This one provides maximum reliability and maximum operating flexibility. Also, it is the most economical and effective configuration for high-density loads. Loads are simultaneously supplied from several feeders. Additionally, voltage regulation is significantly improved in this configuration. [2]

Table 1 Distribution System Configuration Types, adapted from [2]



Another classification of distribution system configuration or layout exists in the literature. Basically, it is a similar classification but with they are more detailed classifications, such as those presented by Faulkenberry: radial, loop, combined, and network types. [6] Such classification is important for network operations and maintenance practices. Also, the protection system design is different; it is based on system layout properties like power flow.

Protection system requirements are based on anticipated hazards, the level of acceptable protection against those hazards, and the relative cost of the protection system. The hazards that protection systems aim to reduce include the following:

- a) Overcurrent such as faults or overload
- b) Electric shock
- c) Fire
- d) Loss of discrimination
- e) Interruption of power supply

Protection must be effective and respond to a disturbance with minimum effect on normal operation. [2] The selection of protective devices considers three different ratings: voltage rating, continuous current rating (maximum load), and interrupting rating. Usually, the overcurrent rating for a fuse is selected to be 30% higher than the maximum load current at the time of installation to allow for future load growth [5].

2.2 Protection Schemes of RDS

The majority of a distribution system is configured in a radial layout. Even though the radial layout has the least reliability compared to other layouts, it is the most economical and suitable for the majority of loads, which are residential. An RDS is identified by one power source (distribution substation) and a single power flow path to loads [7]. At the distribution level, loading

is inherently unbalanced due to the large number of connected single-phase loads and variation of demand. Another advantage of RDS that makes it more economical is the simplicity of protection requirements. The protection problem in RDS is less complex than other configurations because current can flow only in one direction. Fault current as well flows in one direction from source to fault location. Additionally, since RDS is electrically the farthest segment in the power network from generation, changes in generation capacity have minimal effect on the available fault current with RDS [8].

The basic protection scheme for RDS is simple overcurrent: overcurrent relay or fuse. Technically and historically, fuses represent the principal protective device used for RDS protection [8]. Fuses are the most commonly used protective device for distribution systems. Relays and auto-reclosers are also used for RDS protection. Both relays and auto-reclosers are overcurrent protective devices similar to fuses. The operation of protective devices must be coordinated to ensure that protection selectivity is properly maintained. Technically, two solutions exist to coordinate protective device operations: time and communication [4]. The communication solution is limited to protection schemes for transmission network due to the additional cost associated with communication equipment. The time solution is implemented using time-delayed overcurrent relays and auto-reclosers. Similarly, fuses implement such a principle.

The time delay introduced by the time solution to the operation curves of protective devices makes possible coordination between such devices. The device closer to the fault operates faster than devices upstream (closer to the source), clearing the fault. In such a case, the devices upstream will not operate because the time delay allows the downstream device to act faster. In other words, both protective devices see the overcurrent due to the fault, but the operation of the upstream protective device is delayed, allowing the downstream device (closer to the fault) to act. Figure 2

illustrates the coordination principle and shows the increasing time delay of a protection device for locations closer to the power source. On the other hand, the available fault current increases as the fault location gets closer to the power source. This fact introduces a problem with the protection scheme as the operation time is delayed further for higher fault currents. Inverse time-overcurrent curves are used to overcome such a problem [8]. Inverse time-overcurrent curves reduce the operation time of the protective devices as the fault current increases.

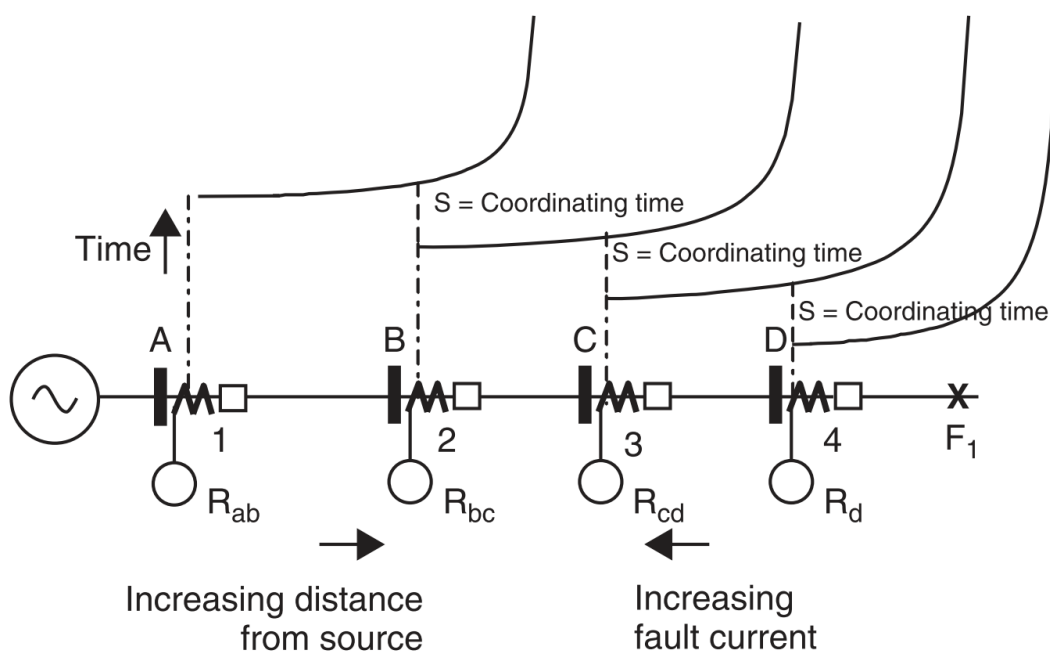


Figure 2 Protective Device Coordination Principles, reprinted from [8]

In RDS, the operation of protective device coordination is achieved by maintaining the coordinating time interval (CTI). CTI is the operating time difference between two consecutive protective devices along a single current path in RDS [4]. The operating time for a protective device in RDS is equal to the sum of the operating time of the near downstream device and the

CTI. Figure 3 illustrates coordination of various protective devices in RDS using inverse time-overcurrent curves.

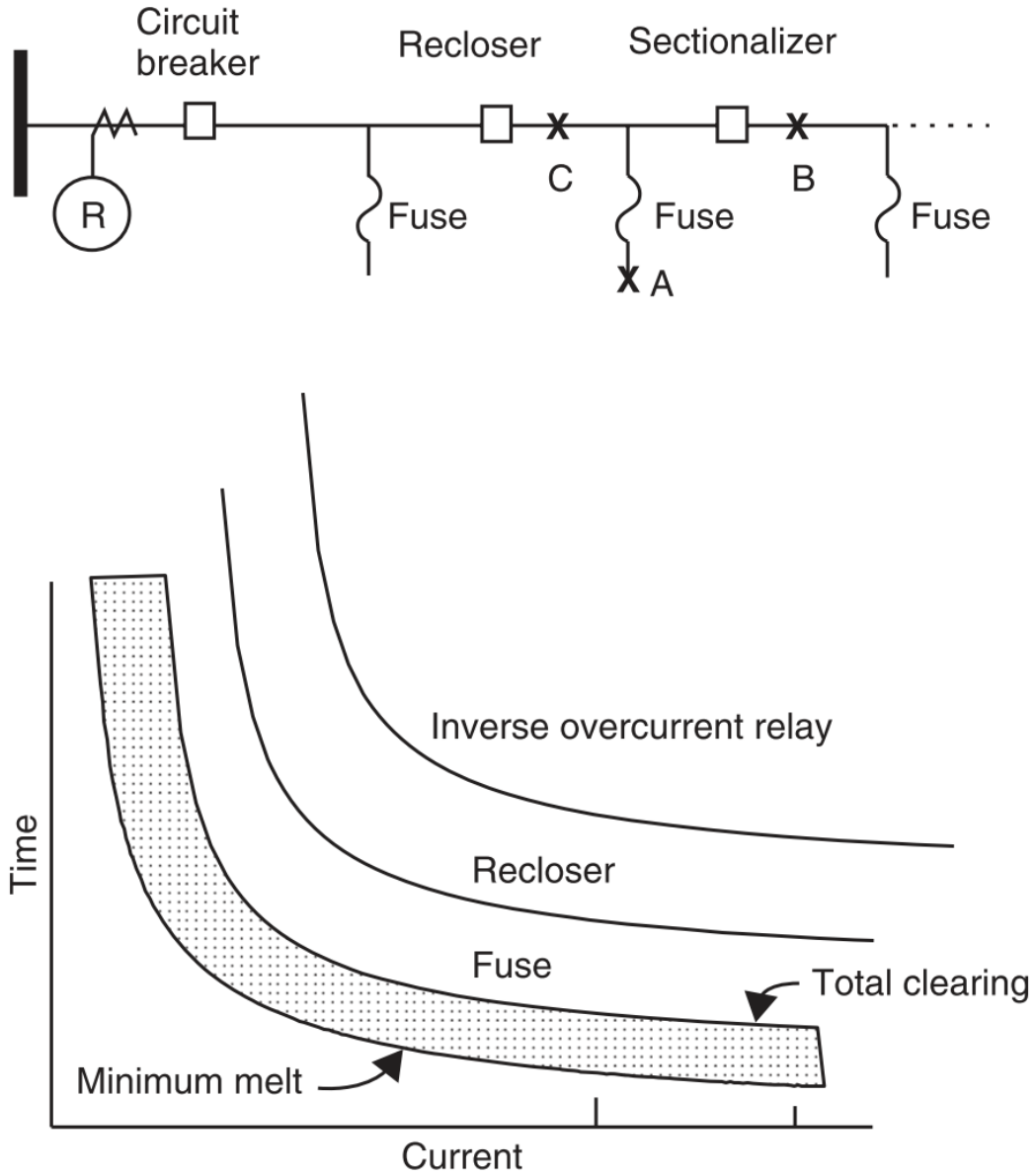


Figure 3 Coordination of Inverse Time-Overcurrent Protective Devices, reprinted from [8]

2.2.1 Relays

Relays are low-voltage electrical devices used for protection and control of a power system at various segments of an electrical network. Relays are complicated devices that have a variety of designs and applications for power systems. Inputs from transducers are wired to relays to provide low-level inputs of voltages, currents, and contacts. Transducers, such as instrument transformers (voltage or current) or status contacts, are located at the electrical node where relay application is required. However, relays are mainly fault- (or abnormality-) sensing devices and need to be associated with electrical interrupting devices such as circuit breakers or reclosers [8].

Relay operation is governed by time-current curves (TCCs) such as those used in inverse time-overcurrent relays. These relays are the most commonly used for RDS protection applications. Relays are required to have proper settings based on the application requirements. Relay or protection engineers perform various studies on the electrical network where the relay is to be applied to come up with required settings. Mainly, overcurrent relays have pickup and TDS. The pickup setting is associated with the abnormality or fault threshold in the electrical system. The TDS is derived from a relay coordination on the specific electrical network. In other words, time-dial control is introduced to relay to delay its operation as required.

Generally, two industry standards exist to identify a family of inverse time-overcurrent curves for overcurrent protection. IEC, which is very popular in Europe, and IEEE, popular in the US, have developed standards for these curves defined by the equations listed in Tables 2 and 3. Each standard defines five curves described by how inverse their characteristics are. Figures 4 and 5 show “extremely inverse” curves on time-current graphs with different TDSs.

Table 2 IEEE C37.112 (US) Inverse Time-Overcurrent Curve Equations, reprinted from [9]

Curve Type	Operating Time	Reset Time
U1 (Moderately Inverse)	$T_p = TD \cdot \left(0.0226 + \frac{0.0104}{M^{0.02} - 1} \right)$	$T_R = TD \cdot \left(\frac{1.08}{1 - M^2} \right)$
U2 (Inverse)	$T_p = TD \cdot \left(0.180 + \frac{5.95}{M^2 - 1} \right)$	$T_R = TD \cdot \left(\frac{5.95}{1 - M^2} \right)$
U3 (Very Inverse)	$T_p = TD \cdot \left(0.0963 + \frac{3.88}{M^2 - 1} \right)$	$T_R = TD \cdot \left(\frac{3.88}{1 - M^2} \right)$
U4 (Extremely Inverse)	$T_p = TD \cdot \left(0.0352 + \frac{5.67}{M^2 - 1} \right)$	$T_R = TD \cdot \left(\frac{5.67}{1 - M^2} \right)$
U5 (Short-Time Inverse)	$T_p = TD \cdot \left(0.00262 + \frac{0.00342}{M^{0.02} - 1} \right)$	$T_R = TD \cdot \left(\frac{0.323}{1 - M^2} \right)$

Table 3 IEC Inverse Time-Overcurrent Curve Equations, reprinted from [10]

Curve Type	Operating Time	Reset Time
C1 (Standard Inverse)	$T_p = TD \cdot \left(\frac{0.14}{M^{0.02} - 1} \right)$	$T_R = TD \cdot \left(\frac{13.5}{1 - M^2} \right)$
C2 (Very Inverse)	$T_p = TD \cdot \left(\frac{13.5}{M - 1} \right)$	$T_R = TD \cdot \left(\frac{47.3}{1 - M^2} \right)$
C3 (Extremely Inverse)	$T_p = TD \cdot \left(\frac{80}{M^2 - 1} \right)$	$T_R = TD \cdot \left(\frac{80}{1 - M^2} \right)$
C4 (Long-Time Inverse)	$T_p = TD \cdot \left(\frac{120}{M - 1} \right)$	$T_R = TD \cdot \left(\frac{120}{1 - M^2} \right)$
C5 (Short-Time Inverse)	$T_p = TD \cdot \left(\frac{0.05}{M^{0.04} - 1} \right)$	$T_R = TD \cdot \left(\frac{4.85}{1 - M^2} \right)$

Where:

- a) T_p = Operating time in seconds
- b) T_R = Electromechanical induction-disk emulation reset time in seconds (if you select electromechanical reset setting)
- c) TD = Time-dial setting (TDS)
- d) M = Applied multiples of pickup current [for operating time (T_p), $M > 1$; for reset time (T_R), $M \leq 1$]

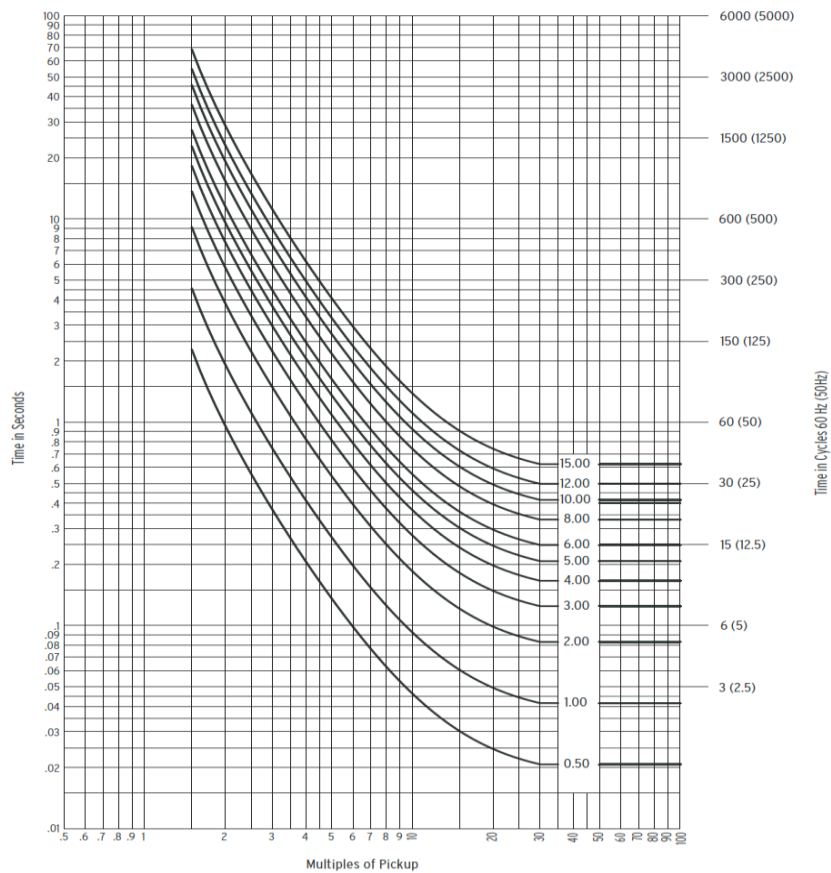


Figure 4 U4 IEEE (US) Extremely Inverse Time-Overcurrent Curves, reprinted from [10]

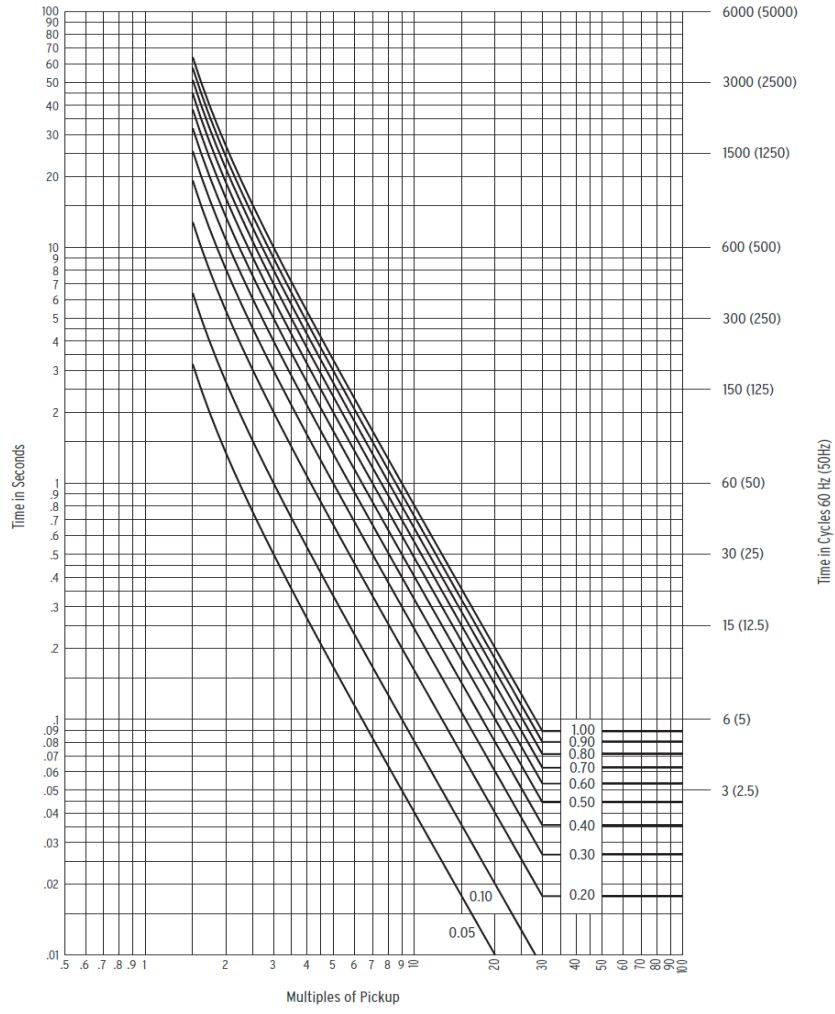


Figure 5 C3 IEC Extremely Inverse Time-Overcurrent Curves, reprinted from [10]

Most of the concepts and jargon for relays are associated with the generation of electromechanical relays. They are still used and valid, even though the industry has moved to microprocessor-based relays. The new relays are multifunctional, smarter, faster, and more accurate compared to electromechanical relays. Additionally, the capability of new relays has increased drastically, allowing more complicated algorithms to be implemented for protection and control of an electrical network.

2.2.2 Auto-Recloser

The auto-recloser is “a self-controlled device for automatically interrupting and reclosing an AC circuit, with a predetermined sequence of opening and reclosing followed by resetting, hold closed, or lockout” [11]. Auto-reclosers, as well as sectionalizers, are used in the protection of radial distribution lines on ≤ 25 -kV voltages. [5]. Compared to circuit breakers, auto-reclosers are compact, lightweight devices that can be pole-mounted. However, the auto-recloser has lower short-circuit-current interrupting capabilities. Also, auto-reclosers are less costly and are maintenance-free. The controller is integrated into the auto-recloser device and is self-powered. It doesn't require AC or DC control power supply. [2] Due to the nature of overhead lines, momentary faults are expected for the majority of interruptions. Auto-reclosers, being less expensive, are a better option compared to circuit breakers for protection against such types of faults. Auto-reclosing can be functional as part of circuit breaker protection and control as well. The auto-reclosing function is sometimes required at the substation breaker to mitigate the effect of temporary faults.

Auto-reclosers can operate at fast or slow curves. The fast curve is used for fuse-saving schemes. In a fuse-saving scheme, the recloser trips faster than the lateral fuse [11]. The objective of this scheme is to avoid tripping a fuse for a temporary fault. Depending on the recloser setting, one or two reclosing attempts are made by the recloser using the fast curve before switching to the slow curve. The slow curve allows the fuse to trip before the recloser takes action. If the fault is within the fuse trip reach, the fuse trips, clearing the fault and allowing the power supply to other parts of the distribution system. If the fault is upstream of the fuse, the auto-recloser will trip permanently after one or two attempts (setting-dependent) using the slow curve. On the other hand, the fuse-blowing scheme doesn't consider fast curve recloser operations.

2.2.3 Fuse

The fuse in the electrical system works as a protective and disconnecting device at the same time. The concept of the fuse is based on thermal heating given by I^2t . High-voltage fuses can be categorized into expulsion, non-expulsion, and current-limiting fuses. [2] As per IEEE 100, the definition of a fuse is “an over-current protective device with a circuit-opening fusible part that is heated and severed by the passage of the overcurrent through it”[4]. A fuse is the simplest protection and interrupting device in an electrical protection system. Fuses are used at distribution voltages to protect feeder circuits of short lines and relatively small loads. Fuses must be selected based on three ratings: voltage, continuous (maximum-load) current, and interrupting rating. [5]. The fuse current rating is usually selected to be 30% larger than maximum load current to allow for future load growth. Also, the fuse interrupting rating should be at least the maximum fault current available at the protected electrical circuit.

At 600+ V, the fuse is called a power fuse. It is designed for transmission, sub-transmission, and distribution levels. It can be installed on poles or inside substations. The fuse link, part of the fuse assembly, is the part replaced after each operation of the fuse (after each trip). Power fuses are used instead of breakers when the cost of a breaker is not justified compared to the number of anticipated operations and service restoration speed after a fault [5].

Fuse operation occurs in a band of the time-current plane. The lower band is the minimum melting time (MMT), and the upper band is the total clearing time (TCT). The time difference between MMT and TCT is the fuse arcing time [4]. Both curves are significant when coordinating operation of protective devices in a power system. In the case of fuse-fuse coordination, the downstream-fuse TCT must be lower than the upstream-fuse MMT. The rule used here is that downstream-fuse TCT must be $\leq 75\%$ compared to upstream MMT [5]. This prevents any damage

to the upstream fuse while the downstream fuse operates for a fault in its zone. This approach extends to the coordination of fuses with other protective devices.

Types of fuses used in power system protection are expulsion, non-expulsion, and current-limiting. The most commonly used type for pole-mounted applications is expulsion [4]. Fuses are also classified based on the speed of operation, in other words, the slope of time-current characteristics. The industry started to develop a standard (later known as ANSI C37.42) in the early 1950s to enable interchangeability. The classification is based on the speed ratio, which is defined in the following equation [5]. The “K” type is for fast fuses, “T” is for slow, and “N” exists as well [4]. Figure 6 shows the characteristics curves for the different speed types of fuses. The benefit of the standard is that utilities can buy and stock fuses from various manufacturers that are interchangeable.

$$\textit{Speed ratio} = \frac{\text{Melting current at 0.1 s}}{\text{Melting current at 300 or 600 s}}$$

These classifications mean that fuse behavior is similar within specific current ranges. In other words, the melt time is expected to be similar for similar fault currents. Fuse current ratings don’t provide information about the characteristics curves. The speed ratio is what specifies the slope of the fuse characteristics curve. The denominator of the speed ratio equation uses 300-second current value for fuses rated 100 A or less and 600 seconds current values for fuses rated over 100 A [12] IEEE C37.42. The words “slow” and “fast,” often associated with types T and K, respectively, are only indicative of fuse relative speed [12] IEEE C37.42. The speed ratio of the K (fast) fuse ranges from 6 to 8.1, while the speed ratio of the T (slow) fuse ranges from 10 to 13 [13]. Other types of fuses exist as well: C, E, and R, which are further described in standards ANSI IEEE C37.42 [12] IEEE C37.42.

It is worth mentioning here that the fuse as a protective device can't identify current or power direction. A directional element is sometimes required to ensure proper protection operation. The fuse, being the simplest protective device, can only respond to current magnitude regardless of direction. Additionally, fuses can't respond to external signals such as trip signals from relays or controllers. This makes the fuse extremely rigid in its operation as a protective device. [14]

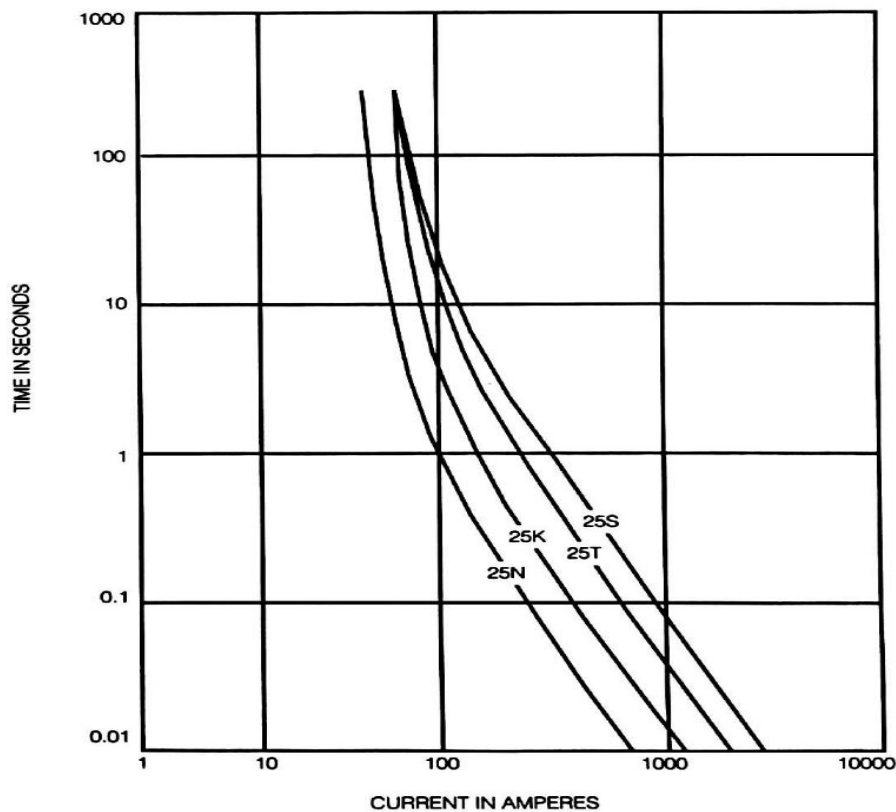


Figure 6 Fuse Speed Ratio Comparison, reprinted from [13]

2.2.4 Directional Element

Being able to determine fault direction is very helpful for some protection schemes. The utilization of a directional element is fundamental to the security and selectivity of protection with

bidirectional power flow. Overcurrent relays, for example, measure the current magnitude in the location of the protected circuit, but they don't provide the direction of the current [5]. Knowing the direction of the fault current (or power) is sometimes required to support the decision of an overcurrent protection scheme. A directional unit is usually applied as part of a scheme [4]. In general, the directional element serves the following purposes: identify the direction of the fault in reference to the relay location, supervise the distance scheme, and create quadrilateral characteristics of ground distance [15]. Communication-assisted directional overcurrent elements are commonly applied for transmission-line primary protection. Usually, directional overcurrent elements are paired with communication-assisted distance schemes such as directional comparison blocking (DCB) and permissive overreaching transfer trip (POTT). With the help of directional elements, these schemes can overcome the limitations of fault resistance associated with ground distance elements. [15]. Directional capability is involved in the functions of three different relays or standard device numbers as per ANSI/IEEE 37.2: device 21, distance relay, device 32, directional power relay, and device 67, AC directional overcurrent relay. Both 21 and 67 are based on the impedance calculation, but 67 doesn't have the distance-to-fault capability. Device 32 is based on the power calculation ($P = \text{Re} [V \times I^*]$) [16].

Directional element output is used in conjunction with overcurrent element output, with either instantaneous or time-inverse characteristics. Therefore, the relay initiates a trip signal if the current magnitude is higher than the minimum operating current (pickup) setting and if the current direction is the desired direction (trip direction). On the other hand, if the current direction is not the desired direction (non-trip direction), the relay will be blocked from initiating trip signal even though the current is higher than the pickup setting [4]. In RDS, the directional element is not required for fault protection because RDS is characterized by unidirectional current (power) flow.

Therefore, RDSs are usually protected by simple overcurrent protective devices like overcurrent relays, reclosers, sectionalizers, and fuses [5]. However, the directional element is required for overcurrent relay applications in looped or networked systems. Both systems are different from RDS due to the existence of bidirectional current flow. In such conditions, determining current direction is a must for the security of the protection scheme. Additionally, adding a directional element to the overcurrent enhances the sensitivity of the scheme and simplifies time coordination [15].

Directional relay provides the current direction based on the relative phase position with respect to a reference: voltage or current [5]. The reference used is usually referred to as polarization. Polarization can be either voltage or current. Therefore, the reference quantity is referred to as the polarizing quantity and monitored current as the operating quantity. The reference quantity must be reasonably constant during the fault to provide an adequate comparison with the fault current. It is common to use voltage as the polarizing quantity since the voltage phase does not change significantly during faults. However, the current phase may shift 180° , resembling a reverse current direction for a fault on the side relative to connected CT on the protected circuit [4]. Figure 7 shows commonly used directional-sensing units. The first two are voltage-polarizing configurations, and the third one is a current-polarizing configuration. The zero-torque line and the maximum-torque line indicate the thresholds for phase comparison. The zero-torque line divides the plane by half into operating and non-operating regions [4]. In the operating region, the current is in the desired direction as the angle difference between the operating quantity, and the polarizing quantity is within the zero-torque line threshold. The maximum-torque line indicates the angle where operating quantity (monitored current) is at a normal forward direction. The angle

of this line depends on the polarizing quantity. This directional element is usually referred to as the classical voltage-polarizing power directional element.

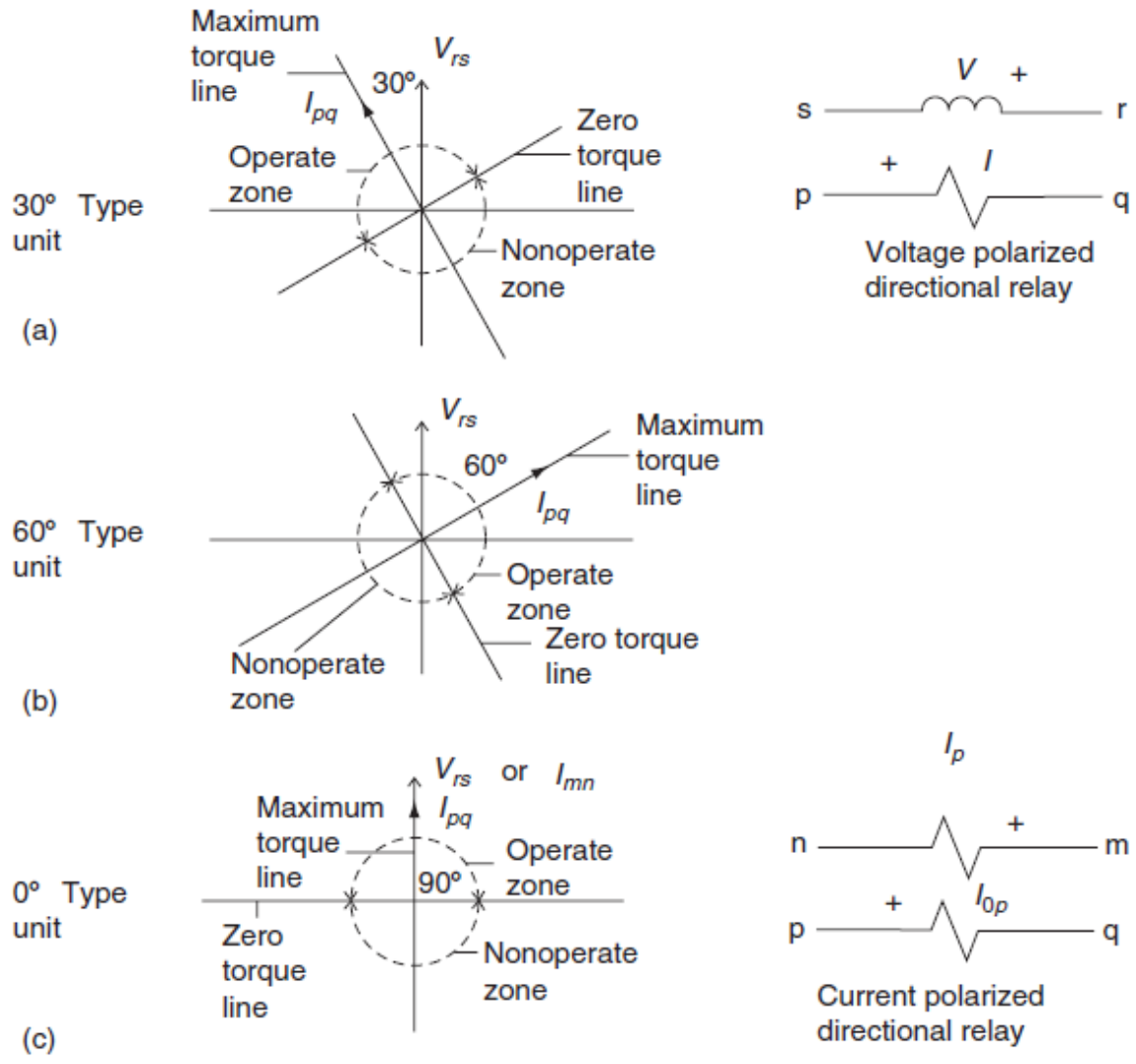


Figure 7 Typical Directional Element Characteristics, reprinted from [4]

Another popular voltage-polarizing directional connection is the 90° connection, which is used for phase overcurrent protection. Table 4 lists the operating and polarizing quantities used for such directional element configurations [15].

Table 4 Quantities for 90° Connected Phase Directional Element, reprinted from [15]

Phase	Operating Quantity (I_{OP})	Polarizing Quantity (V_{POL})
A	I_A	$V_{POL} = V_{BC}$
B	I_B	$V_{POL} = V_{CA}$
C	I_C	$V_{POL} = V_{AB}$

The direction of the fault current is identified using torque (T_{PHASE}). The fault is identified as forward if the torque value for the phase is positive and is identified as reverse if the torque value of the phase is negative. For each phase that is connected at 90°, the torque is calculated using the operating and polarizing quantities as represented in the following equations [15]:

$$T_A = |V_{BC}| \cdot |I_A| \cdot \cos(\angle V_{BC} - \angle I_A)$$

$$T_B = |V_{CA}| \cdot |I_B| \cdot \cos(\angle V_{CA} - \angle I_B)$$

$$T_C = |V_{AB}| \cdot |I_C| \cdot \cos(\angle V_{AB} - \angle I_C)$$

2.2.4.1 Sequence-Quantities Power Directional Elements (32)

Another method to implement a power directional element is using sequence-quantities. Various voltage and current sequence-quantities are utilized as operating and polarizing quantities. Fault types have different characteristics in terms of the sequence-quantities present in the system. Thus, for each fault type, different sequence-quantities are utilized that best match the characteristics of the fault. For balanced faults, positive-sequence currents and voltages are the only present quantities in the system. These quantities are employed to produce the three-phase directional element. However, for phase overcurrent and distance protection, using positive-sequence quantities works for balanced faults only, which means that a separate directional element for unbalanced faults is required. Negative-sequence quantities are present only during

unbalanced conditions. As a result, negative-sequence quantities are used for detecting fault direction during unbalanced faults. Also, zero-sequence quantities are utilized for ground faults due to their presence on such faults only. Different protection schemes use different combinations of these elements, which are selected based on suitability for the system and protection requirements [15].

As per ANSI/IEEE C37.2, the device number for the directional element is 32. For positive-sequence, the device number is defined as 32P. Similarly, for negative-sequence, it is 32Q. However, the zero-sequence voltage polarization uses device number 32V, while zero-sequence current polarization uses device number 32I. All of these elements are further explained in the next sections.

2.2.4.2 Positive-Sequence Power Directional Element (32P)

During balanced system conditions, only positive-sequence quantities are present. The system is considered balanced during the normal balanced power flow state or during balanced fault conditions. Balanced fault conditions are when the fault current is balanced across all phases, including either three-phase faults or three-phase-to-ground faults. Table 5 shows the quantities used in the positive-sequence directional element [15].

Table 5 Quantities for Positive-Sequence Directional Element, reprinted from [15]

Phase	Operating Quantity (I_{OP})	Polarizing Quantity (V_{IPOL})
Three-Phase	$3I_1 \cdot (1 \angle Z_{L1})$	$3 V_1$

Fault direction is identified using the torque produced due to the positive-sequence quantities. The term torque originates from the electromechanical relay time, where the sign of the

torque determines the direction of the three-phase fault current. A positive torque sign indicates a forward fault current, and a negative torque sign indicates a reverse fault current. Positive-sequence directional element torque (T32P) is calculated using the following equation [15]:

$$T_{32P} = |3V_1| \cdot |3I_1| \cdot \cos [\angle 3V_1 - (\angle 3I_1 + \angle Z_{L1})]$$

Where:

$$3I_1 = \text{Positive-sequence current: } 3I_1 = (I_A + a \cdot I_B + a^2 \cdot I_C).$$

$$3V_1 = \text{Positive-sequence voltage: } 3V_1 = (V_A + a \cdot V_B + a^2 \cdot V_C).$$

$$\angle Z_{L1} = \text{Positive-sequence line angle.}$$

$$a = 1 \angle 120^\circ.$$

2.2.4.3 Negative-Sequence Power Directional Element (32Q)

Negative-sequence quantities are only present for unbalanced conditions [17]. Unbalance in the system occurs due to load variation from phase to phase, referred to as “unbalanced loading,” or due to faults that don’t involve all phases. In other words, the unbalanced condition occur when currents or power are differs across phases. Unbalanced faults are faults that are phase-to-ground, phase-to-phase, or phase-to-phase-to-ground. To determine the direction of an unbalanced fault current, the separate directional current element is required. The element is based on negative-sequence quantities and is designated as 32Q. Table 6 shows the quantities used in the negative-sequence directional element [15].

Table 6 Quantities for Traditional Negative-Sequence Directional Element, reprinted from [15]

Operating Quantity (I_{OP})	Polarizing Quantity (V_{2POL})
$3I_2 \cdot (1 \angle Z_{L1})$	$-3 V_2$

Fault direction is identified using the torque produced due to the negative-sequence quantities. The sign of the torque determines the direction of the three-phase fault current. A positive torque sign indicates a forward fault current, and a negative torque sign indicates a reverse fault current. It is important to note here that the polarizing quantity has a (–) negative sign, so the torque expression maintains the forward and reverse convention. Negative-sequence directional element torque (T32Q) is calculated using the following equation [15]:

$$T_{32Q} = |3V_2| \cdot |3I_2| \cdot \cos [\angle -3V_2 - (\angle 3I_2 + \angle Z_{L1})]$$

Where:

$$3I_2 = \text{Negative-sequence current: } 3I_2 = (I_A + a^2 \cdot I_B + a \cdot I_C)$$

$$-3V_2 = \text{Negative-sequence voltage: } -3V_2 = (V_A + a^2 \cdot V_B + a \cdot V_C) \cdot (1 \angle 180^\circ)$$

The angle $\angle Z_{L1}$ usually corresponds to the maximum torque angle (MTA), as shown in Figure 8. The plane describes the relationship between the operating and polarizing quantities for the negative-sequence directional element. Consistent with the torque calculation equation, the polarizing quantity ($3V_2$) is in the negative axis direction [15]:

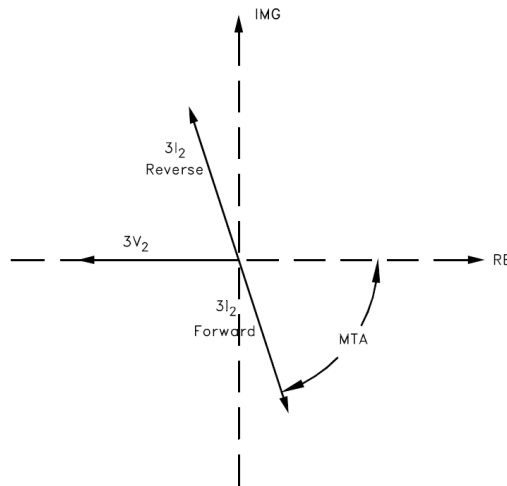


Figure 8 Operating/Polarizing Quantities Plane for Negative-Sequence Directional Element, reprinted from [17]

2.2.4.4 Zero-Sequence Power Directional Element (32V)

Ground faults involve fault current path to ground. For all ground faults, zero-sequence quantities are the most suitable for the directional element [17]. The zero-sequence ground directional element can either use voltage or current as the polarizing quantity. The voltage-polarized ground directional element (32V) uses the zero-sequence voltage (V_0 or $3V_0$) as the polarizing reference. The operating quantity used in this element is $3I_0$. Again, the torque associated with the zero-sequence indicates the fault direction following the same sign convention. The torque calculation equation is as follows [15]:

$$T_{32V} = |3V_0| \cdot |3I_0| \cdot \cos [\angle -3V_0 - (\angle 3I_0 + \angle Z_{L0})]$$

Where:

$$3V_0 = \text{Zero-sequence voltage: } 3V_0 = (V_A + V_B + V_C).$$

$$3I_0 = \text{Zero-sequence current: } 3I_0 = (I_A + I_B + I_C).$$

$$\angle Z_{L0} = \text{Zero-sequence line angle.}$$

For remote ground faults, the ground directional element may fail to provide correct identification of the fault direction because of the small magnitude of the polarizing voltage. With such faults, the polarizing voltage is at its lowest magnitude. The polarizing voltage angle also becomes unreliable, which results in the wrong torque value. To overcome this problem, current is used as an alternative to voltage for the polarizing quantity [15].

2.2.4.5 Zero-Sequence Power Directional Element (32I)

Similar to the previous element, this element is a zero-sequence current ground directional element. However, this element uses an external source current (I_{POL}) as the polarizing quantity. This is the only element explored here that doesn't have voltage as the polarizing quantity. This is useful to overcome the issue of small voltage magnitude during remote ground faults. This element

measures the phase angle difference between the polarizing current (I_{POL}) and the line residual current ($3I_0$). Compared to negative- and positive-sequence voltage polarizing elements, in this element the line residual current ($3I_0$) doesn't involve phase-shifting by line angle. Consistent with other directional elements, the direction of the fault is determined using torque calculation as per following equation [15]:

$$T_{3I} = |I_{POL}| \cdot |3I_0| \cdot \cos(\angle I_{POL} - \angle 3I_0)$$

The directional element for distance relays works based on principles similar to those used for overcurrent relays. Voltages and currents are compared to produce directional characteristics and an impedance plane. This is accomplished by using phase angle comparators. Those comparators examine the angles between various voltage and current quantities to create desired characteristics such as directional, reactance, and mho. Similar to overcurrent relays, the directional element for distance relays uses different polarization quantities as a reference to compare with fault current and to determine direction. Additionally, comparators use various techniques according to application.

It worth mentioning here that negative-sequence has the following advantages [18]:

- Zero-sequence due to mutual coupling has no effect on directional decision based on negative-sequence.
- Higher sensitivity with reasonable security is possible for remote-ground, high-resistance faults. Such faults create more negative-sequence current compared to zero-sequence.
- Insensitivity to shift of VT neutral that might be caused by VT neutral multiple grounds.

The only main disadvantage of the negative-sequence directional element is nonoperational during breaker single-pole operations [18].

2.2.4.6 Negative-Sequence Impedance Directional Element (67_{NEG})

Another way of applying negative-sequence quantities to identify fault current direction is through a negative-sequence impedance. The same quantities are used to apply the negative-sequence impedance directional element, but using a different equation. Negative-sequence impedance is the ratio of negative-sequence voltage to negative-sequence current. This value is used instead of the torque value that is the product of negative-sequence voltage and negative-sequence current. The calculation equation is as follows [17]:

$$Z_2 = 3V_2/3I_2 \text{ or equivalently } V_2/I_2$$

For a forward fault, the negative-sequence current lags the polarizing voltage by the line angle (MTA or $\angle Z_{L1}$). However, for a reverse fault, the negative-sequence current is in the opposite direction, or 180° out-of-phase. In both cases (forward or reverse), the negative-sequence voltage (polarizing quantity) is always negative. Thus, for a forward fault, the negative-sequence impedance value is always negative. On the other hand, for a reverse fault, the negative-sequence impedance values are always positive [17].

An advantage of this method to implement negative-sequence directional element is high sensitivity, even with a very small negative-sequence voltage. This is valid even when the negative-sequence impedance is reduced to zero as the negative-sequence voltage approaches zero. Practically, the zero value for negative-sequence impedance is an indication of a forward fault [17].

2.3 Review of RDS with DER Protection Schemes

Since the late 1990s, the use of DER has gained popularity in electrical networks around the world [19]. DER provides an economical and feasible solution to the increasing demand for energy in electrical grids. DER is installed on the load side, eliminating the need to expand the

capacity of transmission and distribution networks. Such expansion requires huge investments that are avoided by the utilization of DER. However, the interconnection of DER introduces challenges to the protection and operation of distribution networks. The significance of these challenges increases and becomes alarming with the increase of DER penetration in a particular system. Some of the common distribution system protection issues associated with interconnection of DER include the following [19]:

- The introduction of a bidirectional current in RDS. The protection system is designed with the assumption of unidirectional fault current in the RDS.
- Voltage regulation might be affected.
- The islanded operation of DG and the requirements of frequency control.
- The synchronization requirements in the case of connecting two live parts of the system.
- The auto-reclosing scheme needs to be revised.
- System area stability might be affected.

DR is defined as “sources of electric power that are not directly connected to a bulk power transmission system. DR include both generators and energy storage technologies” [1, 20]. Additionally, DG is defined as “electrical generation facilities connected to an area electrical power system through a point of common coupling; a subset of DR” [1, 20]. For the sake of this report, DG and DR are used interchangeably as they have the same effect on protection. DG comes in various capacities: micro-sized below 5 kW, small-sized between 5kW and 5 MW, medium-sized between 5 and 50 MW, and large-sized above 50 MW [21]. Some of the common technologies available for DR are wind generation, solar generation, fuel cells, biomass generator, super magnetic energy storage, mini-turbine modules, sterling-engine-based generators, and

internal combustion engines [21] [19]. Renewable energy technologies are, in general, the most significant enabler of DG deployment.

To eliminate vulnerabilities associated with the interconnection of DG to RDS, various solutions have been proposed in the literature. Besides standards and operational practices, technical solutions have been developed (and continue to be developed) to tackle the aforementioned challenges. In general, adaptive schemes are gaining popularity as a solution to DG interconnection issues. As per IEEE C37.230, adaptive relay schemes are “making automatic real-time adjustments to power system protection schemes to achieve the most dependable and secure distribution system protection for the system conditions at that time” [22] IEEE C37.230. Adaptation on the relays to respond to system changes are driven by internal logic, analog measurements, communication signals from other intelligent electronic devices (IEDs), changes in the monitored status of switch contacts or circuit breakers, or a combination of these inputs [23]. Adaptive protection can be implemented on two levels: devices and systems. When implemented on devices, only local information is available to the IED to respond to changes in the specific local area. On the other hand, adaptive protection systems use information available from the entire system to respond to changes that occur in different parts of the system. Information is interchanged with the system using a communication network [23]. Device implementation is simpler but limited in response to local changes only, whereas system implementation can achieve area-wide optimality and with full dependability in communication.

Aside from adaptive protection schemes, methods proposed in the literature to mitigate DG interconnection impact on distribution system conventional protection can be classified into 1) finding the limit of DG penetration on the distribution system that does not have any effect on protection operation; 2) revising existing protection schemes or settings based on the new

configuration; and 3) limiting DG contribution to fault current using FCLs [3]. An overview of such schemes from the literature is provided in Table 7.

In 1 and 2, the distribution system is divided into zones (or assumed to be divided) and separated by breakers associated with IEDs. Directional overcurrent is implemented in IEDs where the current direction is shared with other IEDs via communication to determine the faulty zone. In 1, no centralized controller/IED is used to avoid a single point of failure, but coordination with fuses and recloser operations are not considered. However, in 2, all current directions are communicated to a centralized IED that runs the algorithm and sends a trip signal to boundary breakers of the faulty zone. Similarly, 3 and 23 use the concept of a divided distribution system with a centralized controller. However, in 3, the faulty zone is identified by calculating the Thevenin equivalent at each node and comparing to a lookup table from offline studies. Estimation of the Thevenin equivalent is a tedious calculation (and prone to errors), especially when distribution system loadings and configurations vary significantly and abruptly. On the other hand, 23 uses the Artificial Neural Network (ANN) algorithm to identify faulty zones.

In 15, directional overcurrent is applied to a divided distribution system as well. However, the directional overcurrent is extended to provide backup to neighboring zones using two-stage TDS. The solution doesn't consider temporary faults. In 25, directional overcurrent is applied to a divided distribution system, but uses definite time curves and a centralized energy management system (EMS) to control the scheme. In 27, the directional element is combined with the current differential in a master-slave architecture to provide protection to a zoned distribution system. In 28, a synchronizing check is added to a communication-assisted directional scheme to allow reclosing for temporary faults.

A microprocessor-based recloser is used in 4 and 9 to restore recloser-fuse coordination. Both need to have real-time monitoring of lateral current. In 5, 7, 8, and 16, the concept of a multiagent system is applied to the protection scheme. In 5, a wavelet coefficient algorithm is applied to identify abnormalities. However, the method is not fully successful to distinguish a fault from transient conditions. In 7, relays are agents with the centralized controller, while in 8, current and voltage transformers are added to the agent level. Both methods are heavily communication-dependent. In 16, Fuzzy C-Means (FCM) clustering and space relative distance are applied to the algorithm of fault identification and location.

In 6 and 12, a recloser setting is proposed to be reviewed after DG interconnection to restore coordination with a fuse. In 6, directional overcurrent in the substation relay is assumed to mitigate false tripping. The approach doesn't consider multiple DG interconnections and assumes that fuse-fuse coordination is not affected. In 12, DG location is optimized by studying various location impacts before interconnection. The recloser setting is revised afterward. This method doesn't provide a structured algorithm to find the optimal DG location. In 10, 18, and 19, FCLs are proposed to limit DG contribution to fault current. In 19, FCL is simply applied to DG interconnection. However, FCL is based on power electronics, which could affect power quality, especially with high penetration of DG. In 18, FCL is combined with relay protection that uses ANN and decision tree algorithms. In addition to FCL power quality issues, the method does not consider coordination with other protective devices. In 10, a superconducting FCL is used.

In 11, the method suggests studying DG interconnection for each application to find a penetration limit that does not have an effect on protection and limits DG capacity accordingly. Considering the nature of varying loads in distribution and varying renewable DG outputs, finding the penetration level limit is very difficult, or at best will have very low utilization of DG. In 13,

the method is based on the positive-sequence current differential concept. The scheme requires advanced communication for real-time sampling and synchronization, which are costly to distribution systems. In 14, the genetic algorithm (GA) optimization technique is applied to update the adaptive overcurrent optimal setting. In 17, the author proposes studying the DG interconnection for each application to decide the minimal number of DGs to be disconnected during a fault. DGs are disconnected by using a gate turn-off (GTO) thyristor that is power-electronic-based. Again, power electronics might compromise power quality. In 20, the author suggests replacing fuses by microprocessor-based reclosers for lateral with DGs to overcome fuse fatigue and nuisance trips, but fuse fatigue is not fully mitigated. In 21, zone 2 adaptive distance settings are suggested assuming inverter-interface DGs only. In 22, a mathematical algorithm is proposed to adaptively change directional overcurrent settings. Also, the scheme employs a hybrid islanding detection method. The scheme has not been tested for multiple DGs or different DG locations on the distribution system. In 24, adaptive voltage relay with a directional element is proposed at each end of the line where DG is interconnected. However, coordination with other protective devices is not considered. In 26, an adaptive directional overcurrent scheme is suggested with settings updated based on calculations using optimized Thevenin-equivalent estimation. Thevenin-equivalent accuracy in the distribution system is very low due to the fast changes in system operating point and configuration.

Table 7 Review of Protection Methods to Mitigate DG Interconnection Impact on RDS

#	Ref	Protection Approach/Method	Protective Element	Adaptive (Yes/No)	Shortfalls
1	[24]	Zonal overcurrent protection for smart RDS with DG: Propose to add breakers to divide RDS into zones based on the balance of DG output and average load. Communication-assisted directional overcurrent is implemented at zonal breaker protection.	Relays	No	<ul style="list-style-type: none"> ▪ Coordination with fuse is not considered ▪ Reclosing is not considered
2	[25]	Implementation of a new protection scheme on a real distribution system in the presence of DG: Distribution network is divided into zones separated by switches. Centralized controller remotely monitors current at DG interconnection point, zonal switches, and laterals without DGs. The faulty zone is identified by comparing system measurements with a lookup table. The lookup table is created from offline load flow and short circuit studies. The centralized controller sends a trip signal to switches associated with identified faulty zone. Reclosing is considered.	Relays	No	High dependency on communication
3	[14]	Development of adaptive protection scheme for distribution systems with high penetration of DG: Divide the distribution system into zones separated by breakers. Monitor current at all sources: substation and DGs. Fault and location are identified by comparing source current contribution to a lookup table that is based on offline calculations. Confirm faulty zone by the directional element at zone boundaries.	Relays	No	<ul style="list-style-type: none"> ▪ Requirement of continuous monitoring of DG status ▪ Difficult to calculate Thevenin equivalent for each network configuration or loading scenario

Table 7 Continued

#	Ref	Protection Approach/Method	Protective Element	Adaptive (Yes/No)	Shortfalls
4	[26]	New adaptive digital relaying scheme to tackle recloser-fuse miscoordination during DG interconnections: Recloser adaptive scheme to reestablish coordination with fuse based on a calculation of the ratio of feeder current and recloser current. TDS of the recloser is automatically adjusted to avoid miscoordination between fuse and recloser.	Microprocessor-based recloser	Yes	Requirements to monitor all laterals with fuses in real time
5	[27]	Isolation of faults in distribution networks with DG: Use of agent-based (relays) algorithm to identify faulty segment RDS. Fault current direction is identified by analyzing wavelet coefficients of the Clarke components of the fault currents. RDS is divided into segments with breakers at boundaries.	Relays	Yes	<ul style="list-style-type: none"> ▪ Not coordinated with OC and fuses ▪ Can't distinguish fault from non-fault transients
6	[28]	A strategy for protection coordination in RDS with DG: Proposal to review the recloser settings after adding DG to restore recloser-fuse coordination. Uses substation relay directional element to eliminate false tripping.	Microprocessor-based recloser Relay	No	<ul style="list-style-type: none"> ▪ Assumes fuse-fuse coordination is not affected, even at neighboring feeder ▪ Does not consider high-impedance faults ▪ Did not consider multi-DGs at the same feeder

Table 7 Continued

#	Ref	Protection Approach/Method	Protective Element	Adaptive (Yes/No)	Shortfalls
7	[29]	<p>A multiagent-system-based protection and control scheme for distribution system with DG integration: Use multiagent system including DG controller and directional overcurrent relays on the RDS. Information from agents is communicated to the central controller to decide on the faulty location and send a signal to trip associated breakers.</p>	Relays	Yes	<ul style="list-style-type: none"> ▪ Significant communication traffic that burdens communication network ▪ Update of agents setting might happen slowly
8	[30]	<p>An adaptive multiagent approach to protection relay coordination with DG in industrial power distribution system: Based on multiagent system algorithm considering DG controller, directional overcurrent relays, CT, and PT as agents.</p>	Relays	Yes	Significant communication traffic that burdens communication network
9	[31]	<p>Microprocessor-based reclosing to coordinate fuse and recloser in a system with high penetration of DG: Restore recloser-fuse coordination by creating user-defined curves in microprocessor-based recloser. The recloser curve is adjusted based on the fuse-to-recloser ratio (FRR).</p>	Microprocessor-based recloser	Yes	Requirement of continuous monitoring of DG status
10	[32]	<p>Use of superconducting fault current limiters for mitigation of DG influences in radial distribution network fuse-recloser protection system: Use of superconducting FCL to mitigate the effect of SM-based DG sources on fuse-recloser protection infrastructure without the requirement of DG disconnection.</p>	FCLs	No	Power electronics might affect power quality

Table 7 Continued

#	Ref	Protection Approach/Method	Protective Element	Adaptive (Yes/No)	Shortfalls
11	[33]	<p>Assessment of DG influences on fuse-recloser protection systems in radial distribution networks: Propose a technique to determine the maximum penetration level of synchronous machine-based DG that doesn't cause loss of fuse-recloser coordination or affect pickup sensitivity of recloser. DG penetration is limited to the capacity as per the assessment to avoid protection issues.</p>	Fuse Recloser	No	<ul style="list-style-type: none"> ▪ Limited to synchronous-based DGs ▪ Does not consider load variation and renewable output variation
12	[34]	<p>A classification technique for recloser-fuse coordination in distribution systems with DG: Determine the best DG locations and change the recloser setting to minimize number of cases classified as "coordination lost." DG location is determined by testing various locations on the system. When "coordination lost" is minimized, settings of recloser are reviewed.</p>	Recloser	No	<ul style="list-style-type: none"> ▪ Location determination algorithm is not optimal ▪ Could lead to situations that have miscoordination
13	[35]	<p>Principle and implementation of current differential protection in distribution networks with high penetration of DGs: Use positive-sequence fault component for current differential at distribution feeder. Current data are communicated to other end of protected zone using dedicated channel or SDH network.</p>	Relays	No	Extensive use of advanced communication and synchronization methods, which are costly for the distribution system
14	[36]	<p>Optimization-technique-based adaptive overcurrent protection in radial system with DG using GA: Use GA optimization technique to adaptively update overcurrent settings.</p>	Relays	Yes	Coordination with fuse and recloser is not considered

Table 7 Continued

#	Ref	Protection Approach/Method	Protective Element	Adaptive (Yes/No)	Shortfalls
15	[37]	<p>A communication-assisted overcurrent protection scheme for RDS with DG: Use communication to implement directional overcurrent scheme in the RDS. Two-stage TDS are used for each relay setting, where the second stage provides backup in case of a failed neighboring protective device.</p>	Relays	No	No recloser coordination solution
16	[38]	<p>Novel protection scheme of single-phase earth fault for RDS with DG: Apply agent-based relay protection scheme to detect a fault based on zero-sequence voltage element. This element is very sensitive to earth faults. Also, the method implements FCM clustering and space relative distance algorithms to discriminate and locate faults and consequently make tripping decisions.</p>	Relays	Yes	Very complicated method without consideration of recloser or fuse coordination
17	[39]	<p>Recloser-fuse coordination protection for DG systems: Methodology and priorities for optimal disconnections: Once DG is interconnected to RDS, impact on coordination is verified. If coordination is affected, a GTO thyristor integrated with a controller is used to disconnect the DG during a fault. DGs that don't cause miscoordination are not included in the disconnection method.</p>	DG controller	No	Power-electronics-dependent, which can affect power quality

Table 7 Continued

#	Ref	Protection Approach/Method	Protective Element	Adaptive (Yes/No)	Shortfalls
18	[40]	Self-adaptive protection strategies for distribution system with DGs and FCLs based on data mining and neural network: Overcurrent protection strategies employing FCLs and relays with communication ability to determine operating states. Uses an operation setting decision tree and topology-adaptive neural network model based on the data processed by fast Fourier transform (FFT).	Relays FCL	Yes	<ul style="list-style-type: none"> ▪ Lack of coordination validation with other protective devices: fuses and reclosers ▪ FCL is power electronics, which may affect power quality
19	[41]	Reducing the impact of DG in distribution network protection using FCLs: Use FCLs to reduce fault current contribution from DGs and consequently restore overcurrent protection coordination.	FCL	No	Power-electronics-dependent, which can affect power quality
20	[42]	An approach to mitigate the impact of DG on the overcurrent protection scheme for radial feeders: Mitigate fuse fatigue and nuisance blowing by replacing fuses with multifunction reclosers for laterals with DGs and adding relays to DG connection point.	*Microprocessor-based recloser *Relays	No	Fuse fatigue is not fully mitigated
21	[43]	An adaptive distance protection scheme for distribution system with DG: Adaptive setting for zone 2 distance protection is presented as zone 1 is not affected by the DG interconnection.	Relays	Yes	Does not work with synchronous-based DGs
22	[44]	A new adaptive current protection scheme of distribution networks with DG: Adaptive directional overcurrent scheme. Settings of the directional element are changed based on a mathematical	Relays	Yes	Does not consider multiple DGs or various DG locations

Table 7 Continued

#	Ref	Protection Approach/Method	Protective Element	Adaptive (Yes/No)	Shortfalls
		algorithm. Also, the scheme proposes the use of a hybrid islanding detection method.			
23	[45]	A protection and reconfiguration scheme for distribution networks with DG: Divide the network into zones based on the balance between DG capacity and average load. ANN is used to determine fault location based on lookup tables from offline calculations. The faulty zone is isolated by a signal from the centralized controller.	Relays	Yes	Intensive communication dependency
24	[46]	A new adaptive voltage protection scheme for distribution network with DG: Relays along with directional element are placed at both ends of the line where the DG is interconnected. An adaptive voltage protection scheme is applied on those relays. An adaptive voltage mathematical model and algorithm are presented.	Relays	Yes	Coordination with fuse and recloser is not considered
25	[47]	Adaptive protection system for distribution networks with DER: Implement directional overcurrent scheme with adaptive settings based on system state and DG output. Information is exchanged between IEDs and EMS via the communication network in real time. EMS runs the algorithm for available short circuit and updates settings accordingly.	Relays	Yes	<ul style="list-style-type: none"> ▪ High dependency on communication ▪ Does not consider coordination with other protective devices: fuses and recloser

Table 7 Continued

#	Ref	Protection Approach/Method	Protective Element	Adaptive (Yes/No)	Shortfalls
26	[3]	<p>An adaptive protection scheme for distribution systems with DGs based on optimized Thevenin-equivalent parameters estimation: Uses adaptive directional overcurrent that is updated based on locally available measurements. The algorithm is based on optimized Thevenin equivalent as an estimation. Available short-circuit current is calculated, considering contribution from DGs during fault and relay settings are updated accordingly.</p>	Relays	Yes	Does not consider coordination with other protective devices: fuses and recloser
27	[48]	<p>The study on fault directional relay in protection system for distribution system under high DG penetration level: Protection scheme based on longitudinal comparison principle. Relays on the distribution system communicate directional element output with the master controller at the substation to identify faulty section and send trip signals to associated breakers. The distribution system is assumed to be divided by breakers controlled by relays.</p>	Relays	No	<ul style="list-style-type: none"> ▪ Extensive use of communication ▪ Temporary faults are not considered
28	[49]	<p>A fast current protection scheme for distribution network with DG: Traditional overcurrent is modified by adding communication, directional element, and sync-check capability. The communication with directional element overcomes the problem of false tripping due to reverse fault and blinding for forward fault. Sync-check allows auto-recloser operation, avoiding synchronization issues when connecting two live systems.</p>	Relays	No	Coordination with fuses is not considered, especially for auto-reclosing

3 PROBLEM FORMULATION FOR AUTO-RECLOSING SCHEME IN RDS WITH DER

3.1 DER Interconnection in RDS Protection Challenges

Distributed generation (DG), or distributed energy resources (DER), are energy sources that supply power to a distribution system at the connection point. In a conventional power system, power is supplied from generation facilities only. Generation facilities are electrically located on the other side of the transmission network across from the distribution system. Power can only flow to an RDS from one source, which is the connection point to the transmission network. DGs are interconnected in the distribution system where the load is. With this interconnection, the assumption of power unidirectionality is not valid any more. Also, any disconnections on the network might create two live systems with separate controls. Distribution systems are not designed considering these facts. Therefore, protection challenges arise as DG is connected to an RDS. Following are major protection issues considered in this work.

3.1.1 Protection Blinding

DG interconnection in an RDS introduces a current source at the load side. This fact changes how a fault current is sourced. On a traditional RDS, the entire fault current is supplied from the main power source (i.e., substation, grid). However, with the presence of DG, the fault current is sourced from all available power sources (i.e., substation and all connected DGs, as shown in Figure 9). Therefore, the amount of fault current from the main power source is reduced due to the contribution from DGs. Consequently, protection devices on the main feeder line sense a smaller amount of current compared to a traditional RDS. The smaller current might be below the pickup setting of the protection device. In this case, the protection device does not react to isolate the faulty section, even though a fault exists [26].

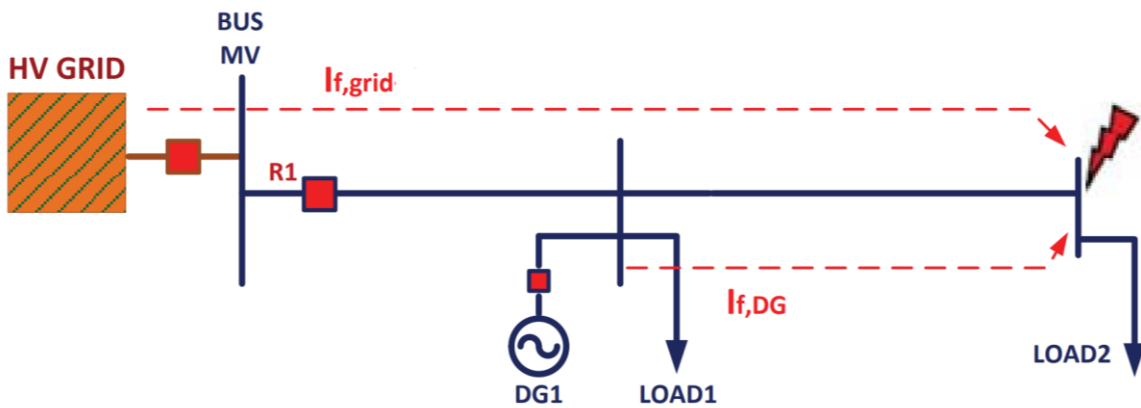


Figure 9 Protection Blinding Due to DG Interconnection

A simple solution might seem to be to lower the pickup value of a protection element to be able to correctly detect a fault. However, the pickup value should be above the current required for the cold start of loads, which is usually estimated at twice the full load, so protection element settings should consider both boundaries to ensure protection acts correctly. With the presence of DG, the margin might be very tight for such a setting.

3.1.2 Miscoordination

One important objective of a protection system is to maintain selectivity at its best. This translates into isolating the smallest possible part of the electrical system where the fault occurs. The system is divided into parts by switching equipment (i.e., circuit breakers, auto-reclosers), so protection devices across the electrical system have to be coordinated with each other for operation during a fault. A fault in a line, for example, should be acted upon by the nearest protection devices to achieve fault isolation. Coordination in an RDS is achieved by introducing a time delay in protection device operation. For a particular system, coordination for all protection devices should be ensured for entire fault current range: from I_{fmin} to I_{fmax} . With the presence of DGs, the

maximum fault current, I_{fmax} , increases, potentially resulting in miscoordination of various protection devices [19].

Reclosers, being overcurrent protection devices, are affected by DG interconnection in an RDS. Frequently, reclosers are miscoordinated with fuses, as shown in Figure 10. In addition to increasing maximum fault current, I_{fmax} , DG interconnection might cause different fault currents to flow into the recloser and fuse. This is affected by the location of DGs and fault with respect to the recloser and fuse.

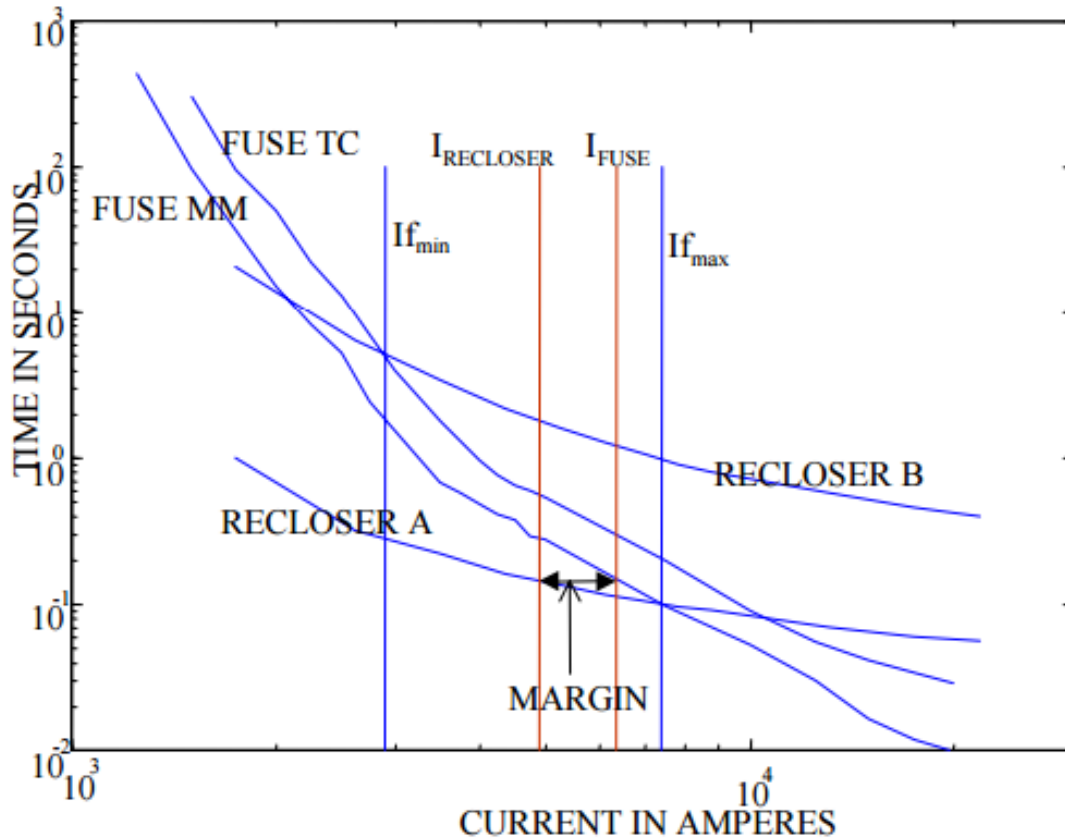


Figure 10 Recloser-Fuse Miscoordination with DG Interconnection, reprinted from [31]

3.1.3 Sympathetic Tripping

DG interconnection in an RDS increases the chance of sympathetic tripping [26]. This is a sort of protection system malfunction where the relay operates for a fault outside its zone or a fault on an adjacent feeder. For example, a distribution system with two radial feeders where a fault occurs in one feeder could lead to a trip on the healthy adjacent feeder, as shown in Figure 11. The added DG power source in the second feeder might contribute to a fault in the first feeder. The feeder breaker might sympathetically trip, disconnecting a healthy system. In a particular system with DG interconnection, the risk of sympathetic tripping varies depending on the size of the distribution system, DG penetration level, fault current, and implemented protection schemes [19].

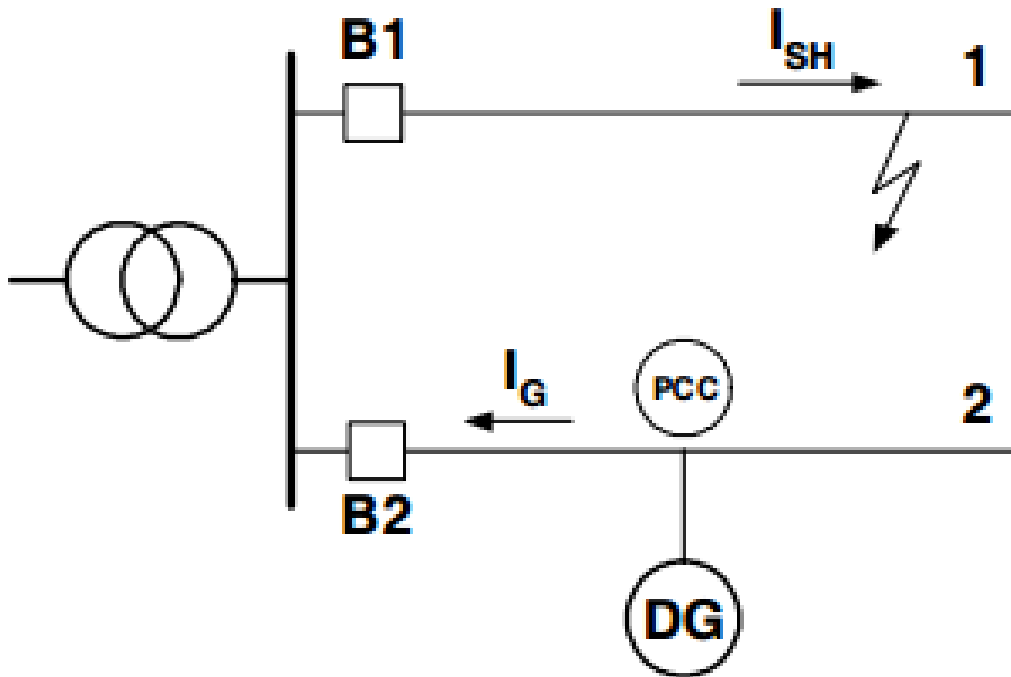


Figure 11 Sympathetic Tripping due to DG, adapted from [26]

3.1.4 Synchronization

As said earlier, DG interconnection in a distribution system creates a new source of power. Once this power source is separated from the grid (main power supply), the DG and its own supplied loads form an island, with the DG acting as the main regulator of frequency and voltage on that island. In power systems, the connection of two live systems requires both systems to be synchronized. This means that voltage, frequency, and angle of both systems have to have a minimal difference. In general, voltage difference can be up to 5%, angle difference in the range of 10 to 20°, and the slip frequency cutoff range from 0.1 to 0.15 Hz [4]. Closing while systems are not synchronized properly may cause severe fluctuation, which is a power quality concern. Moreover, generators (especially DGs) might be at greater risk of improperly synchronized reclosing. Generators can be damaged due to transient torque caused by such reclosing [4].

3.2 Problem Formulation

The main protection scheme in a distribution system is overcurrent protection. Distribution systems mostly consist of overhead line circuits where 80 to 90% of faults are transient. A reclosing scheme is commonly used to address transient faults. The introduction of DG in a distribution system affects reclosing in terms of coordination and synchronization. Both issues are studied in an RDS with interconnected DGs, where a proposed protection scheme for reclosing is explicated. The proposed scheme aims to ensure that reclosing is coordinated with downstream fuses and upstream substation relay. Also, the reclosing scheme aims to avoid any synchronization risks to the system. After a transient fault, no recloser operations to restore power should close on a live system.

The studied reclosing scheme is particular to an RDS divided into zones. The zones are separated by breakers with directional overcurrent protection. In such a system, zonal breakers

isolate the faulty zone while keeping other zones energized and powered by connected DGs. If the fault is temporary, reclosing is required to overcome such phenomena and increase the reliability of power supply. Once the faulty zone is identified by the directional overcurrent scheme and associated breakers are tripped, the reclosing scheme identifies the appropriate breaker to reclose and performs the right sequence of operations.

4 SOLUTION METHODOLOGY

The approach under investigation in this work is specific to a radial topology distribution system. It is an expansion of previous work [14, 25, 50]. The objective of the approach is to add capabilities to the existing protection scheme to tackle temporary faults in an RDS with interconnected DGs. In the previous work, the protection approach is based on dividing the RDS into zones and implementing an adaptive auto-reclosing scheme. Zones are identified based on the location of DG interconnection, DG capacity, and average consumer load. Zones are separated by breakers with an auto-reclosing function and directional overcurrent protection. The proposed expansion to the protection approach is the coordination of auto-reclosing with fuses using an adaptive approach implemented through microprocessor-based control. The following sections are the components of the proposed approach investigated in this work.

The previous work [14, 25, 50] considered only permanent faults in RDS with interconnected DG. The approach divided the RDS to zones separated by breakers as explained in 4.1. To identify the fault, communication-assisted directional overcurrent is used as explained in 4.2. Both [14, 25] used a centralized controller to compare to a lookup table and make a decision identifying the faulty zone. In [50], the centralized controller is eliminated as it represents single point of failure increasing the risk during a cyber-attack. Consequently, [50] suggests the fault current direction to be shared between neighboring protective devices via simple communication. The protective device trips if the current directions match specific conditions. However, none of these works considered the reclosing function or temporary faults. The work here suggests adding the reclosing functionality to the zonal communication-assisted directional overcurrent approach suggested in [50]. In sections 4.3 and 4.4, the approach to add reclosing functionality is explained in detail. In section 4.5, the recloser-fuse coordination is presented.

The approach under investigation aims to enhance the reliability of the power supply. The approach considers restoring power to customers in the case of temporary fault. However, the restoration of the system to a normal state is out of the scope of this approach.

4.1 Zoning

The RDS is divided into zones separated by circuit breakers (CBs). The approach of defining a zone is driven by the intention to supply all loads from the available DG power in the case of an islanded operation [50], [25], [14]. Ultimately, the objective is to enhance system reliability by keeping loads powered as much as possible. Zones are determined based on the balance between DG capacity and total average load. The following steps describe how a zone is formed in the RDS [25]:

- 1- The zone starts at the bus where DG is connected.
- 2- The zone extends downward through the feeder until total average load equals DG capacity.
- 3- While extending the feeder downstream, if the end of the feeder is reached and load-generation balance is not reached yet, the zone is extended upward (from the DG bus) until load matches DG capacity.
- 4- If another DG (or DGs) is found while extending the zone, the capacities of all DGs are added together. Zone extension continues until a balance of average load and generation capacity is reached [25], [14]. This condition can be mathematically described by the following equation:

$$\sum_i P_{DG_i} = \sum_j P_{L_i, Average}$$

where (i) = the total number of DGs in the zone and (j) is the total number of loads in the same zone. In other words, if all zonal breakers are open, the DG capacity should be sufficient to supply the load. Usually, the capacity of generation is kept slightly higher than the average

load to account for load fluctuation. The above equation represents the minimum condition that should be satisfied to form a zone. Figure 12 shows an example of zoning for the RDS with DG interconnection. The figure shows a single line diagram of a typical RDS where two DGs are connected at laterals. The application of the above-mentioned steps yields four zones for this particular system. Three circuit breakers separate the zones from each other. In this example, zone 3 does not have any DG power supply. Based on the level of DG penetration and location on the RDS, there could be conditions where a zone does not have a DG connection [14, 25, 50].

This happens when two DG zones are formed apart from each other, leaving a middle zone without any DG power supply. In the case of a fault in the upstream zone (closer to the substation), the middle zone is left without power. The described situation is not different from a conventional RDS situation. The main advantage of the zoning configuration is eliminating the requirement to disconnect all DGs for any fault in the RDS. This requirement is mandated as per IEEE 1547 concerning DG interconnection to prevent the contribution from DGs during a fault[1].

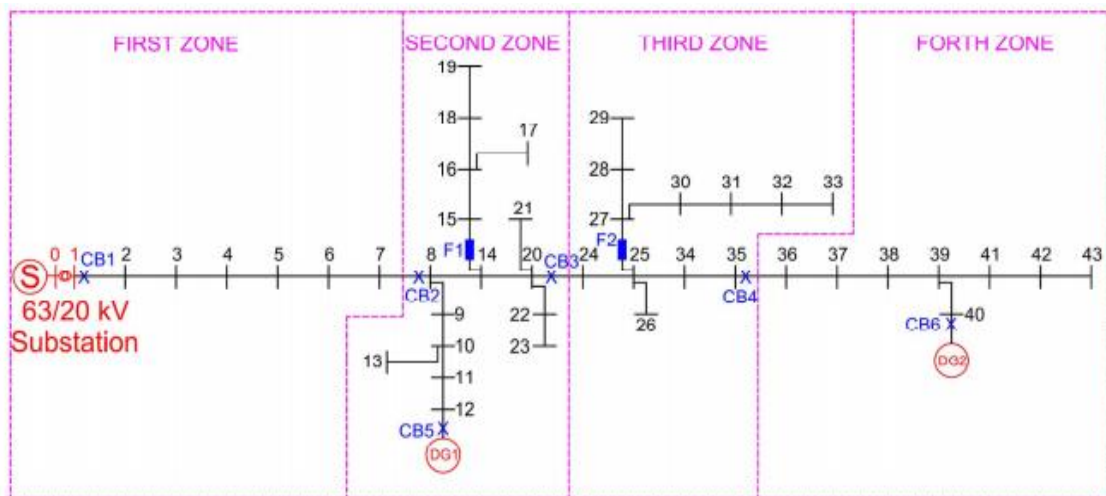


Figure 12 Illustration of Zoning Scheme for RDS with DG Interconnection, reprinted from [25]

4.2 Communication-Assisted Directional Overcurrent

A directional element is important to be able to identify the faulty zone. Bidirectional current flow caused by the interconnection of DGs in an RDS mandates the use of directional element to indicate fault current flow. Figure 13 shows the direction of fault current at each zonal boundary breaker when a fault occurs at a certain location along the RDS. The figure represents the RDS main line with zonal breakers and DG interconnections. Loads are neglected in this figure as they don't significantly contribute to faults. To the left of the diagram is the grid power source represented by substation supply. The black arrow represents the fault location at the RDS main line while the red arrows represent the fault current flow during the fault condition. Since the system is now divided into zones, once the faulty zone is identified, associated zonal breakers are tripped isolating the zone from the rest of the system. Other zones are kept energized either by the main grid or their own DG, if equipped. The directional element determines the fault current direction at each protection device. Although the power flow is bidirectional, the fault current is significantly higher in magnitude, making its direction dominant. If zonal boundary protection devices share fault current direction that point inward (inside the zone), the zone is identified as faulty and all boundary breakers should trip to isolate the fault [50], [14]. Additionally, breakers of all DGs connected to the faulty zone are tripped via communication signal from zonal protective devices. DGs should be disconnected from the faulty zone to prevent feeding the fault. In addition to trip signals, the protection scheme utilizes communication to share directional elements among relevant relays. The next section describes the logic to be implemented in zonal CBs and provides more detail on the concept of the zonal auto-reclosing algorithm. The last zone along the RDS topology is slightly different because it only has one zonal breaker, which doesn't require reception of directional element from other breakers.

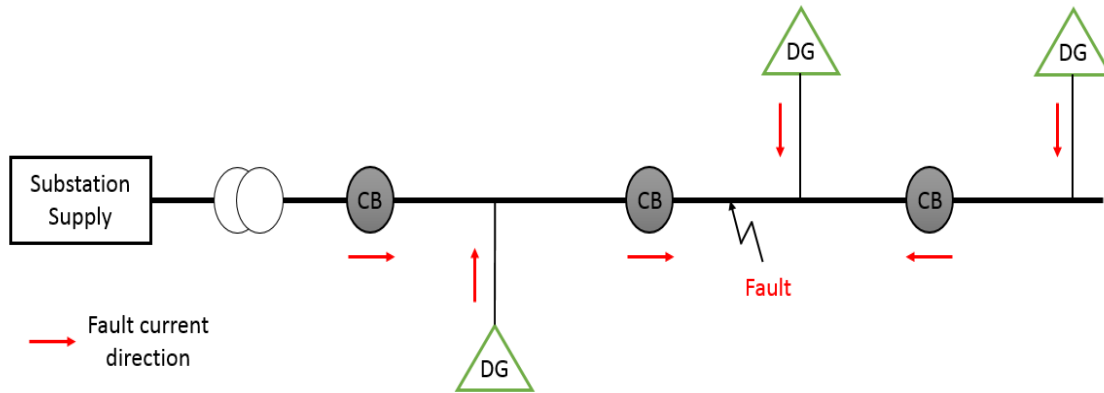


Figure 13 Fault Current Direction

4.3 Zonal Reclosing

Once the faulty zone is isolated, the zone boundary breaker closer to the main power source (grid substation) auto-recloses [14]. The other boundary breakers are blocked from auto-reclosing to avoid synchronization issues. Attempting to reclose at the mentioned boundary breakers might connect downstream live zone to the grid powered zone without proper synchronization. Auto-reclosing permits/blocks are identified using zonal breaker logic. DG breakers in the fault zone are tripped to avoid feeding the fault. The breaker to perform reclosing follows an auto-reclosing sequence of a fast-slow tripping operation before permanently tripping in the case of a permanent fault. The concept is illustrated in Figure 14 with an example system consisting of a typical RDS with 3 interconnected DG and 4 zones. The contribution to fault current from load branches are neglected as they are not significant. If a fault occurs in zone 2 as indicated in the figure, all zonal breakers associated with the faulty zone (zone 2 in this case) trip to isolate the zone from the rest of the system. DG1 protection trips as well to prevent contribution to the fault. In this case, ZB2 is the only breaker permitted to perform auto-reclosing as it is the breaker closest to the main substation or the grid power supply. All other zonal breakers associated with the faulty zone (ZB3

and ZB4 in this case) are blocked from auto-reclosing. By doing so, the requirements to have proper synchronization when connecting two live systems are avoided. In other words, zone 3 or zone 4 are not connected back to the substation power supply by any auto-reclosing attempts.

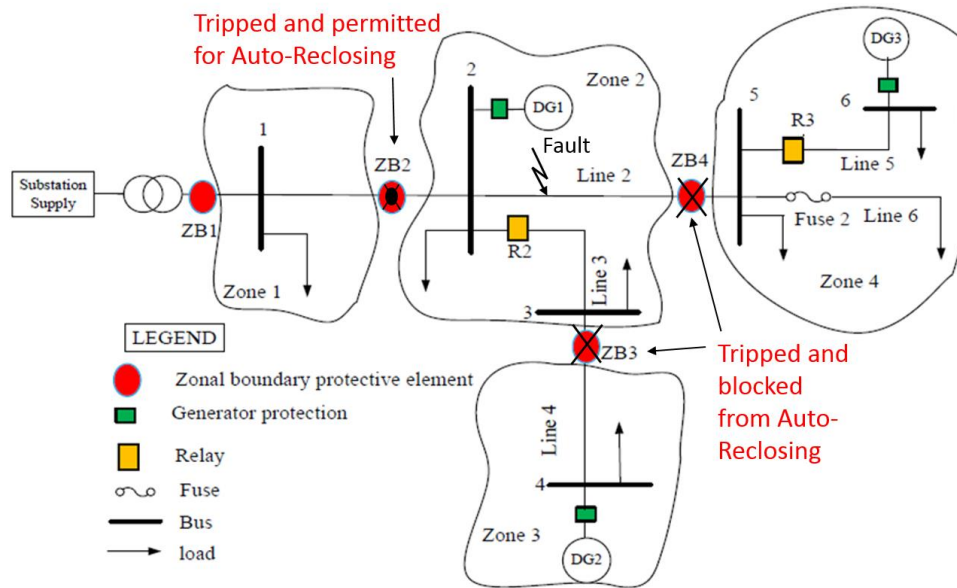


Figure 14 Zonal Auto-Reclosing on the RDS, adapted from [50]

A fuse-saving scheme is usually desired when implementing reclosing. The scheme provides enhanced reliability of power supply. For a temporary fault within a fuse reach, the fuse-saving scheme restores power to loads after the fault is extinguished. The recloser is set to act on a fast curve, preventing the fuse from blowing for a temporary fault within its reach. This requires coordination between the recloser and fuses. To ensure this scheme is functioning properly, all zonal breakers of a faulty zone trip on instantaneous overcurrent except for the breaker responsible for auto-reclosing. Implementing this, coordination between recloser and fuse is made relatively straightforward.

4.4 Zonal Breaker Logic

To make use of protection elements (overcurrent and directional) available at each zonal protective relay, a logic is proposed. The logic was developed during the course of this research. It uses protection information from the zonal relay and from adjacent relays. The logic decide if any particular breaker shall trip using instantaneous overcurrent or trip using inverse-time overcurrent, as well as if the breaker is permitted to perform auto-reclosing or blocked. This logic is intended for implementation at each microprocessor-based relay that controls a zonal breaker. The logic is not concerned with recloser-fuse coordination which is discussed in detail in the next section.

To better understand this logic, we assume two adjacent zones at an arbitrary location along the RDS: Zone- and Zone+. DGs are connected along the RDS where current may flow in both directions. Figure 15 shows these zones and the relative location of zonal breakers. The logic is explained assuming implementation in breaker CB, which is shared between both zones. Zone- is the zone closer to the main substation, and Zone+ is the zone farther from the main substation.

In Case B, a fault occurs in “Zone+” and fault current flows into the zone. Breakers “CB” and “CB+” identify themselves (by sharing current direction) as zonal breakers of the faulty zone and trip. Breaker “CB” identifies itself as upstream of the fault and allows auto-reclosing.

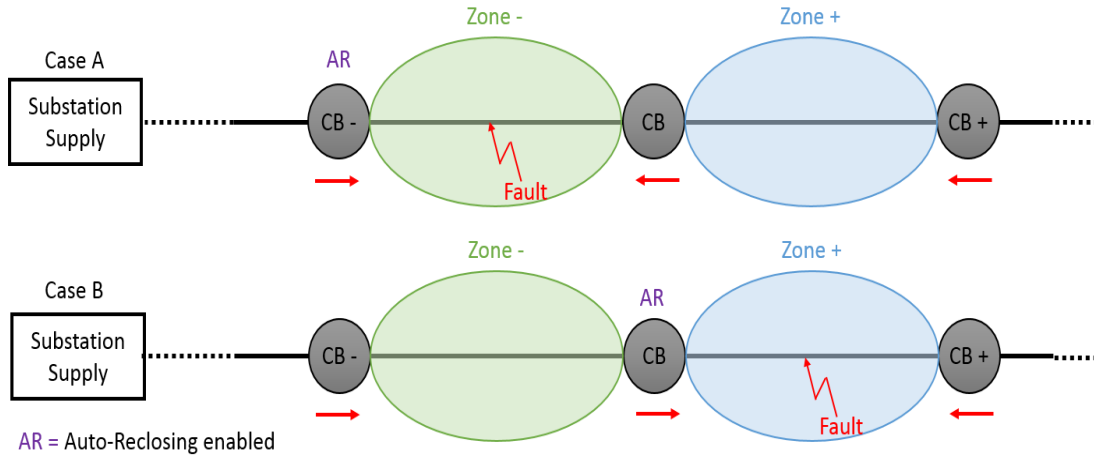


Figure 15 CB Logic Concept

This logic is relative to the breaker, so it is implemented in each breaker and will see breaker/s upstream as “CB–” and breaker/s downstream as “CB+”. Each zonal breaker in the system needs overcurrent and direction from adjacent breakers for the logic to work. However, each logic works independently from other breaker logic. There are other possible current directions, identified in Table 8, where no action is required. Table 8 lists all possible combinations of current directions seen by the relays controlling breakers “CB”, “CB+” and “CB–”. In this table, forward current direction is assumed to have a value of “1” and reverse current direction to have a value of “0”. For any current direction combination, an outcome of trip signal or auto-reclosing permit/block is assigned. Only two combinations shall have an output to react to a fault. Otherwise, the breaker shall have not reacted to a fault. These cases are designated with “False” for trip and “N/A” for auto-reclosing.

This logic is developed into inputs, outputs, and logical gates to be configured inside the relay. In the table, fault current direction from all adjacent relays is considered. Only two combinations of fault direction should initiate a trip. “True–” indicates a trip on instantaneous

settings with a block of auto-reclosing. On the other hand, “True+” indicates a trip on inverse-time overcurrent with permission for auto-reclosing.

Table 8 Zonal Breaker Logic

Current Direction	Forward	1	Reverse	0
CB–	CB	CB+	Trip	Auto-Reclosing
0	0	0	False	N/A
0	0	1	False	N/A
0	1	0	False	N/A
0	1	1	False	N/A
1	0	0	True–	Block AR (Instantaneous Trip)
1	0	1	False	N/A
1	1	0	True+	Permit AR (Inverse-Time Overcurrent Trip)
1	1	1	False	N/A

Considering RDS topology, zones at the beginning and the end of the RDS have slightly different logic. The first zone after the substation breaker does not consider an upstream zone as “Zone+”. The last zone at the end of the RDS does not consider a downstream zone as Zone–.

4.5 Adaptive Reclosing

Once the faulty zone is identified, and corresponding breakers are identified for the right action, the coordination with fuses within the zone is to be considered. The zonal downstream breakers trip on instantaneous overcurrent settings while the DG breakers in the faulty zone trip on an inter-trip signal from zonal breakers. This leaves the zonal upstream breaker (assigned for reclosing) to coordinate with fuses in the zone. The fuses in the zone are downstream from the

reclosing zonal breaker as DGs in the zone are disconnected. If the zone doesn't have any fuse, coordination considerations are not required.

The objective of this proposed approach is to restore coordination between auto-reclosers and fuses. With the presence of DGs in the RDS, the maximum fault current increases, which could result in lost coordination. Protective devices are coordinated for a range of fault currents that is calculated from the electrical system parameters. Establishing coordination between such devices is only important for the range of available fault current. Once DGs are interconnected, the range of available fault current changes, usually increases. Recloser and fuse curves might not coordinate as the maximum fault current increases. Also, the recloser and fuse might see different fault currents based on the relative location of the fault, as well as the relative location of each component (recloser, fuse, and DG) in the RDS. To reestablish coordination, the ratio of recloser current (I_R) to fuse current (I_F) is calculated on a per-phase basis. Figure 16 demonstrates both current flows on a simple RDS, with the relative location of each component shown. The setup shown in the figure is the most possible severe miscoordination due to difference in fault currents seen by protective devices for a recloser-fuse setup with interconnected DG [26]. The severity comes from the large difference between fault current seen by the recloser compared to the fault current seen by the fuse. In this setup, the DG will supply the its maximum available fault current causing the recloser to see very little fault current, probably even below pickup value. The relative locations of the recloser, DG, fuse, and fault represent the scenario where fault current variation is maximized.

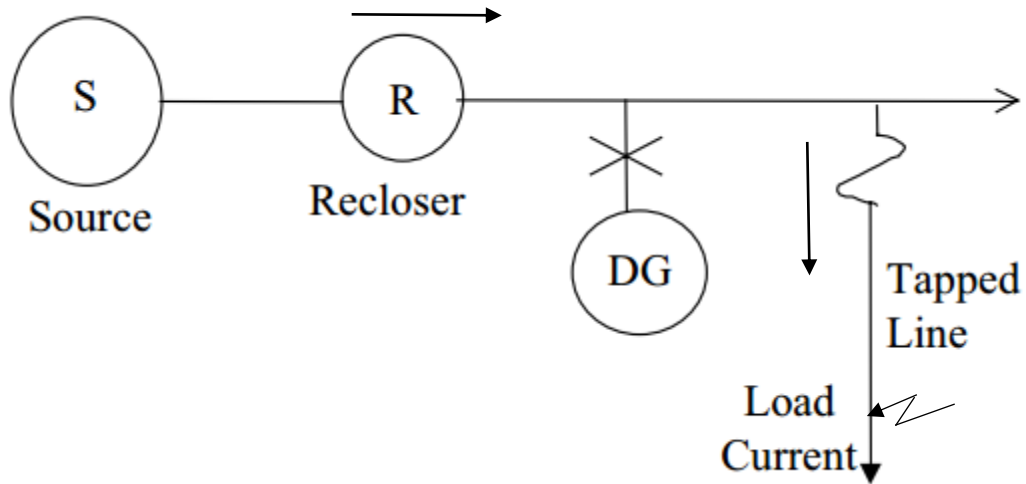


Figure 16 Simple RDS Illustrating Recloser-Fuse Currents, reprinted from [26]

The adaptive approach to restore coordination mainly concerns the fast curve. A recloser operates on two curves, fast and slow. The fast curve trips faster than the fuse to save the fuse from tripping for a temporary fault. However, the slow curve allows time for the fuse to react for a fault in case the fault is permanent. When miscoordination occurs due to DG interconnection, the coordination with fast curve is what is usually affected due to the smaller margin between recloser fast curve and fuse curve. Figure 17 shows the TCC of a typical recloser and fuse coordination. The maximum fault current increases as DGs are added to the RDS. As shown in the figure, for the fault current range (Margin I), the three curves (recloser fast, fuse, and recloser slow) coordinate well. For the fault current range with DG (Margin II), the fuse acts faster than the recloser fast curve which is a miscoordination.

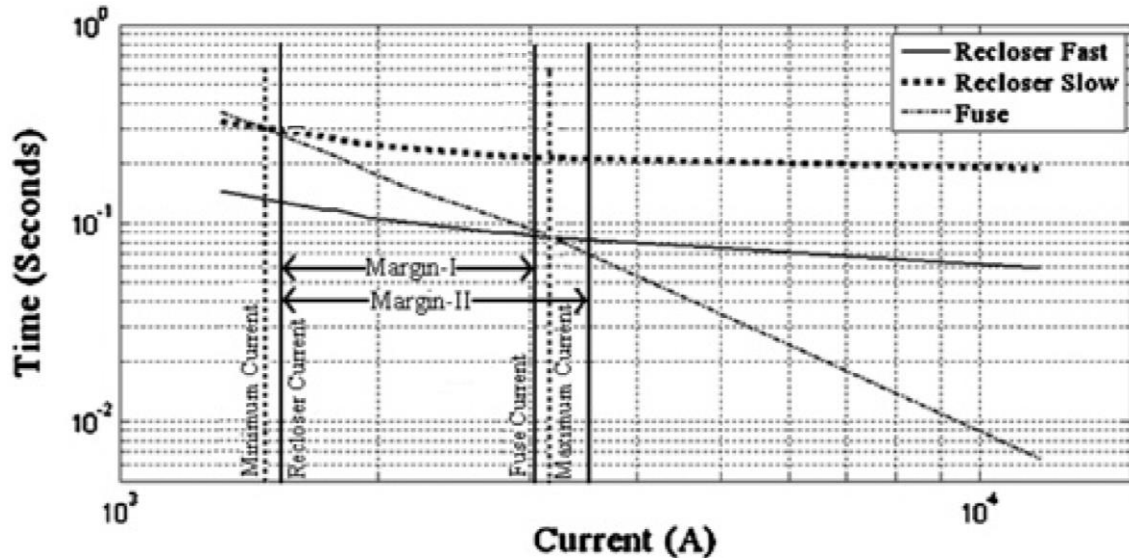


Figure 17 Recloser-Fuse Coordination Curves, reprinted from [26]

To restore coordination, it is suggested to use the ratio of recloser current to fuse current during a fault [26]. The ratio is used as a correction factor to the recloser TDS. The miscoordination is caused by the difference in current seen by each protective device. Therefore, the fault current ratio of a recloser and a fuse is a suitable correction factor that should restore coordination. The ratio I_R/I_F is calculated inside the relay based on the peak value of each current for each phase. If the ratio is lower than unity, the recloser fast curve must be revised by multiplying the time dial by the found ratio: I_R/I_F . In other words, if the fault current seen by the fuse is higher than fault current seen by the recloser, the recloser TDS must be adjusted. This situation occurs due to the DG contribution as described previously and shown in figure 16. The ratio is used to reduce the TDS of the recloser fast curve which shifts the curve down, allowing a trip before the fuse is blown. If the ratio is unity or higher, then the recloser current is higher which will not cause miscoordination and will not require adjustment to recloser TDS.

Considering RDS with interconnected DG where zonal protection is implemented, the zonal breaker assigned to perform auto-reclosing shall coordinate with fuses within the faulty zone. When the other zonal breakers (downstream) of the faulty zone trip on instantaneous overcurrent settings, the upstream zonal breaker (assigned for reclosing) trips on reclosing fast curve. The algorithm to adaptively adjust the TDS of the reclosing fast curve is implemented at this zonal breaker for the reclosing fast trip. The fuses within the faulty zone are the fuses considered in this algorithm for the associated reclosing breaker.

Figure 18 shows a flow chart of the approach for an adaptive recloser. Current at the fuse must be monitored and made available at the zonal breaker (recloser) relay [26]. The algorithm is implemented in the micro-processor based relay that controls the zonal breaker. To start with, both recloser and fuse curves are considered in the algorithm. The value of the currents seen by the recloser and fuse are obtained in the first cycle after the fault. The ratio of the recloser to fuse currents I_R/I_F during a fault is calculated. If the ratio is less than unity, then TDS of the recloser fast curve must be adjusted using the equation depicted in figure 18. Otherwise, the I_R/I_F is higher than unity, so there is not any requirement to adjust the TDS of the recloser fast curve.

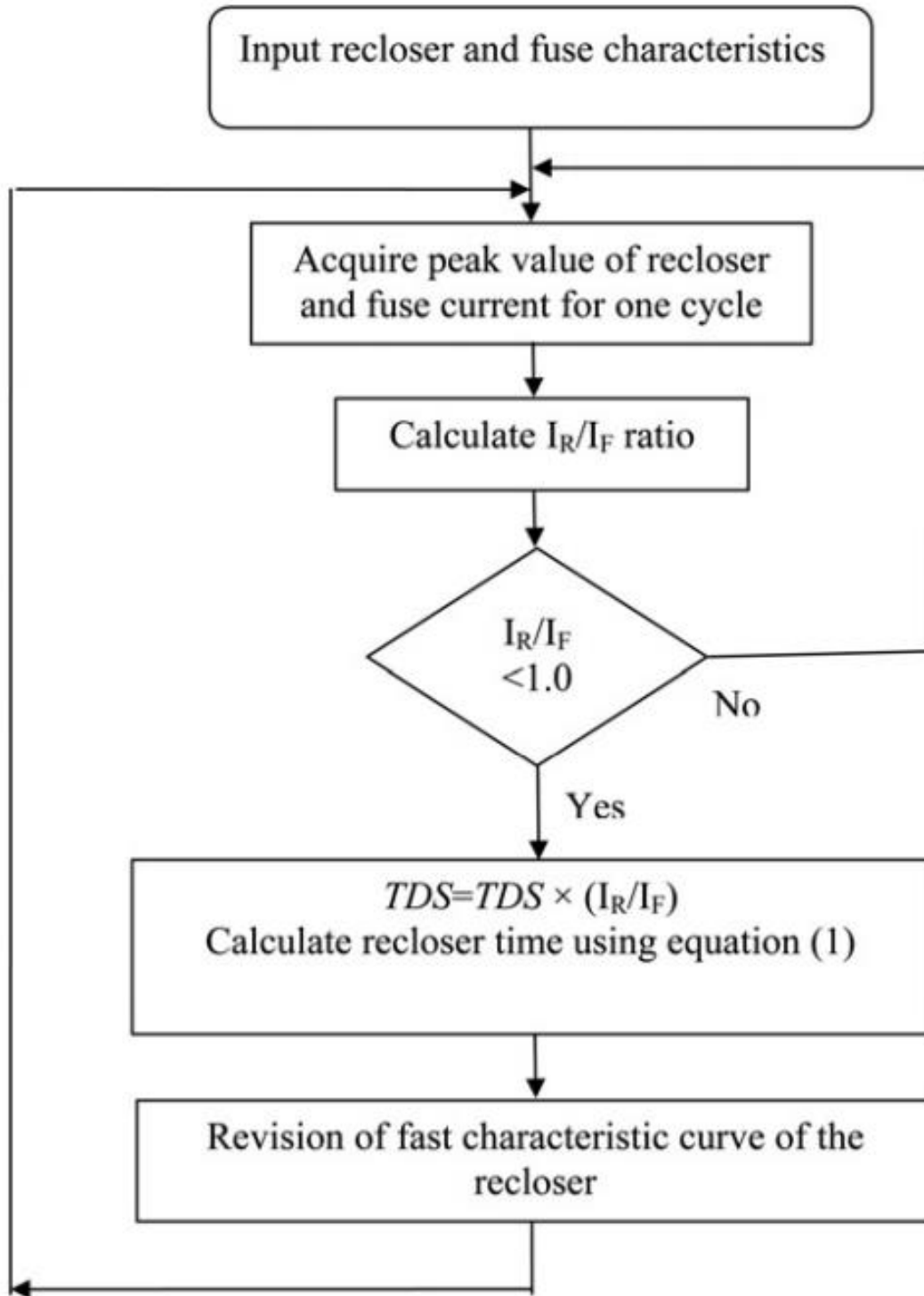


Figure 18 Adaptive Recloser Algorithm for Restoring Fuse Coordination, , reprinted from [26]

5 CASE STUDIES AND FINDINGS

The behavior of the proposed approach introduced in the previous chapter is investigated using several case studies. The approach is implemented in PSCAD/EMTDC simulation software and applied to a test system. This section outlines the details of simulation steps and the implementation of the case studies. Subsequently, the results of the simulation studies are presented and analyzed.

5.1 Test System

The test system is simulated in PSCAD/EMTDC software to investigate the behavior of the suggested auto-reclosing approach. The test system is based on the IEEE 34 Node Test Feeder standard distribution system [51]. Initially, two identical IEEE 34 Node Test Feeders were connected to a distribution substation. The distribution substation is connected to the grid to supply power to both feeders via two power transformers. Figure 19 shows an overall diagram of the test system. The initial simulation was run until steady state to obtain power flow values and verify the correctness of the model compared to IEEE power flow results [51].

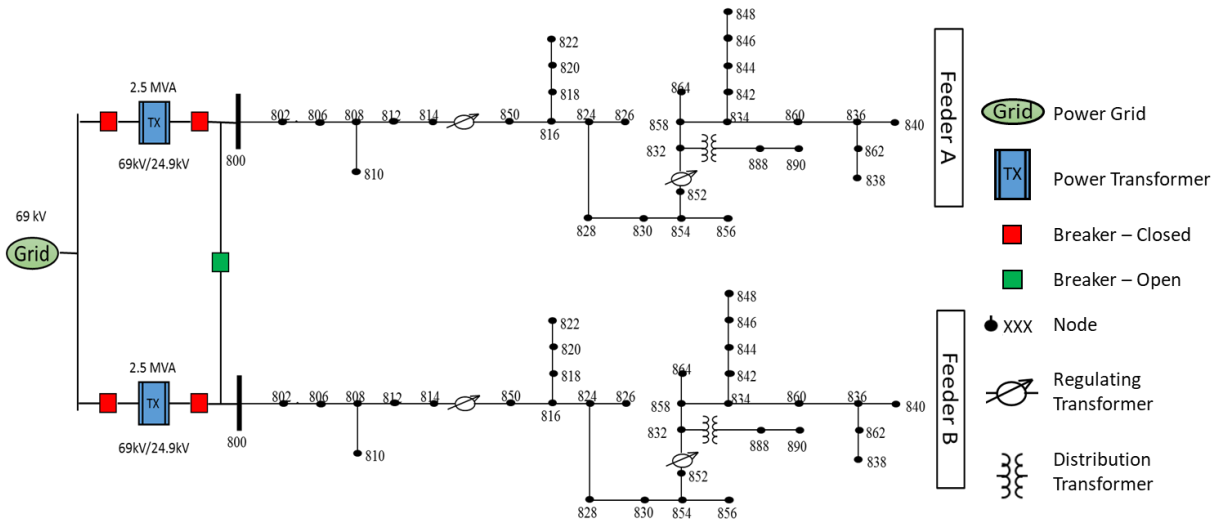


Figure 19 Test System Overall Diagram, adapted from [51]

At this stage of the study, both feeders, Feeder A and Feeder B, were identical. Both feeders were IEEE 34 Node Test standard feeders. The substation has two buses at the secondary side that are connected with a normally open bus tie breaker. Each of the feeders is connected to one of the secondary side buses. The two distribution power transformers are 2.5 MVA each with 69 kV voltage and delta connection at primary, 24.9 kV voltage and grounded wye connection at secondary. Both transformers are connected at the high side to the grid by a power circuit breaker. Also, each transformer is connected at secondary side to a feeder bus by a power circuit breaker. The transformers are based on the substation transformers identified by the IEEE 34 Node Test Feeder original system [51]. Additionally, as in the original IEEE 34 Node Test Feeder, a transformer exists between node 832 and node 888. Table 9 shows transformer data for substation transformers as well as for the distribution transformer at node 832.

Table 9 IEEE 34 Node Test Feeder Transformer Data, reprinted from [51]

Transformer	KVA	kV-High	kV-Low	R - %	X - %
Substation	2500	69 – D	24.9 – Gr. W	1	8
XFM – 1	500	24.9 – Gr. W	4.16 – Gr. W	1.9	4.08

Additionally, two voltage regulating transformers exist between nodes 814 – 850 and 852 – 832. Regulating transformer data is depicted in table 10. Voltage drop is expected to be significant in this feeder due to the length of the line. The voltage regulating transformers are used to adjust the voltage of the line to be within acceptable limits.

Table 10 Regulating Transformers Data, reprinted from [51]

Regulator Data			
Regulator ID:	1		
Line Segment:	814 - 850		
Location:	814		
Phases:	A - B -C		
Connection:	3-Ph,LG		
Monitoring Phase:	A-B-C		
Bandwidth:	2.0 volts		
PT Ratio:	120		
Primary CT Rating:	100		
Compensator Settings:	Ph-A	Ph-B	Ph-C
R - Setting:	2.7	2.7	2.7
X - Setting:	1.6	1.6	1.6
Voltage Level:	122	122	122
Regulator ID:	2		
Line Segment:	852 - 832		
Location:	852		
Phases:	A - B -C		
Connection:	3-Ph, L-G		
Monitoring Phase:	A-B-C		
Bandwidth:	2.0 volts		
PT Ratio:	120		
Primary CT Rating:	100		
Compensator Settings:	Ph-A	Ph-B	Ph-C
R - Setting:	2.5	2.5	2.5
X - Setting:	1.5	1.5	1.5
Voltage Level:	124	124	124

The standard IEEE 34 Node Test Feeder is an actual distribution feeder located in the state of Arizona [51]. It is characterized by long lines with in-line transformer (XFM-1) at one of the laterals as shown in Figure 20. The feeder is lightly loaded, however loading is unbalanced. The loads in this feeder are in various forms: spot, distributed, and shunt capacitors. Some laterals are single phase laterals with more than one node and several loads. The distributed loads are modeled

as uniformly distributed loads [7]. In this model, 2/3 of the load are placed at 1/4 of the line, and 1/3 of the load at the end of the line. The impedance of the line is divided to correspond to the line length and location of the load. Additionally, the feeder has two single-phase in-line voltage regulating transformers. The distribution lines are relatively long which introduce voltage drops at the end of the line. The regulating transformers adjust the voltage to keep it close to nominal value.

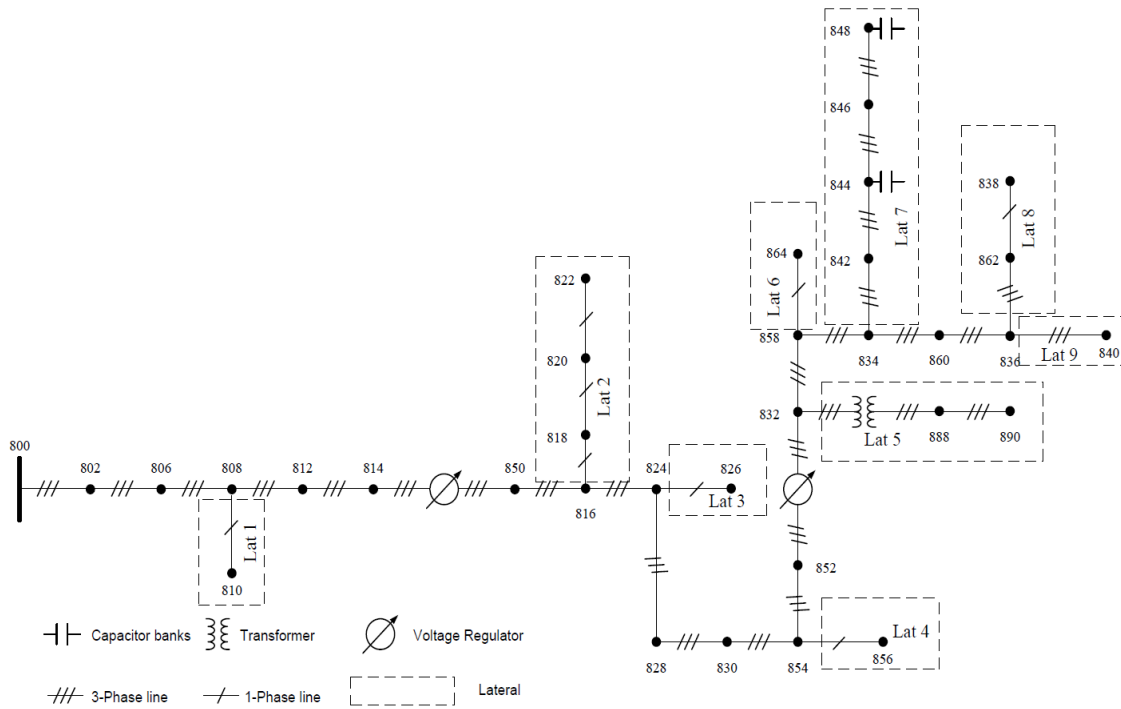


Figure 20 IEEE 34 Node Test Feeder Standard Distribution Feeder, reprinted from [50]

The correctness of the test system model simulated in PSCAD software was verified by running the simulation until study state and obtaining power flow values. The values of the power flow simulation are depicted in Table 11. Since both feeders in the test system were identical at this stage, the power flow values for both feeders were identical to each other as expected. The power flow values for each feeder were compared with results from IEEE 34 Node Test Feeder [51]. The maximum discrepancy from the IEEE power flow values was 4%. The load flow power

values were also used to estimate the loading of each zone as determined in the next stage. Each zone load is used to determine DG's capacity sizing. The power output of each DG is set to be slightly higher than its corresponding zone load.

Table 11 Test System Load Flow Output

Node	Phase	A	B	C	
	Quantity				Units
800	I	53.96	46.03	41.88	A
	V	1.02	1.03	1.04	PU
	P	771.06	675.30	623.38	kW
	Q	178.54	93.70	32.51	kVar
802	I	53.97	46.03	41.88	A
	V	1.02	1.03	1.04	PU
	P	769.22	674.27	622.47	kW
	Q	178.04	93.38	32.54	kVar
806	I	53.98	43.88	40.16	A
	V	1.02	1.03	1.03	PU
	P	767.99	643.54	596.81	kW
	Q	177.70	78.21	18.59	kVar
808	I	54.14	43.88	40.20	A
	V	0.98	1.01	1.02	PU
	P	744.86	632.16	586.34	kW
	Q	170.74	75.10	19.67	kVar
810	I	–	0.42	–	A
	V	–	1.01	–	PU
	P	–	5.39	–	kW
	Q	–	2.69	–	kVar
812	I	54.33	42.71	40.25	A
	V	0.94	0.99	0.99	PU
	P	717.92	603.67	573.88	kW
	Q	161.57	64.84	20.59	kVar
814	I	54.47	42.70	40.28	A
	V	0.91	0.97	0.97	PU
	P	696.42	593.99	563.92	kW
	Q	153.70	62.07	21.04	kVar
816	I	49.52	40.67	38.37	A
	V	1.00	1.02	1.02	PU

Table 11 Continued

Node	Phase	A	B	C	
	Quantity				Units
	P	696.13	593.83	563.76	kW
	Q	153.65	62.05	21.05	kVar
818	I	13.19	–	–	A
	V	1.00	–	–	PU
	P	172.55	–	–	kW
	Q	78.65	–	–	kVar
820	I	10.80	–	–	A
	V	0.98	–	–	PU
	P	135.58	–	–	kW
	Q	67.93	–	–	kVar
822	I	3.63	–	–	A
	V	0.97	–	–	PU
	P	45.09	–	–	kW
	Q	23.32	–	–	kVar
824	I	36.77	40.46	38.24	A
	V	0.99	1.01	1.01	PU
	P	518.82	585.09	557.32	kW
	Q	75.94	62.00	18.27	kVar
826	I	–	3.10	–	A
	V	–	1.01	–	PU
	P	–	40.56	–	kW
	Q	–	19.69	–	kVar
828	I	36.77	37.55	37.96	A
	V	0.99	1.01	1.01	PU
	P	518.44	544.13	552.93	kW
	Q	75.99	42.30	16.25	kVar
830	I	36.32	37.54	37.98	A
	V	0.97	0.99	1.00	PU
	P	502.40	534.63	543.87	kW
	Q	74.10	42.08	15.77	kVar
832	I	21.52	23.59	24.50	A
	V	1.03	1.04	1.04	PU
	P	319.23	350.06	358.03	kW
	Q	-20.37	-46.26	-75.14	kVar
834	I	20.49	22.56	23.39	A
	V	1.03	1.04	1.03	PU

Table 11 Continued

Node	Phase	A	B	C	
	Quantity				Units
	P	301.76	332.26	337.60	kW
	Q	-28.83	-49.98	-82.89	kVar
836	I	1.50	4.41	1.75	A
	V	1.03	1.04	1.03	PU
	P	21.21	58.90	17.33	kW
	Q	6.21	29.01	19.30	kVar
838	I	–	0.70	–	A
	V	–	1.04	–	PU
	P	–	9.36	–	kW
	Q	–	4.66	–	kVar
840	I	0.79	0.79	0.80	A
	V	1.03	1.04	1.03	PU
	P	9.28	9.35	9.34	kW
	Q	7.19	7.24	7.23	kVar
842	I	14.84	16.50	15.25	
	V	1.03	1.04	1.03	
	P	173.80	215.44	186.22	
	Q	-134.03	-118.18	-129.19	
844	I	14.56	16.48	15.24	
	V	1.03	1.04	1.03	
	P	164.71	215.28	186.14	
	Q	-138.71	-117.90	-128.94	
846	I	9.77	9.49	9.82	
	V	1.03	1.04	1.03	
	P	20.79	44.11	20.74	
	Q	-143.00	-134.26	-144.38	
848	I	9.76	9.85	9.81	
	V	1.03	1.04	1.03	
	P	20.78	21.02	20.73	
	Q	-142.87	-145.12	-144.27	
850	I	49.52	40.67	38.37	
	V	1.00	1.02	1.02	
	P	696.40	593.98	563.91	
	Q	153.70	62.07	21.04	
852	I	35.24	36.53	36.71	
	V	0.94	0.96	0.97	

Table 11 Continued

Node	Phase	A	B	C	
	Quantity				Units
	P	471.74	504.20	509.70	
	Q	64.88	38.85	11.68	
854	I	35.12	36.82	36.68	
	V	0.97	0.99	1.00	
	P	486.74	524.51	524.96	
	Q	62.78	37.29	12.41	
856	I	–	0.31	–	
	V	–	0.99	–	
	P	–	4.03	–	
	Q	–	-1.84	–	
858	I	20.93	23.32	24.18	
	V	1.03	1.04	1.04	
	P	309.56	344.77	352.26	
	Q	-22.98	-49.18	-75.45	
860	I	5.87	7.66	5.30	
	V	1.03	1.04	1.03	
	P	75.15	96.71	68.05	
	Q	43.44	60.48	39.58	
862	I	0.00	2.08	0.00	
	V	1.03	1.04	1.03	
	P	0.00	28.08	0.00	
	Q	0.00	13.07	0.00	
864	I	0.14	–	–	
	V	1.03	–	–	
	P	2.01	–	–	
	Q	0.71	–	–	
888	I	70.02	70.07	69.72	
	V	1.00	1.00	1.00	
	P	893.21	902.92	888.35	
	Q	458.35	457.28	468.00	
890	I	70.04	70.08	69.74	
	V	0.91	0.93	0.92	
	P	822.69	842.71	820.45	
	Q	412.20	408.45	418.47	

Modifications were implemented on the system. Various size DG were added to each feeder at different connection points. Each feeder in the test system was divided into 4 zones as shown in Figure 21. The zones were separated by circuit breakers. Directional overcurrent and reclosing schemes were implemented on those breakers. For each zone, one DG is connected to one of the nodes within the zone. DGs were connected to nodes that have all three phases. None of the DGs in this test system was connected to single-phase laterals. Each DG has a different capacity that is relevant to the zone loads. The load of each zone was found from the power flow values obtained earlier. The DGs were sized to be slightly larger than the total load of the zone. Table 12 shows the capacity of each DG along with the connection node at the feeder. DG capacities were determined after running load flow and calculating the total load of each zone.

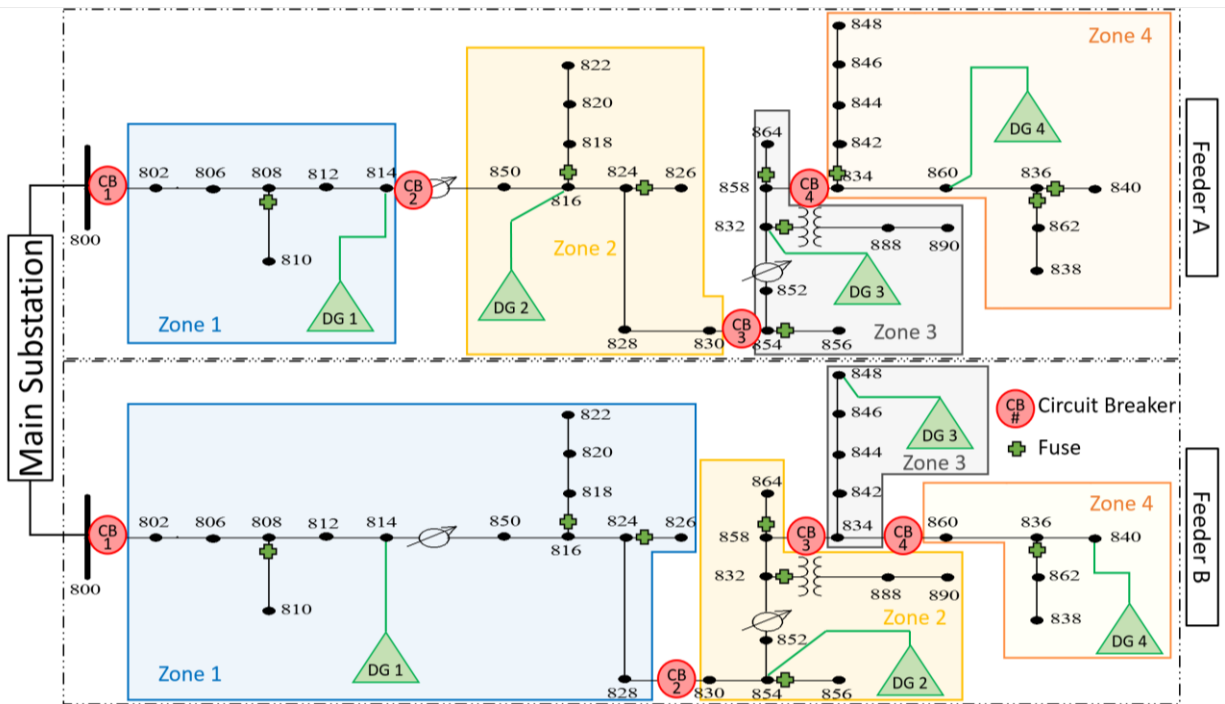


Figure 21 Test System Divided into Zones with DGs.

Table 12 DGs Capacity with Connection Node

Feeder A			Feeder B		
DG/Zone	Connection Node	Capacity (kVA)	DG/Zone	Connection Node	Capacity (kVA)
1	814	250	1	814	500
2	816	300	2	854	700
3	832	700	3	848	900
4	860	1100	4	840	300

Fuses are added to laterals in both feeders. The exception to that are laterals where DG is connected. Fuses are very simple overcurrent protection devices and cannot be controlled to suit DG interconnections. Fuses were selected based on the work of [21] that suggested an overcurrent protection scheme for IEEE 34 Node Test Feeder including fuses. Some laterals are 3-phase and consequently have three single-phase fuses. The three fuses in each phase are designed in this simulation to act simultaneously to avoid single phase trips. On the other hand, other laterals are single phase and have only one fuse. Table 13 shows fuse information at each lateral where fuses are installed. Currents (considering the system with interconnected DGs) at each phase for the operating point of this study are depicted in this table as well. The operating point was considered after running the simulation until study state which turns out to be at 3.0 seconds. This was considered as the point where the study is conducted.

Fuse selection is verified to be suitable for the short circuit current level at each lateral. The short circuit current level bases for the fuse selection [21] matches the ones in the test system. Faults were simulated at each lateral to find the maximum and minimum short circuit current. Table 14 shows the values for available short-circuit currents at all laterals where fuses are installed. For maximum short-circuit current, fault resistance of 0.01Ω was used. For minimum short circuit current, fault resistance of 20Ω was used. Two fault types were applied for three-

phase laterals: a line-to-ground fault which is the most common type and three-phase-to ground which is the most severe fault. This was studied with all DGs connected to the system. In [52], short circuit available current for the standard IEEE 34 Node Test Feeder was provided for all nodes. Obviously, the short circuit level increased after DG interconnection.

Table 13 Laterals' Fuses

Feeder	PHASE Node	Currents			Fuse Size	Manufacturer
		A	B	C		
A	810	-	1.22	-	X4	KEARNEY
	818	13.18	-	-	T15	KEARNEY
	826	-	3.10	-	X4	KEARNEY
	856	-	0.31	-	X4	KEARNEY
	888	11.75	11.76	11.71	Tin-T10	Cooper/McGraw
	864	0.14	-	-	X4	KEARNEY
	842	14.84	16.50	15.25	Tin-K20	Cooper/McGraw
	840	1.50	2.33	1.75	X4	KEARNEY
	838	-	2.08	-	X4	KEARNEY
B	810	-	1.22	-	X4	KEARNEY
	818	13.18	-	-	T15	KEARNEY
	826	-	3.10	-	X4	KEARNEY
	856	-	0.31	-	X4	KEARNEY
	888	11.75	11.76	11.71	Tin-T10	Cooper/McGraw
	864	0.14	-	-	X4	KEARNEY
	838	-	2.08	-	X4	KEARNEY

Table 14 Available Short Circuit Currents at Nodes Where Fuses were installed

1 Phase Laterals		3 Phase Laterals	
Node	SC Current (A)	Node	SC Current (A)
808	L-G	832	L-G
Ph-B Max	590	Ph-A Max	302
Ph-B Min	390	Ph-A Min	239
810	L-G		A-B-C-G
Ph-B Max	530	Ph-A Max	313

Table 14 Continued

1 Phase Laterals		3 Phase Laterals	
Node	SC Current (A)	Node	SC Current (A)
Ph-B Min	360	Ph-A Min	237
816	L-G	Ph-B Max	330
Ph-A Max	410	Ph-B Min	250
Ph-A Min	300	Ph-C Max	318
822	L-G	Ph-C Min	241
Ph-A Max	210	834	L-G
Ph-A Min	170	Ph-A Max	291
824	L-G	Ph-A Min	230
Ph-B Max	400		A-B-C-G
Ph-B Min	300	Ph-A Max	293
826	L-G	Ph-A Min	220
Ph-B Max	385	Ph-B Max	307
Ph-B Min	285	Ph-B Min	231
854	L-G	Ph-C Max	295
Ph-B Max	365	Ph-C Min	224
Ph-B Min	270	848	L-G
856	L-G	Ph-A Max	276
Ph-B Max	275	Ph-A Min	218
Ph-B Min	215		A-B-C-G
858	L-G	Ph-A Max	276
Ph-A Max	300	Ph-A Min	218
Ph-A Min	230	Ph-B Max	290
864	L-G	Ph-B Min	230
Ph-A Max	293	Ph-C Max	279
Ph-A Min	230	Ph-C Min	221
862	L-G	836	L-G
Ph-B Max	288	Ph-A Max	281
Ph-B Min	230	Ph-A Min	222
838	L-G		A-B-C-G
Ph-B Max	280	Ph-A Max	283
Ph-B Min	220	Ph-A Min	220
		Ph-B Max	297
		Ph-B Min	232

Table 14 Continued

1 Phase Laterals		3 Phase Laterals	
Node	SC Current (A)	Node	SC Current (A)
		Ph-C Max	285
		Ph-C Min	223
		840	L-G
		Ph-A Max	279
		Ph-A Min	221
			A-B-C-G
		Ph-A Max	283
		Ph-A Min	217
		Ph-B Max	297
		Ph-B Min	228
		Ph-C Max	285
		Ph-C Min	220

Fuses are coordinated with recloser curves for the fault current range calculated at the respective node. Fuses within a respective zone have to coordinate with the recloser of the zonal breaker closer to the substation. As per suggested approach, the said breaker is the only zonal breaker that is permitted to do reclosing operation for a fault within the specified zone. ETAP software Star™ tool [53] was used to perform the coordination. The Coordination Time Interval (CTI) assumed in the process was 0.2 seconds. Unfortunately, the Star tool does not allow TDS below 0.5 which limits using this tool to coordinate recloser slow curve with fuse curves. Coordination curves using the Star tool are provided in Appendix A. The fast curve TDS was estimated to be 0.2 for all reclosers in this study.

The overcurrent settings of the zonal breakers were calculated based on the current values from load flow results. The current values at nodes where breakers were installed were assumed to be the maximum load current. The pickup (PU) setting for the overcurrent protection was

calculated based on that assumption. The pickup is determined by multiplying the maximum load current by a factor of 1.2 then dividing by the CT ratio. Time Dial Settings (TDS) were determined considering coordination with fuses in the corresponding zone. The coordination was performed using ETAP Star tool as explained previously. Table 15 shows the settings for overcurrent protection in the test system for all zonal breakers. Since most fuses in the test system are installed in single-phase laterals, the coordination between fuses and zonal breakers overcurrent yield different TDS across phases. Some phases don't have load laterals with fuses within a single zone which result in a very low TDS for the zonal breaker overcurrent.

Table 15 Overcurrent Protection Settings

Feeder	Node	Load Flow Current			Breaker	PU			TDS		
		A	B	C		A	B	C	A	B	C
A	800	53.96	46.03	41.88	A1	3.24	2.76	2.51	0.50	3.08	0.50
	814	54.47	42.70	40.28	A2	3.27	2.56	2.42	2.86	2.86	0.50
	830	36.32	37.54	37.98	A3	2.18	2.25	2.28	2.76	2.76	2.76
	858	20.93	23.32	24.18	A4	1.26	1.40	1.45	4.70	4.70	4.70
B	800	53.96	46.03	41.88	B1	3.24	2.76	2.51	2.82	2.82	0.50
	828	36.77	37.55	37.96	B2	2.21	2.25	2.28	2.67	2.67	2.67
	858	20.93	23.32	24.18	B3	1.26	1.40	1.45	0.50	0.50	0.50
	860	5.87	7.66	5.30	B4	0.35	0.46	0.32	0.50	11.98	0.50

5.2 PSCAD Model

The standard IEEE 34-Node Test Feeder PSCAD/EMTC simulation software model is based on the model provided by Tomas Yebra and Mayssam Amiri (University of Manitoba) [52]. It was used as a base to construct the PSCAD model and the consequently, the test system. The model was modified to provide power quantities at all nodes on the standard feeder. Two identical copies of the feeder were made to constitute Feeder A and Feeder B. As described in the previous

section, the distribution substation is connected to the grid. The parameters of Grid model in PSCAD are depicted in Table 16. The Grid was connected to one bus where both distribution substation transformers are connected via circuit breakers. Downstream both transformers, a connection was made to a bus for each transformer via a circuit breaker as well. For the purpose of this study, the breakers were set closed all the time without any protection or control elements. Each transformer supplies power to a feeder through one bus. The buses are connected via a bus tie circuit breaker. Following the specifications of substation transformer in the standard IEEE 34 Node Test Feeder, transformers capacity is 2500kVA, primary side voltage is 69kV, and the secondary side is 24.9kV. Full transformer information was provided in the previous section.

Table 16 Grid Parameters

Parameter	Values
Source Impedance type	Ideal (R=0)
Configuration	Grounded Star
Specified parameters	At the terminal
Voltage ramp up time	0.005 [s]
Frequency	60 [Hz]
Base Voltage (L-L,RMS)	69.0 [kV]
Base MVA	2.5 [MVA]
Terminal Voltage	1.05 [pu]
Phase angle	60 [deg]

Distribution line is modeled based on the configuration of each section and relevant line parameters. Length, Impedance, and Susceptance of each line section are used as specified by original standard test feeder line data. Loads on the feeder are either spot or distributed. For a distributed load, the load is split to 2/3 placed ¼ of the line length and 1/3 placed at the end of the line. This method accounts for line losses and voltage drop on the line. It is commonly used to model distributed loads in distribution systems.

After placing the zonal breakers as described early in this chapter, protection elements were added to the control breaker. PSCAD provides overcurrent functions device numbers 50 and 51, instantaneous and inverse-time delayed overcurrent. Current from each phase is used as input to the overcurrent element. Based on the settings, the element outputs a high signal indicating overcurrent condition. Current transformers (CTs) are considered in this implementation with ratio 100:5 for all relays. Additionally, voltage transformers (VTs) used have turns ratio of 125.

Detection of fault current direction is essential in the overcurrent scheme to determine the faulty zone. A voltage polarizing directional element was selected for this application. Negative sequence current (T32Q) was used for unbalanced faults and positive sequence current (T32P) for balanced fault [50]. PSCAD has a ready component for the T32Q element. The component takes negative sequence current and negative sequence voltage quantities to output the current direction. However, the T32P element was implanted using the difference between positive sequence current and positive sequence voltage and a range comparator to the line angle.

The directional setting particular to the test system is depicted in table 17. The table shows the settings for each zonal breaker which corresponds to the zone line. For T32Q settings, the reverse setting (Z2R) is always more than the forward setting (Z2F). In general, the forward setting is half the line positive-sequence impedance. The reverse setting is simply 0.1 Ω more than the forward setting. The line length at each zone is used in the calculation of this settings. Consequently, the element determines the fault to be forward if the measured negative-sequence impedance is below the forward setting (Z2F) and reverse if the measured negative-sequence impedance is higher than reverse setting (Z2R) [17]. The line angle and positive-sequence impedance range are used for the settings of the T32P settings.

Table 17 Directional Element Settings

Breaker	A1	A2	A3	A4	B1	B2	B3	B4
Length (mi)	19.65	6.02	8.00	2.16	25.68	8.00	1.10	1.05
Z2F (Ω)	1.96	0.60	0.80	0.21	2.56	0.80	0.11	0.10
Z2R (Ω)	2.06	0.70	0.90	0.31	2.66	0.90	0.21	0.20
Line Angle ($^\circ$)	73.21							
Z1 Range ($^\circ$)	-16.79 to 163.21							

The logic presented earlier in 4.4 is implemented at every breaker to determine the right response to a fault. The initial step is to continuously monitor and compare the current direction of the zonal breaker, adjacent zonal breakers, and the overcurrent condition. Following the logic, if the breaker is identified to be a zonal breaker of the faulty section, the breaker will trip either on instantaneous setting or fast curve recloser curve. When fault current is in reverse direction, the breaker will permanently trip on the instantaneous setting. When fault current is in the forward direction, the breaker will first compute IR/IF to adjust the TDS of the recloser fast curve and trip accordingly implementing the fuse saving scheme. Each breaker has current signals from fuses within the zone to allow for current ratio calculation. Also, the inter-trip signal is sent via communication to DG or DGs within the zone to trip permanently. The re-energization of the zone relies on the power available from the grid main substation. First reclose is attempted after 0.2 seconds. The recloser now switches to slow curve and trips accordingly if the fault persists. A second reclose attempt happens after 0.4 seconds. Again, if the fault persists, the breaker will trip on slow curve permanently. Figure 22 shows the sequence of operation of the breaker in the zonal scheme. Starting from the negative/positive sequence fault detection, the diagram describes the sequence of protection and breaker operation. Depending on the fault direction, the breaker will either trip on instantaneous or time delayed settings. If the fault is forward, the sequence progresses

to execute the auto-reclosing attempts. In case the fault is extinguished at any reclosing attempt, then the sequence will be suspended. In other words, the breaker will not trip again and no further action will occur. PSCAD software sequence components are used here to implement the breaker operation as described.

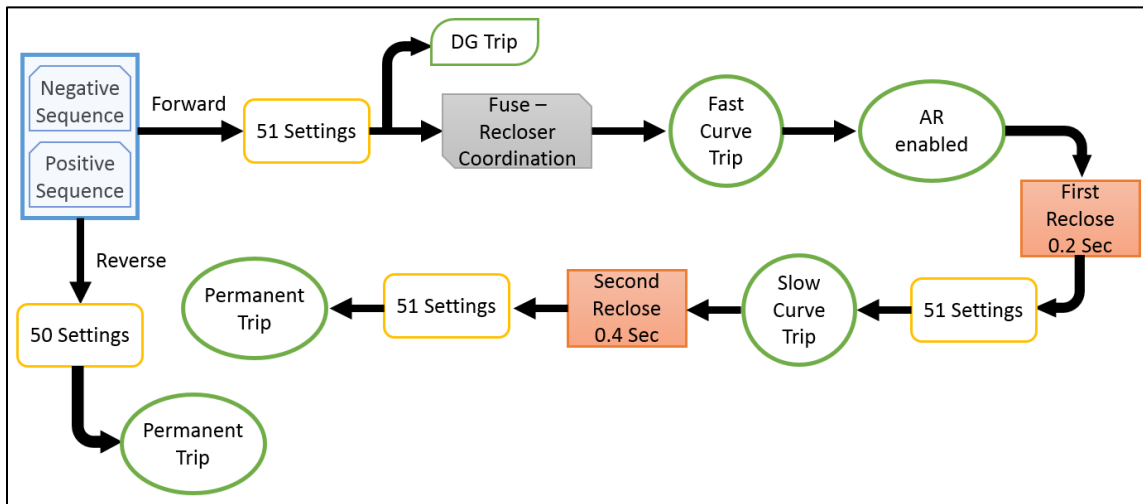


Figure 22 Sequence of Breaker Operation

DGs are modeled in this study as synchronous machines. As shown in figure 23, a standard PSCAD synchronous machine model was used with simple AC exciter, AC1A type. The output of the generator is rated at 480VL-L. A transformer was used to step up the voltage to 24.9kV which is the study system nominal voltage rating. Also, a breaker was added at the connection point responding to the inter-trip signal from zonal breakers. No further protection was used for the DGs.

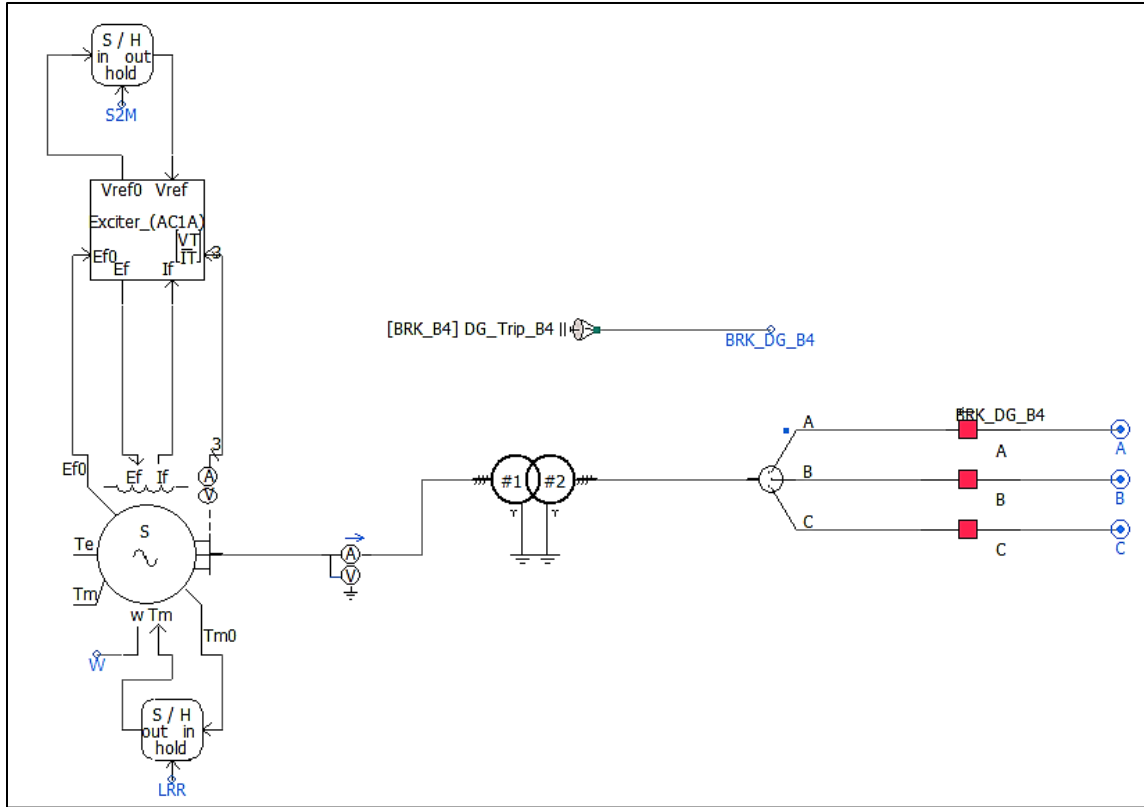


Figure 23 Synchronous Machine Model for DGs

5.2.1 Fuse Model

PSCAD/EMTDC does not provide a ready model for power fuse. Model from [54] was used to simulate fuse function in the test system. The model consists of 4 components. The first component is a multimeter connected in series with a circuit breaker. The multi-meter provides an instantaneous current reading of the current passing through the fuse. The breaker serves as the disconnection mean for the model representing when the fuse is disconnected.

The second component is time delay logic that takes instantaneous current from the multi-meter as an input to empirical tables. Based on the fuse instantaneous current, those tables calculate the times corresponding to Minimum Melting Time (MMT) and Total Clearing Time (TCT) which

are dictated by the fuse characteristic curves. For each fuse, the manufacturer provides such characteristic curves to describe the behavior of the fuse at different current values.

The third component is the fuse active logic. Fuse instantaneous current is compared with fuse continuous current capacity to activate fuse for instantaneous current values higher than fuse capacity only. This logic ensures fuse is not active below capacity value. These values are usually twice the fuse name designation number.

The fourth component is the fuse trip logic. Fuse active condition and fuse bypass switch (optional) are checked to allow two times to start. The times are dependent on the values obtained from time delay logic corresponding to fuse MMT and TCT. The trip signal is asserted if TCT timer is elapsed causing the breaker in the first component to open. Thus, the fuse is considered blown or tripped. The other counter is related to MMT time which is important to indicate the possibility of fuse damage. Usually, this condition occurs when fuse experiences high current, but it is cleared by another protective device, i.e. breaker or auto-recloser. Figure 24 shows a PSCAD diagram for the components of a single-phase fuse model. The same components are duplicated corresponding to each phase to simulate a three-phase fuse model. It is reported that this model is able to mimic the fuse characteristic and operation within 2.5% error from MMT and TCT time [54].

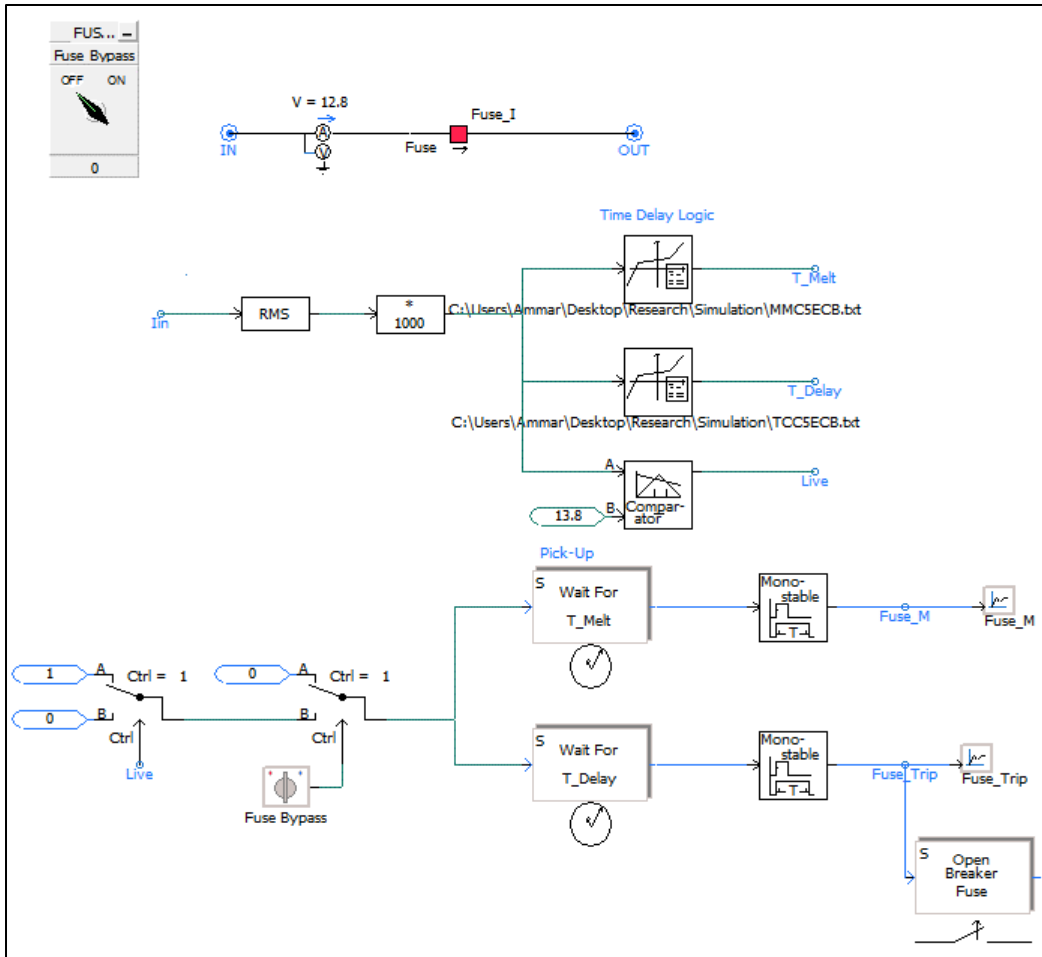


Figure 24 Fuse Custom Model in PSCAD

5.3 Case Studies

The study system with previously mentioned modifications and protection scheme was implemented in PSCAD simulation software. The objective of the simulation was to investigate the behavior of the adaptive reclosing scheme. The focus of the study is the validity of the logic to determine the right zonal breaker for the auto-reclosing sequence as well as the behavior of the adaptive reclosing algorithm. To start with, the test system with DG's interconnected was simulated until study state was reached at 3.0 seconds time. This point was decided to be the operating point for the simulation study. In other words, all faults at the case studies were applied

at that moment. The power supply values from each source (substation and DGs) at 3.0 seconds simulation time are depicted in table 18. Also, the voltage regulating transformers taps are shown in the table.

Table 18 Study System Simulation Operating Point

		P (kW)	Q (kVAR)	I (A)	VR-1 Tap			VR-2 Tap		
					A	B	C	A	B	C
Feeder A	S/S (A1)	837.20	322.30	20.81	11	8	8	13	13	11
	DG 1	181.66	37.33	4.30						
	DG 2	201.65	81.75	5.05						
	DG 3	409.84	241.48	11.03						
	DG 4	703.20	-82.30	16.42						
Feeder B	S/S (B1)	641.20	347.80	16.92	7	2	2	9	8	8
	DG 1	356.47	123.20	8.75						
	DG 2	431.63	94.35	10.25						
	DG 3	486.06	-255.30	12.73						
	DG 4	193.40	92.50	4.97						

Faults were applied in different setups to investigate the proposed approach at different fault scenarios. Fault duration, resistance, type, and location were changed one at a time for every simulation run. Fault duration was assumed to be 0.2 seconds for temporary fault. The value was chosen considering the reclosing timing. On the other hand, for permanent fault, the duration was assumed to be 3.0 seconds. The entire simulation time is 6.0 seconds. After 3.0 seconds, the system was found to be running in study state. At 3.0 seconds, the fault is applied for each simulation run. So, permanent fault duration is basically from the 3.0 second time mark until the end of the run. Fault resistance had two values, 0.01 Ω for low resistance fault or 20 Ω for high resistance fault. The fault resistance values were selected to match the available short-circuit currents study of IEEE 34 Node Test Feeder [52]. Also, all possible fault types were simulated at each node where

the fault is applied. If the fault is applied to single phase lateral, only a line-to-ground fault type is simulated. For main line and 3 phase laterals, line-to-ground, line-to-line, line-to-line-to-ground, three-line, and three-line-to-ground fault types were considered. As shown in figure 25, faults were applied at all laterals just downstream of the lateral fuse. These locations are the most critical to test the proposed approach as it involves fuses, and it represents the highest possible fault current at the lateral. Also, fault locations in the simulation run are considered the end of the lateral and main line in some zones.

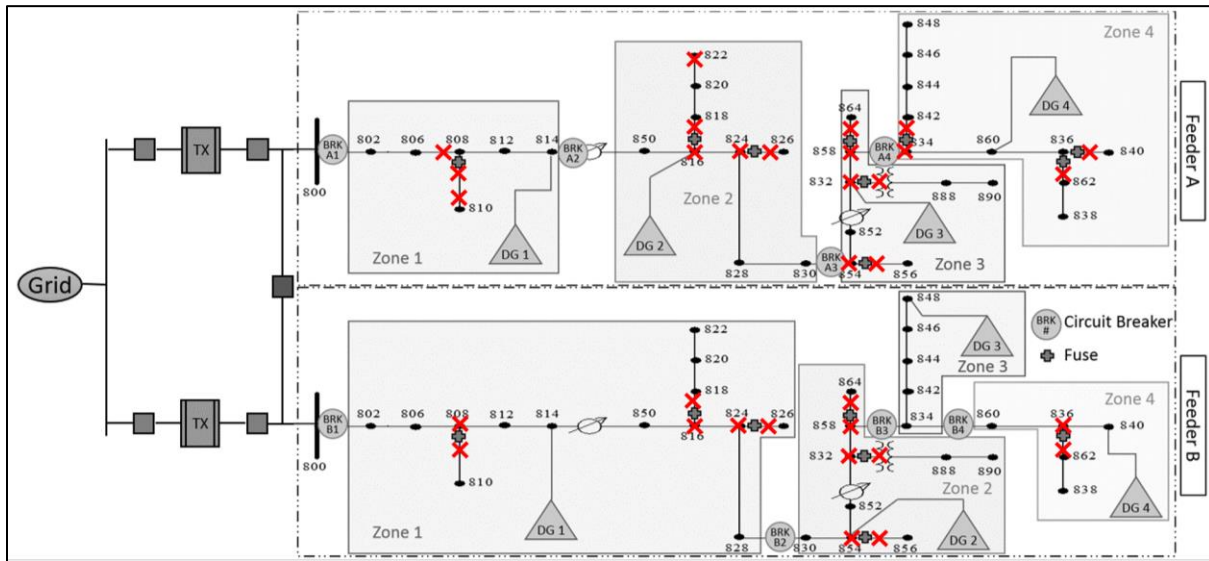


Figure 25 Fault Locations on Test System

In following sections, a few selected cases will be discussed explicitly to provide a detailed understanding of the simulation runs and the outcome analysis. Later in this section, information from all cases with simulation results are provided. The overall result of the simulation of the investigated approach is discussed as well.

5.3.1 Case 1: Feeder A Zone 1 lateral at 808-810

This is a single-phase lateral consisting of phase B. Consequently, the only phase-ground fault can be applied at this lateral. In this case, four fault scenarios were applied, varying fault duration (temporary or permanent) and fault resistance (low or high). For each scenario, a diagram of status for zonal breakers, DG breaker, and the fuse will be shown and explain. In the diagram, the high status reflects breaker open and a low status reflects breaker closed and the same applies to fuse status.

Starting with a temporary and low-impedance fault, scenario is shown in figure 26 status of zonal breakers A1 and A2, DG A1 breaker, and fuse at lateral 808-810. All devices were closed during normal operation study-state. At time 3.0 seconds, the fault was applied and lasted for 0.2 seconds ending at 3.2 seconds. The first device to react is breaker A2 which trips on instantaneous setting at 3.02 seconds (response time 0.02 seconds). Next, breaker A1 trips at 3.05 seconds on recloser fast curve (response time 0.05 seconds). At the same time, DG A1 breaker tripped on an inter-trip signal from breaker A1. The fuse did not react to the fault due to fast curve trip from recloser, A1 zonal breaker.

Now, the faulty zone is completely de-energized. Reclosing sequence at breaker A1 recloses at 3.24 seconds (0.2-second recloser cycle) re-energizing the zone. By that time, the fault is already extinguished since it is a temporary fault. Breaker A1 stays closed for the rest of the simulation. The fuse was saved from blowing for a temporary fault reflecting successful fuse-saving scheme.

The TDS adjustment for the recloser was 0.92 due to the recloser-fuse fault current ratio (I_R/I_F). Breakers A2 and DG A1 stay open as expected. Loads are re-energized back improving the reliability of power supply. However, the system is not back to normal operation as DG A1 and

breaker A2 need to be closed manually by a system operator after synchronization conditions are met. The scheme responded as expected where the logic to identify the breaker to reclose was successful and fuse saving was successful.

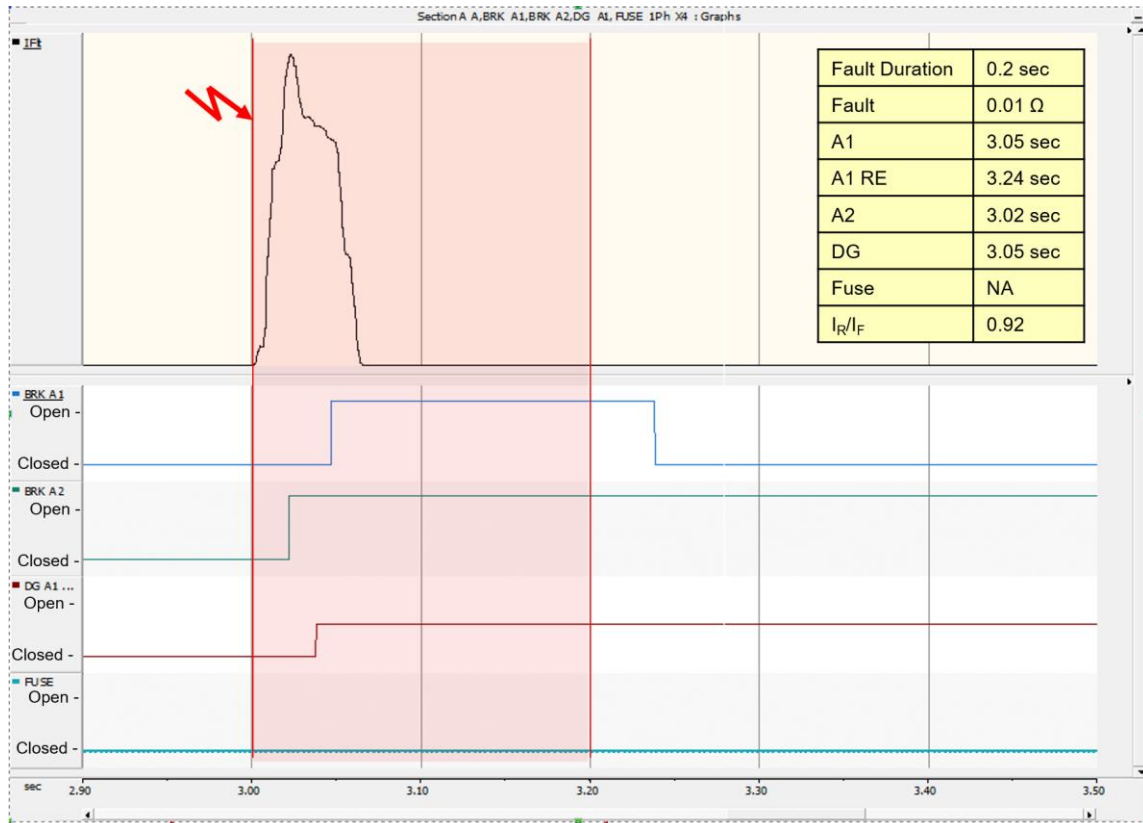


Figure 26 Time Diagram for Case 1 Scenario 1

The second scenario is temporary high impedance fault. As the fault resistance increases for a particular node, the fault current decreases. As shown in figure 27, in this scenario there was not any change from the first scenario in breakers response and timing. Even though this is a high resistance fault, the fault current was still relatively high. The recloser to fuse current ratio (I_R/I_F) is the same since fault current has reduced for both devices proportionally. The scheme responded

as expected where the logic to identify a breaker to reclose was successful and fuse saving was successful.

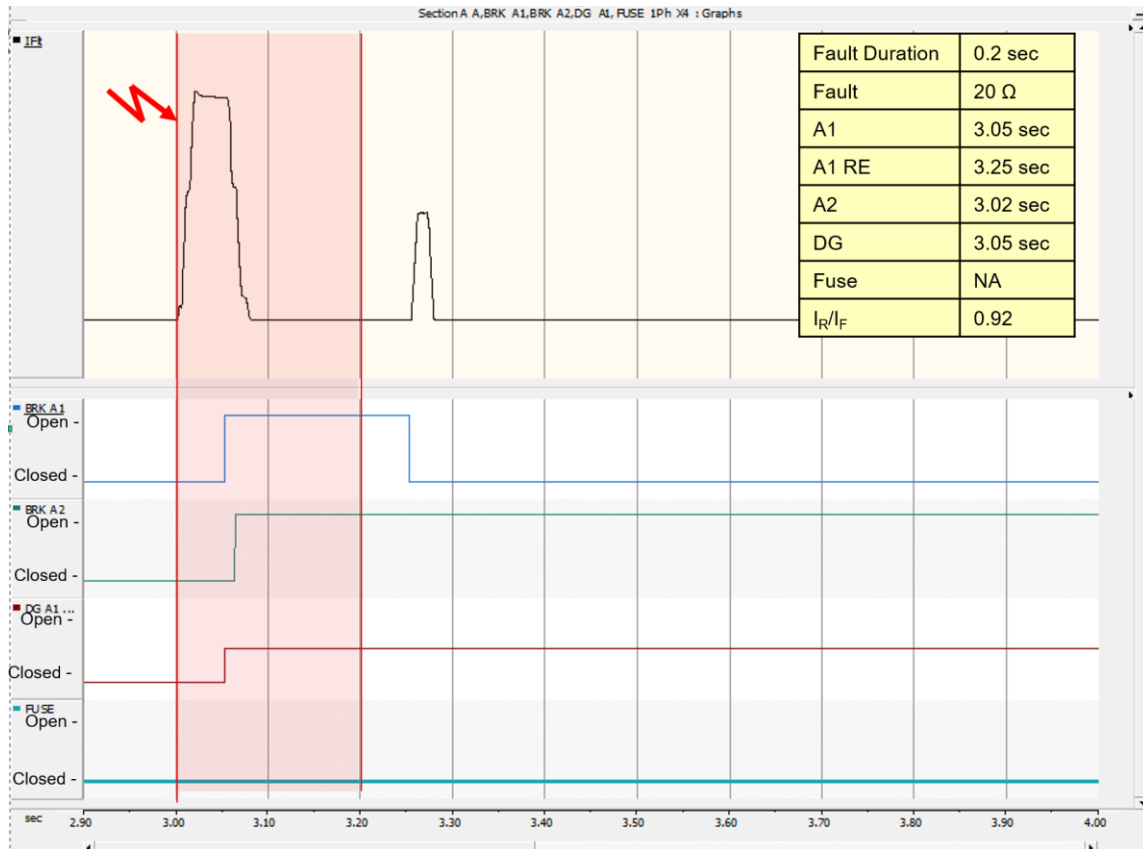


Figure 27 Time Diagram for Case 1 Scenario 2

The third scenario is permanent low impedance fault. As shown in figure 28, the fault is applied at 3.0 seconds and lasts to the end of simulation time. The first device to react is breaker A2 which trips on instantaneous setting at 3.02 seconds (response time 0.02 seconds). Next, breaker A1 trips at 3.05 seconds on recloser fast curve (response time 0.05 seconds). At the same time, DG A1 breaker tripped on an inter-trip signal from breaker A1. The fuse did not react to the fault due to fast curve trip from recloser, A1 zonal breaker.

Now, the faulty zone is completely de-energized. Reclosing sequence at breaker A1 recloses at 3.24 seconds (0.2-second recloser cycle) re-energizing the zone. Unlike the previous scenarios, the fault persists. The recloser breaker (i.e. breaker A1) now shifts to the slow curve allowing the fuse enough time to trip if the fault is within fuse reach. In this case, the fault is in the fuse reach and the fuse trips at 3.31 seconds, 0.07 seconds after first recloser attempt. Recloser breaker A1 stays closed as the fault was cleared by the fuse blowing.

The TDS adjustment for the recloser was 0.91 due to the recloser-fuse fault current ratio (I_R/I_F). Breakers A2 and DG A1 stay open as expected. The fault was cleared by the right protective device maintaining proper selectivity. The system is not back to normal operation as DG A2 and breaker A2 needs to be closed manually by a system operator after synchronization conditions are met. The scheme responded as expected where the logic to identify breaker to reclose was successful and fuse saving was successful. The coordination time interval (CTI) between recloser and fuse at this fault level is 0.02 seconds.

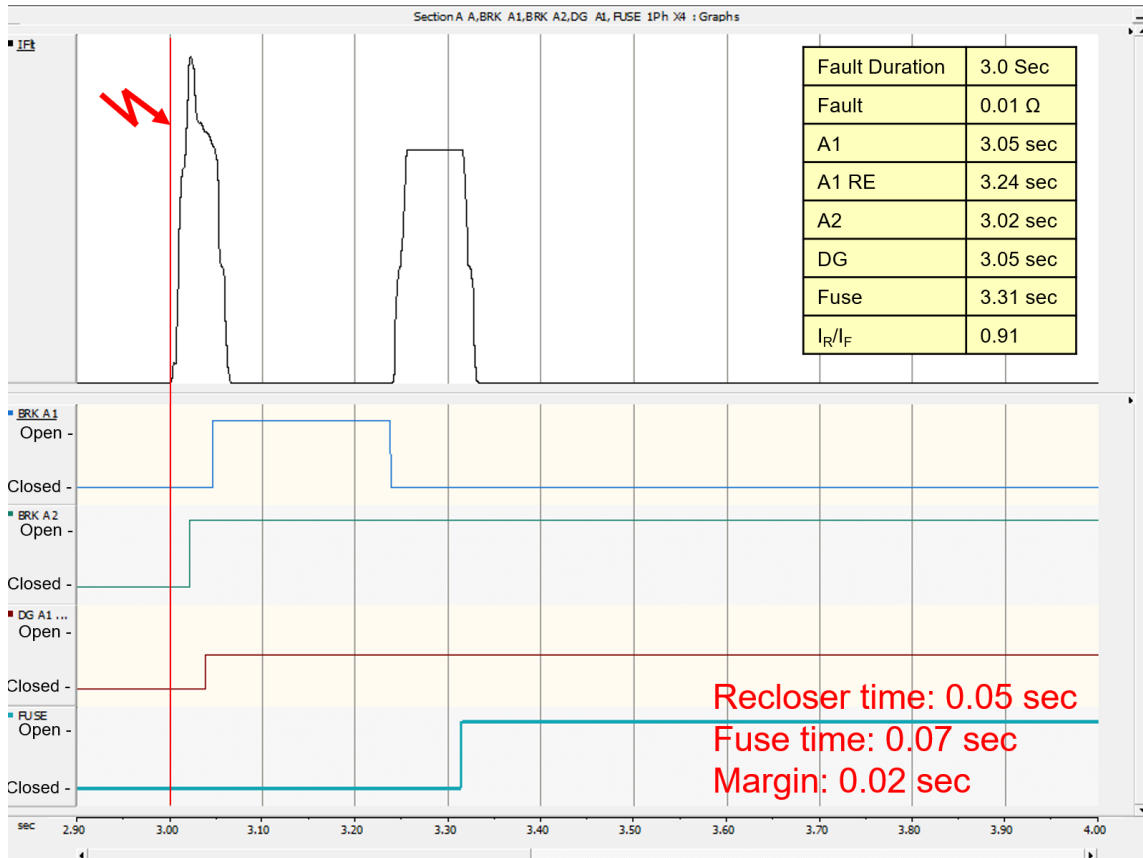


Figure 28 Time Diagram for Case 1 Scenario 3

The fourth scenario is permanent high impedance fault. Again, the fault current is less than the previous scenario since the impedance increased. As shown in figure 29, in this scenario there was not any change from scenario 3 in breakers response and timing. Even though this is a high resistance fault, the fault current was still relatively high. However, the fuse response time has increased in this scenario. Fuse trip time is 3.39 increasing the response time to 0.14 seconds. The recloser to fuse current ratio (I_R/I_F) is the same since the fault current has reduced for both devices proportionally. The fault was cleared by the right protective device maintaining proper selectivity. The system is not back to normal operation as DG A2 and breaker A2 need to be closed manually by a system operator after synchronization conditions are met. The scheme responded as expected

where the logic to identify a breaker to reclose was successful and fuse saving was successful. The coordination time interval (CTI) between recloser and fuse at this fault level is 0.09 seconds which is higher than the previous scenario.

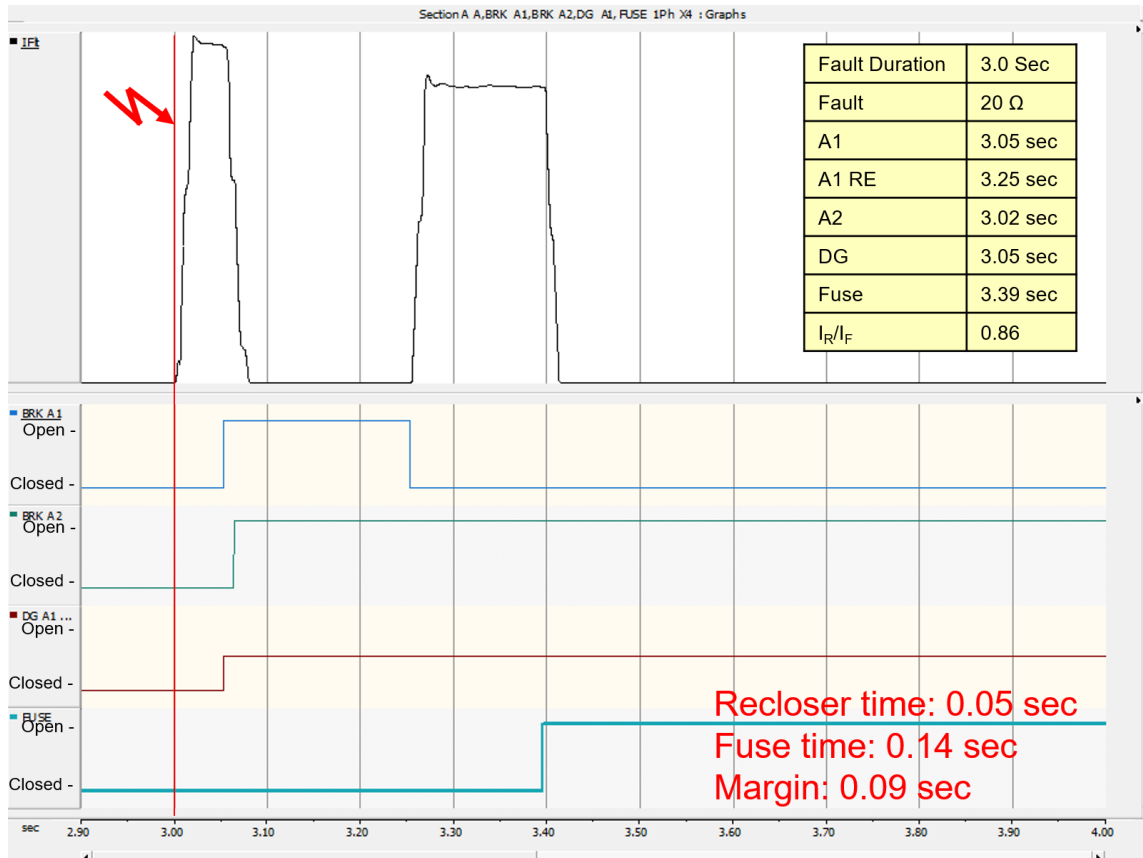


Figure 29 Time Diagram for Case 1 Scenario 4

5.3.2 Case 2: Feeder A Zone 3 lateral at 832-Transformer

This is a three-phase lateral feeding a transformer. All types of faults are possible at this fault location. Even though all types were simulated, only line-to-ground and three-phase-to-ground faults are presented and discussed in this case. Line-to-ground fault type represents the most common fault type to occur in real life. Three-phase-to-ground is the most severe type of

fault (i.e. the highest fault current). In this case, the only permanent fault is discussed but both high and low impedance faults are presented.

The first scenario is line-to-ground low impedance fault. The faulted phase in this scenario is phase A. as shown in figure 30, the first device to react is breaker A4 which trips on instantaneous setting at 3.02 seconds. Next, breaker A3 trips at 3.07 seconds on recloser fast curve. At the same time, DG A3 breaker tripped on an inter-trip signal from breaker A3. The fuse did not react to the fault due to fast curve trip from recloser, A3 zonal breaker.

Now, the faulty zone is completely de-energized. Reclosing sequence at breaker A3 recloses at 3.26 seconds re-energizing the zone. Since this fault is permanent, the recloser breaker (i.e. breaker A3) now shifts to the slow curve allowing the fuse enough time to trip if the fault is within fuse reach. In this case, the fault is in the fuse reach and the fuse trips at 3.50 seconds, 0.24 seconds after first recloser attempt. Recloser breaker A3 stays closed as the fault was cleared by the fuse blowing.

The TDS adjustment for the recloser was 0.76 due to the recloser-fuse fault current ratio (IR/IF). Breakers A4 and DG A3 stay open as expected. The fault was cleared by the right protective device maintaining proper selectivity. The system is not back to normal operation as DG A3 and breaker A4 need to be closed manually by a system operator after synchronization conditions are met. The scheme responded as expected where the logic to identify a breaker to reclose was successful and fuse saving was successful. The coordination time interval (CTI) between recloser and fuse at this fault level is 0.18 seconds.

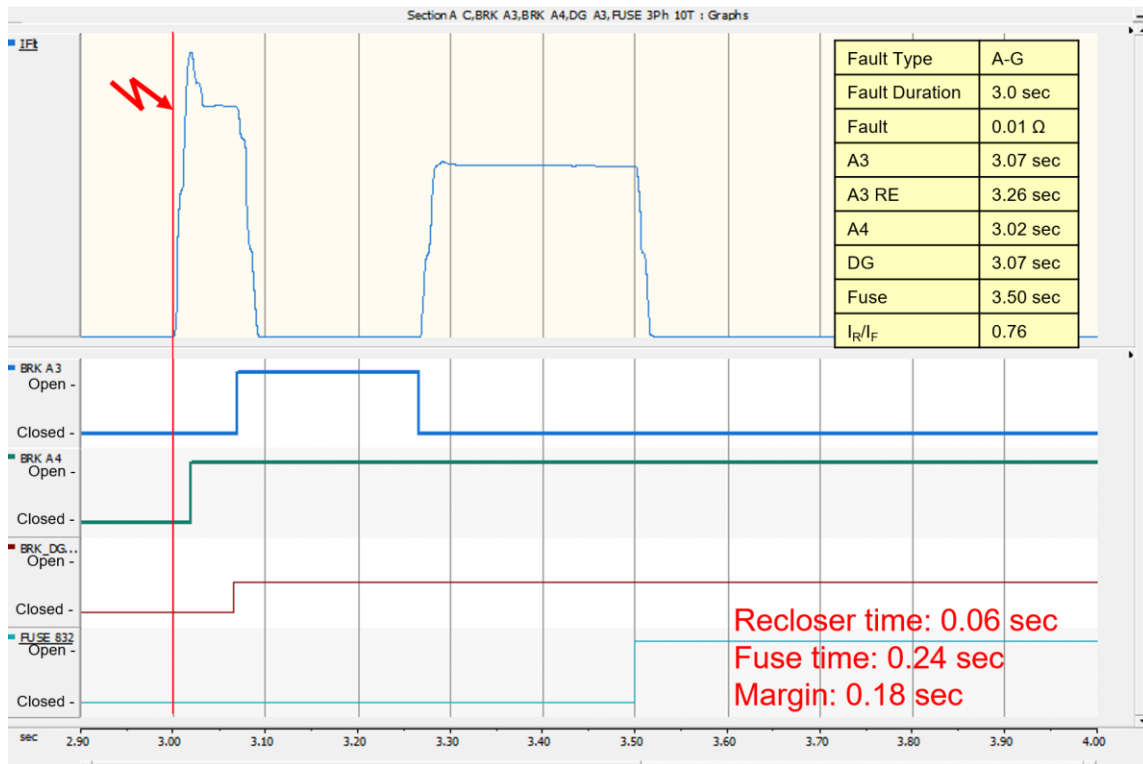


Figure 30 Time Diagram for Case 2 Scenario 1

In scenario 2, the fault resistance was increased to 20 Ω, high fault resistance. The fault current decreased accordingly. As indicated in figure 31, the reaction to the fault was similar to the previous scenario but reaction time was longer. The first device to react is breaker A4 which trips on instantaneous setting at 3.02 seconds. Next, breaker A3 trips at 3.08 seconds on recloser fast curve. At the same time, DG A3 breaker tripped on an inter-trip signal from breaker A3. Fuse did not react to the fault due to fast curve trip from recloser, A3 zonal breaker.

Now, the faulty zone is completely de-energized. Reclosing sequence at breaker A3 recloses at 3.28 seconds re-energizing the zone. Since this fault is permanent, the recloser breaker (i.e. breaker A3) now shifts to the slow curve allowing the fuse enough time to trip if the fault is within fuse reach. In this case, the fault is in the fuse reach and the fuse trips at 3.57 seconds, 0.29

seconds after first recloser attempt. Recloser breaker A3 stays closed as the fault was cleared by the fuse blowing.

The TDS adjustment for the recloser was 0.77 due to the recloser-fuse fault current ratio (IR/IF). Breakers A4 and DG A3 stay open as expected. The fault was cleared by the right protective device maintaining proper selectivity. The system is not back to normal operation as DG A3 and breaker A4 need to be closed manually by a system operator after synchronization conditions are met. The scheme responded as expected where the logic to identify a breaker to reclose was successful and fuse saving was successful. The coordination time interval (CTI) between recloser and fuse at this fault level is 0.21 seconds.

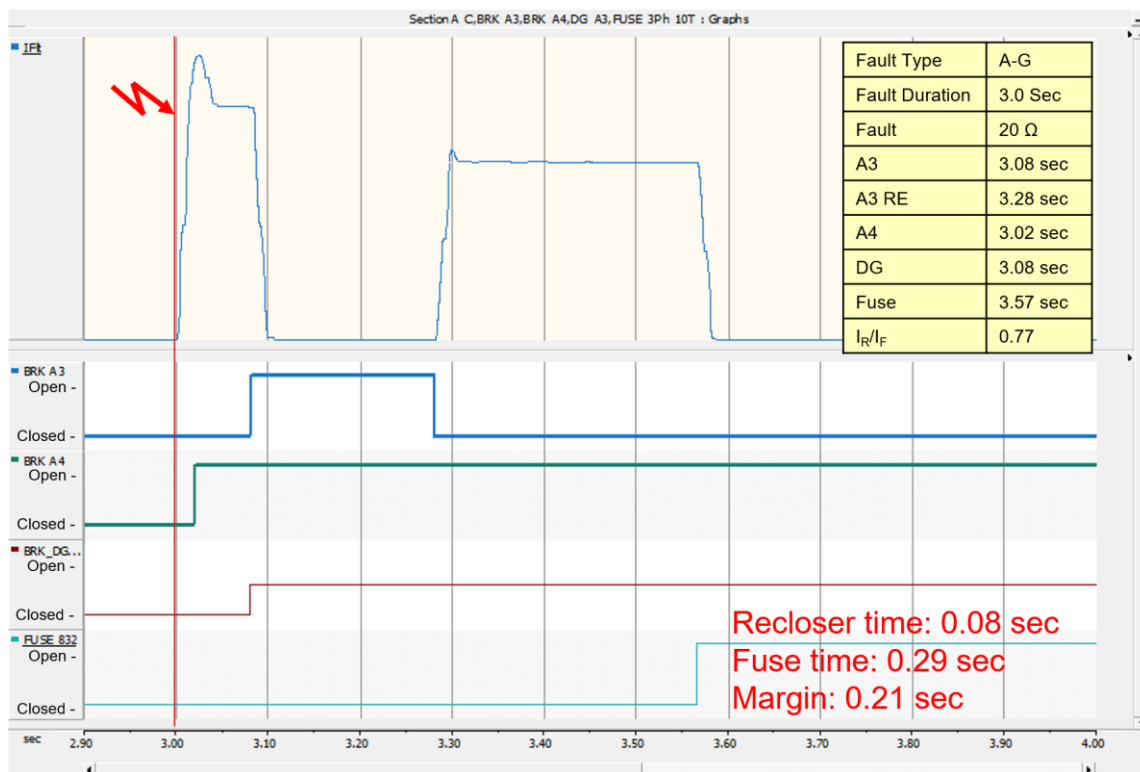


Figure 31 Time Diagram for Case 2 Scenario 2

In scenario 3, the fault applied is three-phase-to-ground low impedance fault. The three-phase-to-ground fault is the most severe type of fault where the fault current is the highest possible. As shown in figure 32, the protective devices reaction sequence is similar to line-to-ground faults presented in scenario 1 and 2. However, the response time of each device has shortened except for breaker A4 which trips on instantaneous settings maintaining 0.02 seconds response time. The fuse tripped at 3.43 seconds making response time of fuse 0.17 seconds. The TDS adjustment for the recloser was 0.76 due to the recloser-fuse fault current ratio (I_R/I_F). The coordination time interval (CTI) between recloser and fuse at this fault level is 0.11 seconds.

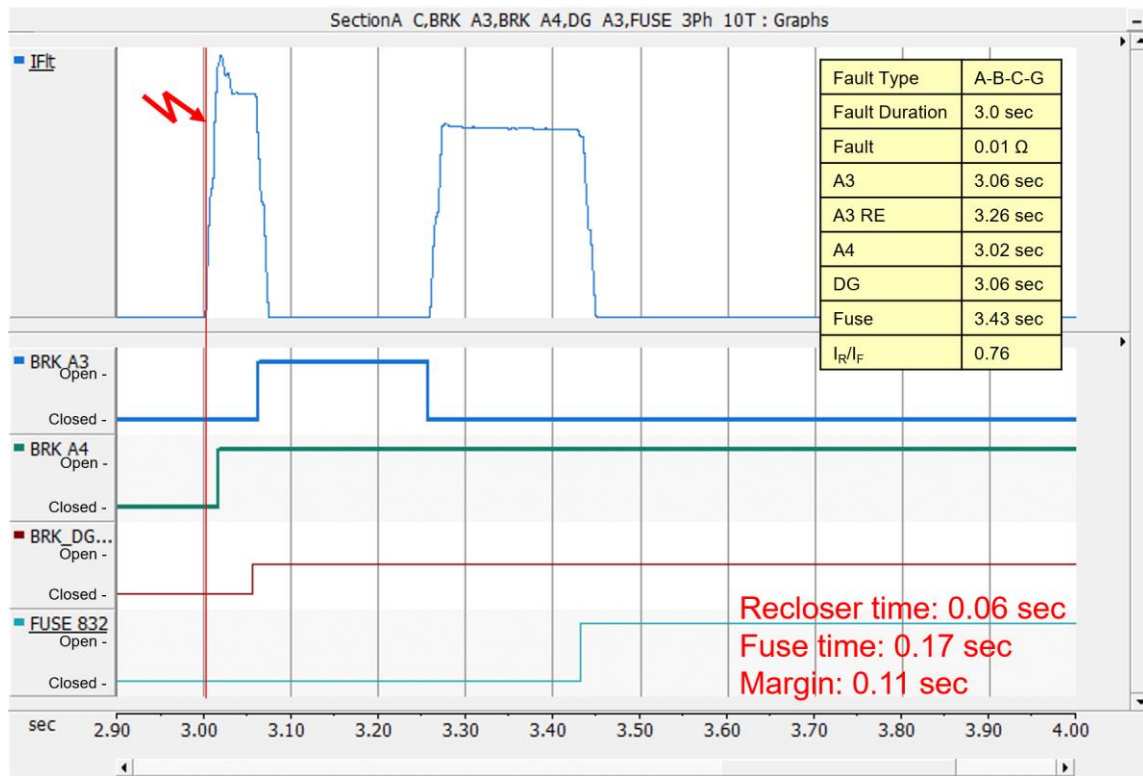


Figure 32 Time Diagram for Case 2 Scenario 3

In scenario 4, the fault resistance was increased to simulated three-phase-to-ground high impedance fault. The fault current is less than the previous scenario but still relatively high. As

shown in figure 33, again, the sequence of protective devices operations did not change except for timing. The fuse operation time was 3.48 seconds making response time of the fuse 0.20 seconds. The TDS adjustment for the recloser was 0.76 due to the recloser-fuse fault current ratio (I_R/I_F). The coordination time interval (CTI) between recloser and fuse at this fault level is 0.12 seconds.

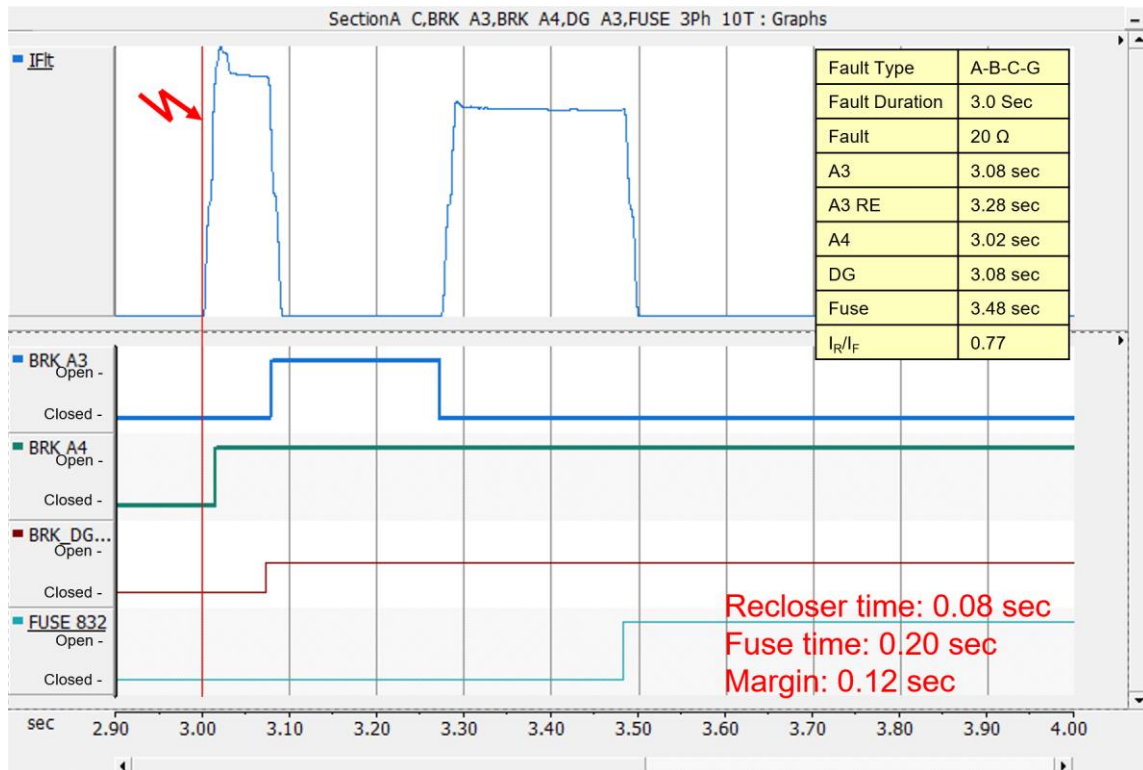


Figure 33 Time Diagram for Case 2 Scenario 4

5.3.3 Case 3: Feeder B Zone 4 lateral at 862-838

This is a single-phase lateral consisting of phase B. Consequently, the only phase-ground fault can be applied at this lateral. In this case, four fault scenarios were applied varying fault duration (temporary or permanent) and fault resistance (low or high). As this zone is at the end of the feeder, there was only one zonal breaker that is closer to the substation. In other words, there is not a breaker at the end of the zone to trip on instantaneous settings.

The first scenario is temporary low impedance fault. As shown in figure 34, the fault applied had 0.2 seconds duration. Zonal breaker B4 trips at 3.03 seconds on recloser fast curve. At the same time, DG B4 breaker tripped on an inter-trip signal from breaker B4. The fuse did not react to the fault due to fast curve trip from recloser, B4 zonal breaker.

Now, the faulty zone is completely de-energized. Reclosing sequence at breaker B4 recloses at 3.22 seconds (0.2-second recloser cycle) re-energizing the zone. By that time, the fault is already extinguished since it is a temporary fault. Breaker B4 stays closed for the rest of the simulation. The fuse was saved from blowing for a temporary fault reflecting successful fuse-aving scheme.

The TDS adjustment for the recloser was 0.94 due to the recloser-fuse fault current ratio (I_R/I_F). Breaker DG B4 stayed open as expected. Loads are re-energized back improving the reliability of power supply. However, the system is not back to normal operation as DG B4 needs to be closed manually by a system operator after synchronization conditions are met. The scheme responded as expected where the logic to identify breaker to reclose was successful and fuse saving was successful.

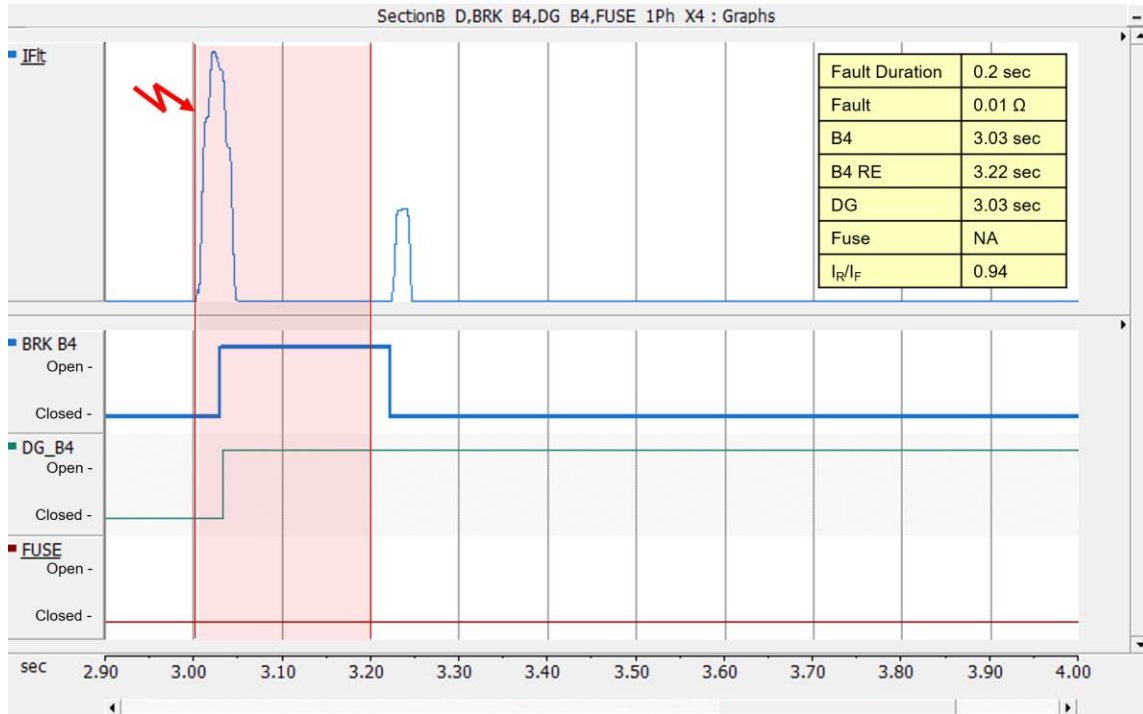


Figure 34 Time Diagram for Case 3 Scenario 1

In scenario 2, the impedance was increased to simulate high impedance fault. The fault applied was still a temporary fault. The fault current was reduced due to an increase of fault resistance. However, the change in fault current was not significant. The results of this scenario were the same as scenario 1 as shown in figure 35.



Figure 35 Time Diagram for Case 3 Scenario 2

In scenario 3, the fault applied was permanent low impedance fault. As shown in figure 36, breaker B4 trips at 3.03 seconds on recloser fast curve. At the same time, DG B4 breaker tripped on an inter-trip signal from breaker B4. The fuse did not react to the fault due to fast curve trip from recloser, B4 zonal breaker.

Now, the faulty zone is completely de-energized. Reclosing sequence at breaker B4 recloses at 3.22 seconds (0.2-second recloser cycle) re-energizing the zone. Unlike previous scenarios, the fault persists. The recloser breaker (i.e. breaker B4) now shifts to the slow curve allowing the fuse enough time to trip if the fault is within fuse reach. In this case, the fault is in the fuse reach and the fuse trips at 3.45 seconds, 0.23 seconds after first recloser attempt. Recloser breaker B4 stays closed as the fault was cleared by the fuse blowing.

The TDS adjustment for the recloser was 0.94 due to the recloser-fuse fault current ratio (IR/IF). Breaker DG B4 stayed open as expected. The fault was cleared by the right protective device maintaining proper selectivity. The system is not back to normal operation as DG B4 needs to be closed manually by system operator after synchronization conditions are met. The scheme responded as expected where the logic to identify a breaker to reclose was successful and fuse saving was successful. The coordination time interval (CTI) between recloser and fuse at this fault level is 0.20 seconds.

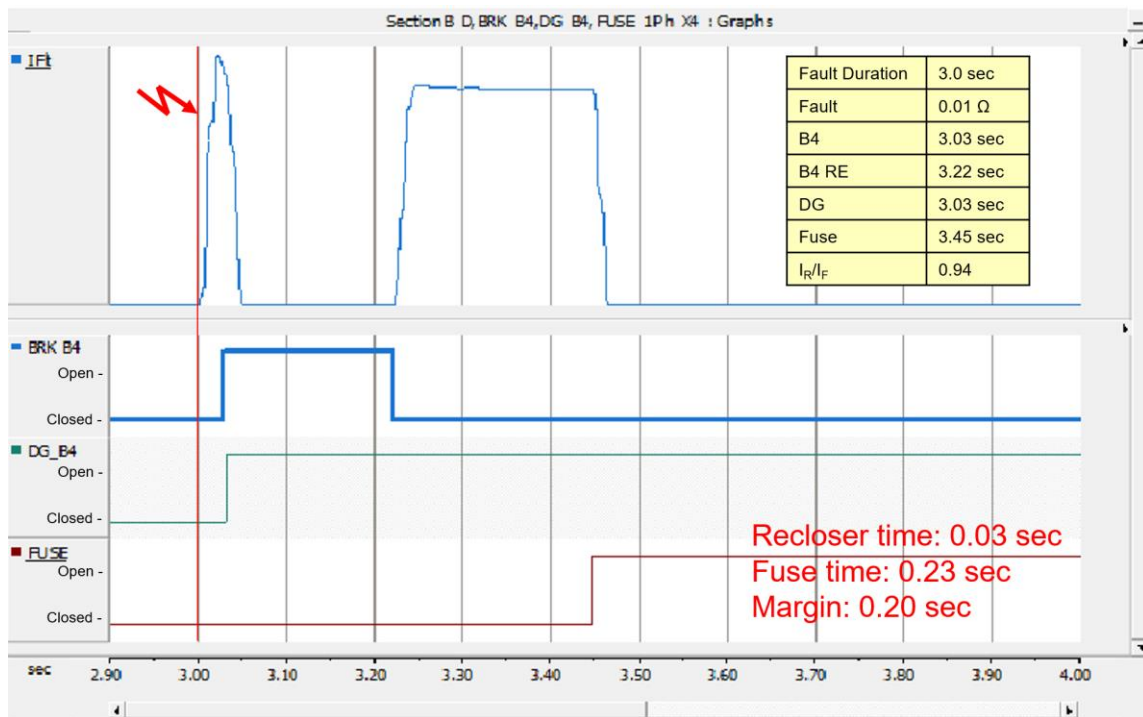


Figure 36 Time Diagram for Case 3 Scenario 3

The fourth scenario was permanent high impedance fault. Again, the fault current is less than the previous scenario since the impedance was increased. As shown in figure 37, in this scenario there was not any change from scenario 3 in breaker response and timing. Since this fault is at the end of the feeder, the change in fault current due to change in fault resistance was not

significant enough to cause a change in the protection response times. However, the fuse was an exception as the response time has increased in this scenario. Fuse trip time is 3.55 increasing the response time to 0.33 seconds. The recloser to fuse current ratio (I_R/I_F) is the same since fault current has reduced for both devices proportionally. The fault was cleared by the right protective device maintaining proper selectivity. The system is not back to normal operation as DG B4 needs to be closed manually by system operator after synchronization conditions are met. The scheme responded as expected where the logic to identify a breaker to reclose was successful and fuse saving was successful. The coordination time interval (CTI) between recloser and fuse at this fault level is 0.30 seconds which is higher than the previous scenario.

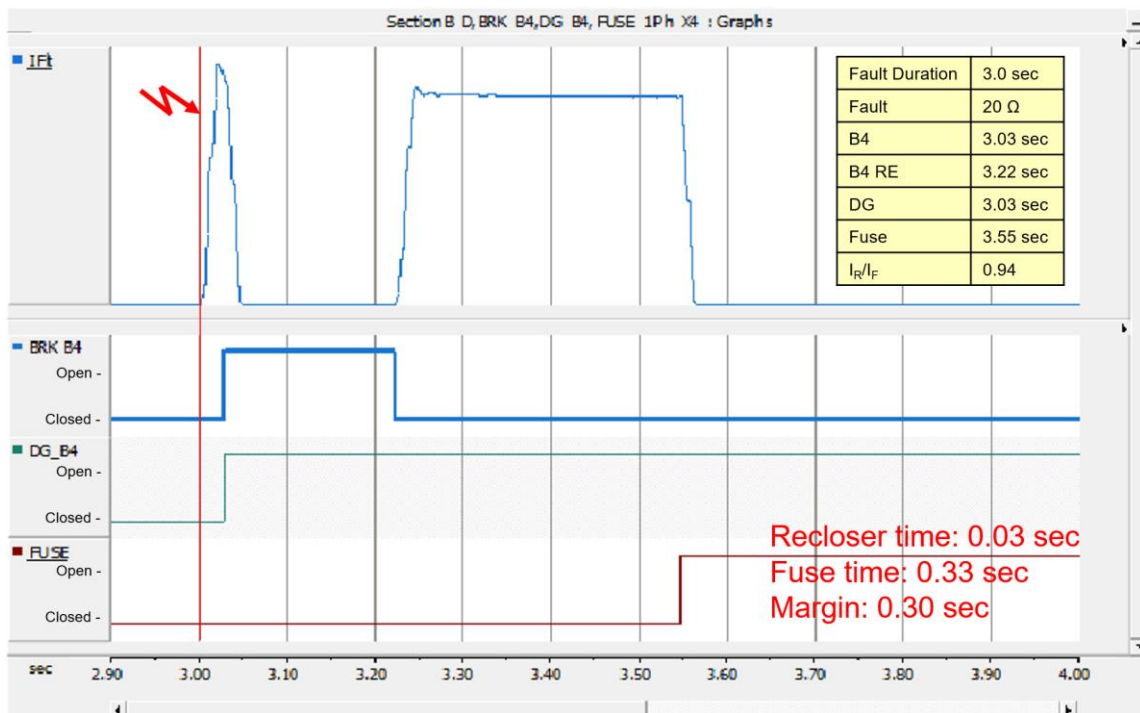


Figure 37 Time Diagram for Case 3 Scenario 4

5.4 Results

As explained at the beginning of the previous section, various faults were simulated at different locations on the test system. The previously discussed cases explain in detail a few examples of how a fault simulation is setup and how the results are obtained and then analyzed. The same applies to all other fault simulation runs discussed in this section. The results of all fault simulations are shown and discussed in this section. The results are divided into three segments based on the focus of test.

The first segment of the results considers only permanent faults at laterals with fuses. In such faults, coordination of recloser and fuse is the focus. Table 19 shows the information of this result segment. In the table at Fault Location column, the Fuse XXX DS indicates a fault just downstream from the fuse at node XXX where Lateral XXX End indicates fault at the end of the lateral with node XXX.

When a permanent fault is applied, the proper operation sequence to implement fuse-saving scheme is to trip the recloser using fast curve then switch to slow curve to allow the fuse to react to the fault if the fault is within fuse reach. In this results segment, all the faults applied are permanent and within fuse reach. Therefore, the fuse should react to the fault after the first reclosing attempt, where the recloser shifts to slow curve. Then, the recloser should stay closed and should not trip. For all the cases discussed in this result segment, this proper sequence was achieved with 100% success rate.

The other aspect to consider in this segment is timing and coordination. The difference between the response time of the recloser and response time of the fuse represents the Coordination Time Interval (CTI). For a protection scheme to be well coordinated, the CTI minimum value should be 0.2 seconds. This value is important to ensure correct operation sequence of protective

devices. The value is based on response time and different accuracies of various protective devices. Although in this result segment the proper sequence was fully maintained, the minimum CTI was not achieved in most cases. Out of 84 simulated cases, only 33 cases (representing 39%) had a CTI of 0.2 seconds or higher. Ten (10) cases (representing 12%) had a CTI below 0.1 seconds. The I_R/I_F factor (ranging from 0.62 to 0.99) that adjusts the TDS of the recloser fast curve was successful in restoring the sequence of operation but did not meet the CTI minimum value requirements. This could be a result of the increase in fault current which shortens the response time of the fuse leaving a very little margin to coordinate with recloser fast curve. In other words, the fuse acts too fast for the recloser fast curve to be able to coordinate with while maintaining proper CTI.

Table 19 Laterals Permanent Fault Simulation Results

Feeder	Zone	Fault Location	Fault Type	Fault Phase	Fault Resistance (Ω)	Fault Current (A)	Recloser Time (sec)	Fuse Time (sec)	CTI	R/F Ratio
A	1	Fuse 810 DS	Ph-G	B	0.01	590	0.05	0.06	0.01	0.92
A	1	Fuse 810 DS	Ph-G	B	20	390	0.05	0.14	0.09	0.86
A	1	Lateral 810 End	Ph-G	B	0.01	554	0.05	0.07	0.02	0.92
A	1	Lateral 810 End	Ph-G	B	20	390	0.05	0.14	0.09	0.86
A	2	Fuse 818 DS	Ph-G	A	0.01	393	0.07	0.29	0.22	0.80
A	2	Fuse 818 DS	Ph-G	A	20	297	0.09	0.41	0.32	0.85
A	2	Lateral 822 End	Ph-G	A	0.01	393	0.06	0.30	0.24	0.80
A	2	Lateral 822 End	Ph-G	A	20	297	0.09	0.40	0.31	0.85
A	2	Fuse 826 DS	Ph-G	B	0.01	423	0.06	0.19	0.13	0.74
A	2	Fuse 826 DS	Ph-G	B	20	302	0.08	0.29	0.21	0.78
A	2	Lateral 826 End	Ph-G	B	0.01	423	0.06	0.20	0.14	0.74
A	2	Lateral 826 End	Ph-G	B	20	302	0.08	0.29	0.21	0.78
A	3	Fuse 856 DS	Ph-G	B	0.01	384	0.05	0.24	0.19	0.72
A	3	Fuse 856 DS	Ph-G	B	20	281	0.07	0.33	0.26	0.75
A	3	Lateral 856 End	Ph-G	B	0.01	384	0.05	0.24	0.19	0.72
A	3	Lateral 856 End	Ph-G	B	20	281	0.07	0.33	0.26	0.75
A	3	Fuse 832 DS	Ph-G	A	0.01	280	0.07	0.24	0.17	0.74

Table 19 Continued

Feeder	Zone	Fault Location	Fault Type	Fault Phase	Fault Resistance (Ω)	Fault Current (A)	Recloser Time (sec)	Fuse Time (sec)	CTI	R/F Ratio
A	3	Fuse 832 DS	Ph-G	A	20	235	0.08	0.29	0.21	0.76
A	3	Fuse 832 DS	Ph-G	B	0.01	310	0.07	0.22	0.15	0.72
A	3	Fuse 832 DS	Ph-G	B	20	254	0.09	0.28	0.19	0.73
A	3	Fuse 832 DS	Ph-G	C	0.01	314	0.07	0.23	0.16	0.72
A	3	Fuse 832 DS	Ph-G	C	20	258	0.09	0.28	0.19	0.72
A	3	Fuse 832 DS	Ph-Ph	A-B	0.01	261	0.07	0.21	0.14	0.81
A	3	Fuse 832 DS	Ph-Ph	A-B	20	233	0.08	0.25	0.17	0.82
A	3	Fuse 832 DS	Ph-Ph	B-C	0.01	267	0.07	0.21	0.14	0.80
A	3	Fuse 832 DS	Ph-Ph	B-C	20	244	0.09	0.25	0.16	0.78
A	3	Fuse 832 DS	Ph-Ph	C-A	0.01	263	0.06	0.21	0.15	0.79
A	3	Fuse 832 DS	Ph-Ph	C-A	20	234	0.07	0.24	0.17	0.79
A	3	Fuse 832 DS	Ph-Ph-G	A-B	0.01	338	0.06	0.18	0.12	0.67
A	3	Fuse 832 DS	Ph-Ph-G	A-B	20	269	0.08	0.21	0.13	0.62
A	3	Fuse 832 DS	Ph-Ph-G	B-C	0.01	284	0.06	0.19	0.13	0.82
A	3	Fuse 832 DS	Ph-Ph-G	B-C	20	234	0.08	0.22	0.14	0.80
A	3	Fuse 832 DS	Ph-Ph-G	C-A	0.01	294	0.06	0.21	0.15	0.76
A	3	Fuse 832 DS	Ph-Ph-G	C-A	20	244	0.07	0.26	0.19	0.77
A	3	Fuse 832 DS	3-Ph	A-B-C	0.01	316	0.06	0.17	0.11	0.76
A	3	Fuse 832 DS	3-Ph	A-B-C	20	298	0.06	0.19	0.13	0.74
A	3	Fuse 832 DS	3-Ph-G	A-B-C	0.01	318	0.06	0.17	0.11	0.76
A	3	Fuse 832 DS	3-Ph-G	A-B-C	20	252	0.08	0.20	0.12	0.77
A	3	Fuse 864 DS	Ph-G	A	0.01	274	0.07	0.44	0.37	0.77
A	3	Fuse 864 DS	Ph-G	A	20	230	0.09	0.61	0.52	0.76
A	4	Fuse 834 DS	Ph-G	A	0.01	277	0.04	0.29	0.25	0.78
A	4	Fuse 834 DS	Ph-G	A	20	225	0.04	0.40	0.36	0.83
A	4	Fuse 834 DS	Ph-Ph	B-C	0.01	251	0.05	0.28	0.23	0.84
A	4	Fuse 834 DS	Ph-Ph	B-C	20	231	0.05	0.34	0.29	0.86
A	4	Fuse 834 DS	Ph-Ph-G	C-A	0.01	276	0.04	0.20	0.16	0.83
A	4	Fuse 834 DS	Ph-Ph-G	C-A	20	234	0.04	0.31	0.27	0.82
A	4	Fuse 834 DS	3-Ph	A-B-C	0.01	299	0.04	0.19	0.15	0.81
A	4	Fuse 834 DS	3-Ph	A-B-C	20	282	0.04	0.23	0.19	0.80
A	4	Fuse 834 DS	3-Ph-G	A-B-C	0.01	301	0.04	0.20	0.16	0.80
A	4	Fuse 834 DS	3-Ph-G	A-B-C	20	241	0.05	0.30	0.25	0.84
A	4	Fuse 838 DS	Ph-G	B	0.01	285	0.04	0.06	0.02	0.81
A	4	Fuse 838 DS	Ph-G	B	20	236	0.05	0.40	0.35	0.81
A	4	Fuse 840 DS	Ph-G	A	0.01	269	0.04	0.34	0.30	0.83

Table 19 Continued

Feeder	Zone	Fault Location	Fault Type	Fault Phase	Fault Resistance (Ω)	Fault Current (A)	Recloser Time (sec)	Fuse Time (sec)	CTI	R/F Ratio
A	4	Fuse 840 DS	Ph-G	A	20	220	0.05	0.45	0.40	0.82
A	4	Fuse 840 DS	Ph-Ph	B-C	0.01	247	0.04	0.08	0.04	0.86
A	4	Fuse 840 DS	Ph-Ph	B-C	20	227	0.05	0.39	0.34	0.84
A	4	Fuse 840 DS	Ph-Ph-G	C-A	0.01	271	0.04	0.03	0.01	0.85
A	4	Fuse 840 DS	Ph-Ph-G	C-A	20	225	0.05	0.35	0.30	0.88
A	4	Fuse 840 DS	3-Ph	A-B-C	0.01	291	0.04	0.03	0.01	0.81
A	4	Fuse 840 DS	3-Ph	A-B-C	20	275	0.04	0.31	0.27	0.78
A	4	Fuse 840 DS	3-Ph-G	A-B-C	0.01	293	0.04	0.02	0.02	0.82
A	4	Fuse 840 DS	3-Ph-G	A-B-C	20	236	0.04	0.38	0.34	0.85
B	1	Fuse 810 DS	Ph-G	B	0.01	660	0.04	0.08	0.04	0.82
B	1	Fuse 810 DS	Ph-G	B	20	402	0.05	0.15	0.10	0.85
B	1	Fuse 822 DS	Ph-G	A	0.01	403	0.08	0.35	0.27	0.71
B	1	Fuse 822 DS	Ph-G	A	20	306	0.12	0.50	0.38	0.74
B	1	Fuse 826 DS	Ph-G	B	0.01	442	0.07	0.23	0.16	0.65
B	1	Fuse 826 DS	Ph-G	B	20	313	0.09	0.32	0.23	0.67
B	2	Fuse 856 DS	Ph-G	B	0.01	400	0.05	0.25	0.20	0.69
B	2	Fuse 856 DS	Ph-G	B	20	295	0.07	0.33	0.26	0.69
B	2	Fuse 832 DS	Ph-G	A	0.01	275	0.08	0.23	0.15	0.71
B	2	Fuse 832 DS	Ph-G	A	20	218	0.1	0.28	0.18	0.73
B	2	Fuse 832 DS	Ph-Ph	B-C	0.01	277	0.08	0.21	0.13	0.74
B	2	Fuse 832 DS	Ph-Ph	B-C	20	247	0.09	0.24	0.15	0.72
B	2	Fuse 832 DS	Ph-Ph-G	C-A	0.01	301	0.06	0.19	0.13	0.70
B	2	Fuse 832 DS	Ph-Ph-G	C-A	20	240	0.08	0.22	0.14	0.73
B	2	Fuse 832 DS	3-Ph	A-B-C	0.01	324	0.06	0.17	0.11	0.99
B	2	Fuse 832 DS	3-Ph	A-B-C	20	302	0.07	0.19	0.12	0.70
B	2	Fuse 832 DS	3-Ph-G	A-B-C	0.01	327	0.06	0.17	0.11	0.71
B	2	Fuse 832 DS	3-Ph-G	A-B-C	20	252	0.07	0.22	0.15	0.73
B	2	Fuse 864 DS	Ph-G	A	0.01	266	0.08	0.48	0.40	0.71
B	2	Fuse 864 DS	Ph-G	A	20	214	0.1	0.63	0.53	0.74
B	4	Fuse 838 DS	Ph-G	B	0.01	287	0.03	0.23	0.20	0.94
B	4	Fuse 838 DS	Ph-G	B	20	234	0.03	0.33	0.30	0.94

In the second result segment, temporary faults on laterals with fuses were considered. The recloser scheme is aimed at protecting the distribution system against the temporary fault. Additionally, fuse-saving scheme protect the fuse from blowing for a temporary fault by making the recloser act on a fast curve, faster than the fuse. In this result segment, the fault applied is temporary within the fuse reach. If the scheme is successful, the recloser should respond to the fault and reclose without the fuse blowing. For studies shown in table 20, the aforementioned fault is applied to all laterals with fuses one at a time. The scheme was successful to clear the fault by the recloser fast curve protecting the fuse from blowing with 100% success rate. The fuse never operated in all simulated cases in this result segment.

Table 20 Laterals Temporary Fault Simulation Results

Feeder	Zone	Fault Location	Fault Type	Fault Phase	Fault Resistance (Ω)	Fault Current	Recloser Trip Time	Fuse Time	R/F Ratio
A	1	Fuse 810 DS	Ph-G	B	0.01	590	0.05	NA	0.92
A	1	Fuse 810 DS	Ph-G	B	20	390	0.05	NA	0.86
A	1	Lateral 810 End	Ph-G	B	0.01	554	0.05	NA	0.92
A	1	Lateral 810 End	Ph-G	B	20	390	0.05	NA	0.86
A	2	Fuse 818 DS	Ph-G	A	0.01	393	0.07	NA	0.80
A	2	Fuse 818 DS	Ph-G	A	20	297	0.09	NA	0.85
A	2	Lateral 822 End	Ph-G	A	0.01	393	0.06	NA	0.80
A	2	Lateral 822 End	Ph-G	A	20	297	0.09	NA	0.85
A	2	Fuse 826 DS	Ph-G	B	0.01	423	0.06	NA	0.74
A	2	Fuse 826 DS	Ph-G	B	20	302	0.08	NA	0.78
A	2	Lateral 826 End	Ph-G	B	0.01	423	0.06	NA	0.74
A	2	Lateral 826 End	Ph-G	B	20	302	0.08	NA	0.78
A	3	Fuse 856 DS	Ph-G	B	0.01	384	0.05	NA	0.72
A	3	Fuse 856 DS	Ph-G	B	20	281	0.07	NA	0.75
A	3	Lateral 856 End	Ph-G	B	0.01	384	0.05	NA	0.72
A	3	Lateral 856 End	Ph-G	B	20	281	0.07	NA	0.75
A	3	Fuse 832 DS	Ph-G	A	0.01	280	0.07	NA	0.74
A	3	Fuse 832 DS	Ph-G	A	20	235	0.08	NA	0.76

Table 20 Continued

Feeder	Zone	Fault Location	Fault Type	Fault Phase	Fault Resistance (Ω)	Fault Current	Recloser Trip Time	Fuse Time	R/F Ratio
A	3	Fuse 832 DS	Ph-G	B	0.01	310	0.07	NA	0.72
A	3	Fuse 832 DS	Ph-G	B	20	254	0.09	NA	0.73
A	3	Fuse 832 DS	Ph-G	C	0.01	314	0.07	NA	0.72
A	3	Fuse 832 DS	Ph-G	C	20	258	0.09	NA	0.72
A	3	Fuse 832 DS	Ph-Ph	A-B	0.01	261	0.07	NA	0.81
A	3	Fuse 832 DS	Ph-Ph	A-B	20	233	0.08	NA	0.82
A	3	Fuse 832 DS	Ph-Ph	B-C	0.01	267	0.07	NA	0.80
A	3	Fuse 832 DS	Ph-Ph	B-C	20	244	0.09	NA	0.78
A	3	Fuse 832 DS	Ph-Ph	C-A	0.01	263	0.06	NA	0.79
A	3	Fuse 832 DS	Ph-Ph	C-A	20	234	0.07	NA	0.79
A	3	Fuse 832 DS	Ph-Ph-G	A-B	0.01	338	0.06	NA	0.67
A	3	Fuse 832 DS	Ph-Ph-G	A-B	20	269	0.08	NA	0.62
A	3	Fuse 832 DS	Ph-Ph-G	B-C	0.01	284	0.06	NA	0.82
A	3	Fuse 832 DS	Ph-Ph-G	B-C	20	234	0.08	NA	0.80
A	3	Fuse 832 DS	Ph-Ph-G	C-A	0.01	294	0.06	NA	0.76
A	3	Fuse 832 DS	Ph-Ph-G	C-A	20	244	0.07	NA	0.77
A	3	Fuse 832 DS	3-Ph	A-B-C	0.01	316	0.06	NA	0.76
A	3	Fuse 832 DS	3-Ph	A-B-C	20	298	0.06	NA	0.74
A	3	Fuse 832 DS	3-Ph-G	A-B-C	0.01	318	0.06	NA	0.76
A	3	Fuse 832 DS	3-Ph-G	A-B-C	20	252	0.08	NA	0.77
A	3	Fuse 864 DS	Ph-G	A	0.01	274	0.07	NA	0.77
A	3	Fuse 864 DS	Ph-G	A	20	230	0.09	NA	0.76
A	4	Fuse 834 DS	Ph-G	A	0.01	277	0.04	NA	0.78
A	4	Fuse 834 DS	Ph-G	A	20	225	0.04	NA	0.83
A	4	Fuse 834 DS	Ph-Ph	B-C	0.01	251	0.05	NA	0.84
A	4	Fuse 834 DS	Ph-Ph	B-C	20	231	0.05	NA	0.86
A	4	Fuse 834 DS	Ph-Ph-G	C-A	0.01	276	0.04	NA	0.83
A	4	Fuse 834 DS	Ph-Ph-G	C-A	20	234	0.04	NA	0.82
A	4	Fuse 834 DS	3-Ph	A-B-C	0.01	299	0.04	NA	0.81
A	4	Fuse 834 DS	3-Ph	A-B-C	20	282	0.04	NA	0.80
A	4	Fuse 834 DS	3-Ph-G	A-B-C	0.01	301	0.04	NA	0.80
A	4	Fuse 834 DS	3-Ph-G	A-B-C	20	241	0.05	NA	0.84
A	4	Fuse 838 DS	Ph-G	B	0.01	285	0.04	NA	0.81
A	4	Fuse 838 DS	Ph-G	B	20	236	0.05	NA	0.81
A	4	Fuse 840 DS	Ph-G	A	0.01	269	0.04	NA	0.83
A	4	Fuse 840 DS	Ph-G	A	20	220	0.05	NA	0.82

Table 20 Continued

Feeder	Zone	Fault Location	Fault Type	Fault Phase	Fault Resistance (Ω)	Fault Current	Recloser Trip Time	Fuse Time	R/F Ratio
A	4	Fuse 840 DS	Ph-Ph	B-C	0.01	247	0.04	NA	0.86
A	4	Fuse 840 DS	Ph-Ph	B-C	20	227	0.05	NA	0.84
A	4	Fuse 840 DS	Ph-Ph-G	C-A	0.01	271	0.04	NA	0.85
A	4	Fuse 840 DS	Ph-Ph-G	C-A	20	225	0.05	NA	0.88
A	4	Fuse 840 DS	3-Ph	A-B-C	0.01	291	0.04	NA	0.81
A	4	Fuse 840 DS	3-Ph	A-B-C	20	275	0.04	NA	0.78
A	4	Fuse 840 DS	3-Ph-G	A-B-C	0.01	293	0.04	NA	0.82
A	4	Fuse 840 DS	3-Ph-G	A-B-C	20	236	0.04	NA	0.85
B	1	Fuse 810 DS	Ph-G	B	0.01	660	0.04	NA	0.82
B	1	Fuse 810 DS	Ph-G	B	20	402	0.05	NA	0.85
B	1	Fuse 822 DS	Ph-G	A	0.01	403	0.08	NA	0.71
B	1	Fuse 822 DS	Ph-G	A	20	306	0.12	NA	0.74
B	1	Fuse 826 DS	Ph-G	B	0.01	442	0.07	NA	0.65
B	1	Fuse 826 DS	Ph-G	B	20	313	0.09	NA	0.67
B	2	Fuse 856 DS	Ph-G	B	0.01	400	0.05	NA	0.69
B	2	Fuse 856 DS	Ph-G	B	20	295	0.07	NA	0.69
B	2	Fuse 832 DS	Ph-G	A	0.01	275	0.08	NA	0.71
B	2	Fuse 832 DS	Ph-G	A	20	218	0.1	NA	0.73
B	2	Fuse 832 DS	Ph-Ph	B-C	0.01	277	0.08	NA	0.74
B	2	Fuse 832 DS	Ph-Ph	B-C	20	247	0.09	NA	0.72
B	2	Fuse 832 DS	Ph-Ph-G	C-A	0.01	301	0.06	NA	0.70
B	2	Fuse 832 DS	Ph-Ph-G	C-A	20	240	0.08	NA	0.73
B	2	Fuse 832 DS	3-Ph	A-B-C	0.01	324	0.06	NA	0.99
B	2	Fuse 832 DS	3-Ph	A-B-C	20	302	0.07	NA	0.70
B	2	Fuse 832 DS	3-Ph-G	A-B-C	0.01	327	0.06	NA	0.71
B	2	Fuse 832 DS	3-Ph-G	A-B-C	20	252	0.07	NA	0.73
B	2	Fuse 864 DS	Ph-G	A	0.01	266	0.08	NA	0.71
B	2	Fuse 864 DS	Ph-G	A	20	214	0.1	NA	0.74
B	4	Fuse 838 DS	Ph-G	B	0.01	287	0.03	NA	0.94
B	4	Fuse 838 DS	Ph-G	B	20	234	0.03	NA	0.94

Although previous result segments provide sufficient information about the behavior of the proposed approach, the third segment considers only main line faults to look at cases where fuses

should not be involved. In table 21, the result of faults simulated at the main line is depicted where both permanent and temporary faults were considered. The main line is always three-phase in the test system for this work. The term “OC 50” indicates the zonal breaker that should trip on instantaneous setting as per the reclosing logic. The logic was successful to identify the right zonal breakers to identify the faulty zone and identify the right reclosing breaker and the breaker to trip on instantaneous settings with 100% success rate. The fuse did not operate in any of these cases. For the last zone on the feeder, the logic was slightly different in terms that there is only one zonal breaker. The logic was fully successful and valid as well.

Table 21 Main Line Fault Simulation Results

Feeder	Zone	Fault Node	Fault Type	Fault Phase	Fault Duration	Fault Resistance (Ω)	Fault Current	Recloser Fault Current	OC 50 Fault Current	DG Current	Recloser 1st Trip Time	Recloser 1st Reclose Time	Recloser 2nd Trip Time	Recloser 2nd Reclose Time	Permanent Trip	OC 50 Trip Time	DG Trip Time
A	1	808	Ph-G	B	0.20	0.01	590	541	112	19.5	3.05	3.24	NA			3.02	3.04
					3.00								3.67	4.06	4.09		
					0.20	20	390	336	86	14	3.05	3.25	NA			3.06	3.05
					3.00								3.83	4.23	4.26		
A	2	816	Ph-G	A	0.20	0.01	393	315	97.2	18.9	3.07	3.26	NA			3.02	3.07
					3.00								4.04	4.44	4.48		
					0.20	20	297	252	58	16	3.09	3.29	NA			3.02	3.09
					3.00								4.31	4.70	4.75		
A	2	824	Ph-G	B	0.20	0.01	423	313	129	21	3.06	3.25	NA			3.02	3.06
					3.00								3.87	4.26	4.30		
					0.20	20	302	236	71	15	3.08	3.27	NA			3.02	3.08
					3.00								4.05	4.44	4.49		
A	3	854	Ph-G	B	0.20	0.01	384	227	82	35	3.05	3.25	NA			3.02	3.06
					3.00								3.84	4.24	4.28		
					0.20	20	281	211	45	27	3.07	3.27	NA			3.02	3.08
					3.00								4.02	4.41	4.45		
A	3	832	Ph-G	C	0.20	0.01	314	227	132	50	3.07	3.26	NA			3.02	3.07
					3.00								4.09	4.49	4.53		
					0.20	20	258	185	73	33	3.09	2.28	NA			3.02	3.09
					3.00								4.26	4.66	4.70		
A	3	832	Ph-Ph	B-C	0.20	0.01	267	214	104	50	3.07	3.26	NA			3.02	3.08
					3.00								4.05	4.45	4.49		
					0.20	20	244	190	75	40	3.08	3.27	NA			3.02	3.09
					3.00								4.15	4.55	4.59		

Table 21 Continued

Feeder	Zone	Fault Node	Fault Type	Fault Phase	Fault Duration	Fault Resistance (Ω)	Fault Current	Recloser Fault Current	OC 50 Fault Current	DG Current	Recloser 1st Trip Time	Recloser 1st Reclose Time	Recloser 2nd Trip Time	Recloser 2nd Reclose Time	Permanent Trip	OC 50 Trip Time	DG Trip Time
A	3	832	Ph-Ph-G	A-B	0.20	0.01	338	228	88	52	3.06	3.26	NA			3.02	3.06
					3.00								3.89	4.28	4.32		
					0.20	20	269	166	54	37	3.08	3.28	NA			3.02	3.08
					3.00								4.04	4.44	4.49		
A	3	832	3-Ph	A-B-C	0.20	0.01	316	240	96	58	3.06	3.26	NA			3.02	3.06
					3.00								3.88	4.27	4.30		
					0.20	20	298	220	76	50	3.06	3.26	NA			3.02	3.07
					3.00								3.93	4.33	4.36		
A	3	832	3-Ph-G	A-B-C	0.20	0.01	318	241	96	58	3.06	3.26	NA			3.02	3.06
					3.00								3.87	4.27	4.30		
					0.20	20	252	194	52	41	3.08	3.28	NA			3.02	3.08
					3.00								4.05	4.45	4.50		
A	3	858	Ph-G	A	0.20	0.01	274	212	77	34	3.07	3.27	NA			3.02	3.07
					3.00								4.08	4.48	4.52		
					0.20	20	230	174	52	30	3.09	3.28	NA			3.02	3.09
					3.00								4.27	4.67	4.70		
A	4	834	Ph-G	A	0.20	0.01	277	216		48	3.04	3.24	NA				3.04
					3.00								3.93	4.32	4.35		
					0.20	20	225	186		38	3.04	3.24	NA				3.04
					3.00								4.03	4.42	4.45		
A	4	834	Ph-Ph	B-C	0.20	0.01	251	212		77	3.04	3.24	NA				3.04
					3.00								3.98	4.38	4.42		
					0.20	20	231	198		58	3.04	3.24	NA				3.04
					3.00								4.06	4.46	4.49		

Table 21 Continued

Feeder	Zone	Fault Node	Fault Type	Fault Phase	Fault Duration	Fault Resistance (Ω)	Fault Current	Recloser Fault Current	OC 50 Fault Current	DG Current	Recloser 1st Trip Time	Recloser 1st Reclose Time	Recloser 2nd Trip Time	Recloser 2nd Reclose Time	Permanent Trip	OC 50 Trip Time	DG Trip Time						
A	4	834	Ph-Ph-G	C-A	0.20	0.01	276	230		82	3.04	3.24	NA				3.04						
					3.00								3.86	4.26	4.28								
					0.20	20	234	192					NA					3.05					
					3.00								3.96	4.35	4.38								
A	4	834	3-Ph	A-B-C	0.20	0.01	299	242		91	3.04	3.23	NA			3.04							
					3.00								3.91	4.31	4.33								
					0.20	20	282	225					NA				3.04						
					3.00								3.93	4.33	4.36								
A	4	834	3-Ph-G	A-B-C	0.20	0.01	301	241		92	3.04	3.24	NA			3.04							
					3.00								3.93	4.32	4.35								
					0.20	20	241	202					NA				3.04						
					3.00								4.00	4.39	4.42								
B	1	808	Ph-G	B	0.20	0.01	660	540	102	29.5	3.04	3.23	NA			3.02		3.05					
					1.50								3.63	4.02	4.05								
					0.20	20	402	343					52	20	3.05		3.24		NA			3.02	3.05
					1.50														3.78	4.17	4.20		
B	1	816	Ph-G	A	0.20	0.01	403	288	112	30	3.08	3.27	NA			3.02	3.08						
					3.00								4.16	4.56	4.60								
					0.20	20	306	226					76	25	3.11			3.30	NA			3.02	3.11
					3.00														4.48	4.88	4.94		
B	1	824	Ph-G	B	0.20	0.01	442	287	154	34	3.06	3.26	NA			3.02	3.06						
					3.00								4.03	4.43	4.46								
					0.20	20	313	210					92	25	3.09			3.29	NA			3.02	3.09
					3.00														4.28	4.68	4.72		

Table 21 Continued

Feeder	Zone	Fault Node	Fault Type	Fault Phase	Fault Duration	Fault Resistance (Ω)	Fault Current	Recloser Fault Current	OC 50 Fault Current	DG Current	Recloser 1st Trip Time	Recloser 1st Reclose Time	Recloser 2nd Trip Time	Recloser 2nd Reclose Time	Permanent Trip	OC 50 Trip Time	DG Trip Time
B	2	854	Ph-G	B	0.20	0.01	400	276	99	47	3.05	3.25	NA			3.02	3.05
					3.00								3.84	4.23	4.27		
					0.20	20	295	205	59	32	3.08	3.28	NA			3.02	3.08
					3.00								4.00	4.40	4.45		
B	2	832	Ph-G	A	0.20	0.01	275	195	80	29	3.07	3.27	NA			3.02	3.07
					3.00								4.07	4.47	4.51		
					0.20	20	218	160	58	26	3.10	3.30	NA			3.02	3.10
					3.00								4.28	4.67	4.71		
B	2	832	Ph-Ph	B-C	0.20	0.01	277	204	112	39	3.08	3.27	NA			3.02	3.08
					3.00								4.03	4.43	4.47		
					0.20	20	247	178	82	32	3.09	3.28	NA			3.02	3.09
					3.00								4.15	4.54	4.59		
B	2	832	Ph-Ph-G	C-A	0.20	0.01	301	212	105	41	3.07	3.27	NA			3.02	3.07
					3.00								3.90	4.30	4.34		
					0.20	20	240	176	65	32	3.08	3.28	NA			3.02	3.08
					3.00								4.08	4.48	4.52		
B	2	832	3-Ph	A-B-C	0.20	0.01	324	232	101	47	3.06	3.26	NA			3.02	3.06
					3.00								3.86	4.26	4.30		
					0.20	20	302	212	84	43	3.07	3.27	NA			3.02	3.07
					3.00								3.92	4.31	4.35		
B	2	832	3-Ph-G	A-B-C	0.20	0.01	327	232	101	47	3.06	3.26	NA			3.02	3.06
					3.00								3.87	4.26	4.30		
					0.20	20	252	184	60	36	3.09	3.28	NA			3.02	3.09
					3.00								4.06	4.46	4.50		

Table 21 Continued

Feeder	Zone	Fault Node	Fault Type	Fault Phase	Fault Duration	Fault Resistance (Ω)	Fault Current	Recloser Fault Current	OC 50 Fault Current	DG Current	Recloser 1st Trip Time	Recloser 1st Reclose Time	Recloser 2nd Trip Time	Recloser 2nd Reclose Time	Permanent Trip	OC 50 Trip Time	DG Trip Time
B	2	858	Ph-G	A	0.20	0.01	266	188	81	28	3.08	3.28	NA			3.02	3.08
					3.00								4.11	4.50	4.56		
					0.20	20	214	159	58	25	3.10	3.30	NA			3.02	3.10
					3.00								4.30	4.70	4.75		
B	4	858	Ph-G	B	0.20	0.01	287	269	█	42	3.03	3.22	NA			█	3.03
					3.00								4.40	4.79	4.82		
					0.20	20	234	221	█	39	3.03	3.22	NA			█	3.03
					3.00								4.45	4.84	4.86		

5.5 Summary

A test system was simulated in PSCAD software to investigate the behavior of the adaptive reclosing approach. The test system is a modified dual IEEE 34 Node Radial Test Feeders. The test system was modified by dividing each radial feeder into 4 zones separated by 4 zonal breakers with directional overcurrent and reclosing protection. In each zone, a synchronous-based DG was interconnected and sized to match the load of the zone. Also, fuses were added to the laterals without DG interconnection. The scheme investigated was built in the zonal breakers by implementing the logic for recloser and fuse current monitoring.

The suggested approach was tested for various scenarios. Faults were applied to different locations on the test system, on laterals and the main line. Also, fault types, fault resistance, and fault duration were varied in each simulation run. High and low impedance faults, as well as temporary and permanent faults, were considered. These combinations provide sufficient varieties of cases to accomplish an acceptable level of testing of the reclosing scheme.

A few cases were selected to be explained in detail to provide an understanding of the pattern of testing approach and how results are obtained. The overall results of all simulations provided a comprehensive understanding of the behavior of the adaptive reclosing scheme. The scheme functions flawlessly in the aspect of identifying the right zonal breaker to trip permanently and the breaker to perform the reclosing. Also, the reclosing and fuse sequence of operations was proper for all cases simulated. Fuse-saving scheme performed with the right sequence of operation. However, the scheme did not meet the minimum coordination time requirements. For most of the cases, the operation of the recloser fast curve and fuse were too fast to provide enough margin that ensures proper coordination is maintained.

6 CONCLUSIONS AND FUTURE WORK

6.1 Study Work

The work in this thesis aimed to investigate the behavior of a proposed adaptive reclosing approach in RDS with interconnected DERs. The adaptive reclosing approach is based on overcurrent zonal protection approach. It is an extension of previous work by a Power System Automation Lab (PSAL) researcher [50]. The zonal protection used communication assisted overcurrent and current direction to identify the faulty zone. However, the work assumed all zonal breakers have auto-reclosing function that works successfully. In such a system, the auto-reclosing function is not simple. The auto-reclosing scheme must consider proper synchronization since the RDS with interconnected DERs has more than one power source. Also, the auto-reclosing scheme must consider proper coordination with fuses and the implementation of fuse-saving scheme. The aforementioned is the focus of the work in this thesis.

In the literature, researchers have suggested many approaches and schemes to overcome the challenges of successful auto-reclosing schemes in RDS with DERs. Also, other algorithms tackle the coordination between recloser and fuse. The work in this thesis suggests to use only one of the zonal breakers for reclosing. While all zonal breakers trip if the zone is identified to be faulty, only the breaker closest to the grid power source is enabled to auto-reclose. Depending on the location of the zonal breaker relative to the faulty zone, a logic was developed to identify the right breaker and enable auto-reclosing. The next step re-establishes the coordination of the recloser with fuses in the zone. Miscoordination is caused by different fault current magnitudes seen by fuse and recloser. A factor of the currents ratio of I_R/I_F (I_R : recloser current, I_F : fuse current) is used to adjust the TDS for the recloser fast curve. However, if the ratio is larger than 1, the TDS

adjustment is not required as coordination is maintained in this situation. The factor shall restore coordination with fuses in the zone for a successful fuse-saving scheme.

The behavior of the suggested approach was investigated in this work. A test system consisting of dual RDS feeders based on IEEE 34 node test feeders with interconnected DERs was simulated in PSCAD. The proposed adaptive reclosing approach was implemented in PSCAD and applied to the test system. Various fault scenarios were applied to the test systems at different locations. Temporary and permanent faults were applied to investigate the reclosing scheme. Also, fault location was varied from single phase laterals to main line. The response of the zonal breakers and fuse was reported. The developed logic was responsible for identifying the correct breakers to trip and the correct zonal breaker to reclose. Also, the timing of the breakers and fuse was reported to study the behavior of the adaptive approach to restore the coordination between fuse and recloser.

6.2 Summary of Findings and Conclusions

To start with, the identification of faulty zone depends on the determination of fault current direction at each zonal breaker. The technique to use voltage polarizing positive and negative sequence current quantities to determine fault current direction was successful in all case studies. Hand in hand with the developed logic, the faulty zone and the correct auto-reclosing breaker were identified in all case studies as well. The developed logic in this work was able to identify the zonal breaker closer (relative to the faulty zone) to the grid power supply. This breaker performed auto-reclosing as suggested by the approach. The success rate of this part of the approach was 100% in all case studies conducted by this work. Also, the reclosing and fuse sequence of operations was proper for all cases simulated. Fuse-saving scheme was working with the right sequence of operation.

The next part is the adaptive reclosing algorithm based on the ratio I_R/I_F to restore coordination between fuse and recloser. The results of the case studies exhibited proper fuse-recloser sequence of operation. However, the minimum CTI requirement (0.2 seconds) to ensure proper coordination was not satisfied in 61% of the cases. Furthermore, 12% of the cases had a CTI below 0.1 seconds. The I_R/I_F factor (ranging from 0.62 to 0.99) that adjust the TDS of the recloser fast curve was successful in restoring the sequence of operation but did not meet the CTI minimum value requirements.

The scheme functions flawlessly in the aspect of identifying the right zonal breaker to trip permanently and the breaker to perform the reclosing. Also, the reclosing and fuse sequence of operations was proper for all cases simulated. Fuse-saving scheme performed with the right sequence of operation. However, the scheme did not meet the minimum coordination time requirements. For most of the cases, the operation of the recloser fast curve and fuse were too fast to provide enough margin that ensures proper coordination is maintained. This could be a result of the increase in fault current which shortens the response time of the fuse leaving a very little margin to coordinate with recloser fast curve. Additionally, this coordination was successfully restored in lab environment (i.e. using simulation software) but that doesn't mean it would be successful in real implementation. Actually, this approach will be difficult to implement in real life due to the margin and the monitoring requirement.

6.3 Future Work

Aside from studying the system with different assumptions or operating points, the following are suggested for future work. First, in this study all zones were interconnected with DERs. Future work may consider having zoning without any DER interconnection. This would change the logic for which zonal breakers to trip and reclose in the case of a fault. Second, future

work may consider the restoration of the system to normal condition after successful auto-reclosing. This includes connecting back all the DERs and closing all zonal breakers. Third, future work may consider another practical way to restore fuse-recloser coordination with better coordination timing.

REFERENCES

1. *IEEE Standard for Interconnecting Distributed Resources with Electric Power Systems - Amendment 1*, in *IEEE Std 1547a-2014 (Amendment to IEEE Std 1547-2003)*. 2014. p. 1-16.
2. Pabla, A.S., *Electric Power Distribution*. 2005, New Delhi: McGraw Hill. 878.
3. Shen, S., et al., *An Adaptive Protection Scheme for Distribution Systems With DGs Based on Optimized Thevenin Equivalent Parameters Estimation*. *IEEE Transactions on Power Delivery*, 2017. **32**(1): p. 411-419.
4. Blackburn, J.L. and T.J. Domin, *Protective Relaying Principles and Applications*. 3rd ed. 2007, Boca Raton, FL: CRC Press. 633.
5. Anderson, P.M., *Power System Protection*. 1999, IEEE Press.
6. Faulkenberry, L.M. and W. Coffey, *Electrical Power Distribution and Transmission*. 1996, Englewood Cliffs, New Jersey: Prentice Hall. 582.
7. Kersting, W.H., *Distribution System Modeling and Analysis, Third Edition*. 2012: Taylor & Francis.
8. Horowitz, S.H., A.G. Phadke, and J.K. Niemira, *Power System Relaying*. 2013, Wiley.
9. *IEEE Standard Inverse-Time Characteristic Equations for Overcurrent Relays*, in *IEEE Std C37.112-1996*. 1997.
10. Schweitzer Engineering Laboratories, I., *SEL 351 Instruction Manual*, I. Schweitzer Engineering Laboratories, Editor. 2017.
11. Short, T.A., *Electric Power Distribution Handbook*. 2004, CRC Press.
12. *IEEE Standard Specifications for High-Voltage (>1000 V) Fuses and Accessories*. *IEEE Std C37.42-2016*, 2017: p. 1-59.

13. Cooper Power Systems, I., *Components & Protective Equipment - Fusing Manual*, C. Industries, Editor. 1992: USA.
14. Brahma, S.M. and A.A. Girgis, *Development of adaptive protection scheme for distribution systems with high penetration of distributed generation*. IEEE Transactions on Power Delivery, 2004. **19**(1): p. 56-63.
15. Jeff Roberts and A. Guzmán, *Directional Element Design and Evaluation*.
16. Horak, J. *Directional overcurrent relaying (67) concepts*. in *59th Annual Conference for Protective Relay Engineers, 2006*. 2006.
17. Fleming, B., *Negative-Sequence Impedance Directional Element*. 1998, Schweitzer Engineering Laboratories, Inc.
18. Jeff Roberts and I. E. O. Schweitzer, *Distance Relay Element Design*.
19. D3, P.-P.W.G., *Impact of Distributed Resources on Distribution Relay Protection*. 2004.
20. Davis, M., D. Costyk, and A. Narang, *Distributed and Electric Power System Aggregation Model and Field Configuration Equivalency Validation Testing*. 2003, National Renewable Energy Laboratory.
21. Butler-Purry, K.L. and H.B. Funmilayo. *Overcurrent protection issues for radial distribution systems with distributed generators*. in *2009 IEEE Power & Energy Society General Meeting*. 2009.
22. *IEEE Guide for Protective Relay Applications to Distribution Lines*. IEEE Std C37.230-2007, 2007: p. 1-100.
23. Li, Z., et al. *Study on Adaptive Protection System of Power Supply and Distribution Line*. in *2006 International Conference on Power System Technology*. 2006.

24. Ituzaro, F.A., R.H. Douglin, and K.L. Butler-Purry. *Zonal overcurrent protection for smart radial distribution systems with distributed generation*. in *2013 IEEE PES Innovative Smart Grid Technologies Conference (ISGT)*. 2013.
25. Javadian, S.A.M. and M.R. Haghifam. *Implementation of a New Protection Scheme on a Real Distribution System in Presence of DG*. in *2008 Joint International Conference on Power System Technology and IEEE Power India Conference*. 2008.
26. Shah, P.H. and B.R. Bhalja, *New adaptive digital relaying scheme to tackle recloser-fuse miscoordination during distributed generation interconnections*. IET Generation, Transmission & Distribution, 2014. **8**(4): p. 682-688.
27. Perera, N., A.D. Rajapakse, and T.E. Buchholzer, *Isolation of Faults in Distribution Networks With Distributed Generators*. IEEE Transactions on Power Delivery, 2008. **23**(4): p. 2347-2355.
28. Zamani, A., T. Sidhu, and A. Yazdani. *A strategy for protection coordination in radial distribution networks with distributed generators*. in *IEEE PES General Meeting*. 2010.
29. Liu, Z., et al., *A Multiagent System-Based Protection and Control Scheme for Distribution System With Distributed-Generation Integration*. IEEE Transactions on Power Delivery, 2017. **32**(1): p. 536-545.
30. Wan, H., K.K. Li, and K.P. Wong, *An Adaptive Multiagent Approach to Protection Relay Coordination With Distributed Generators in Industrial Power Distribution System*. IEEE Transactions on Industry Applications, 2010. **46**(5): p. 2118-2124.
31. Brahma, S.M. and A.A. Girgis. *Microprocessor-based reclosing to coordinate fuse and recloser in a system with high penetration of distributed generation*. in *2002 IEEE Power*

- Engineering Society Winter Meeting. Conference Proceedings (Cat. No.02CH37309).*
2002.
32. Wheeler, K., M. Elsamahy, and S. Faried, *Use of superconducting fault current limiters for mitigation of distributed generation influences in radial distribution network fuse-recloser protection systems.* IET Generation, Transmission & Distribution, 2017. **11**(7): p. 1605-1612.
 33. Wheeler, K.A., S.O. Faried, and M. Elsamahy. *Assessment of distributed generation influences on fuse-recloser protection systems in radial distribution networks.* in *2016 IEEE/PES Transmission and Distribution Conference and Exposition (T&D)*. 2016.
 34. Naiem, A.F., et al., *A Classification Technique for Recloser-Fuse Coordination in Distribution Systems With Distributed Generation.* IEEE Transactions on Power Delivery, 2012. **27**(1): p. 176-185.
 35. Gao, H., J. Li, and B. Xu, *Principle and Implementation of Current Differential Protection in Distribution Networks With High Penetration of DGs.* IEEE Transactions on Power Delivery, 2017. **32**(1): p. 565-574.
 36. Pujiantara, M., et al. *Optimization technique based adaptive overcurrent protection in radial system with DG using genetic algorithm.* in *2016 International Seminar on Intelligent Technology and Its Applications (ISITIA)*. 2016.
 37. Nikolaidis, V.C., E. Papanikolaou, and A.S. Safigianni, *A Communication-Assisted Overcurrent Protection Scheme for Radial Distribution Systems With Distributed Generation.* IEEE Transactions on Smart Grid, 2016. **7**(1): p. 114-123.

38. Wang, Y., et al., *Novel Protection Scheme of Single-phase Earth Fault for Radial Distribution Systems with Distributed Generators*. IEEE Transactions on Power Delivery, 2017. **PP**(99): p. 1-1.
39. Gutierrez, L.F.F., G. Cardoso, and G. Marchesan. *Recloser-fuse coordination protection for distributed generation systems: Methodology and priorities for optimal disconnections*. in *12th IET International Conference on Developments in Power System Protection (DPSP 2014)*. 2014.
40. Tang, W.J. and H.T. Yang. *Self-adaptive protection strategies for distribution system with DGs and FCLs based on data mining and neural network*. in *2017 IEEE International Conference on Environment and Electrical Engineering and 2017 IEEE Industrial and Commercial Power Systems Europe (EEEIC / I&CPS Europe)*. 2017.
41. Agheli, A., et al. *Reducing the impact of DG in distribution networks protection using fault current limiters*. in *2010 4th International Power Engineering and Optimization Conference (PEOCO)*. 2010.
42. Funmilayo, H.B. and K.L. Butler-Purry. *An approach to mitigate the impact of distributed generation on the Overcurrent Protection scheme for radial feeders*. in *2009 IEEE/PES Power Systems Conference and Exposition*. 2009.
43. Jing, M., L. Jinlong, and W. Zengping. *An adaptive distance protection scheme for distribution system with distributed generation*. in *2010 5th International Conference on Critical Infrastructure (CRIS)*. 2010.
44. Yi, H., H. Xuehao, and Z. Dongxia. *A new adaptive current protection scheme of distribution networks with distributed generation*. in *2009 International Conference on Sustainable Power Generation and Supply*. 2009.

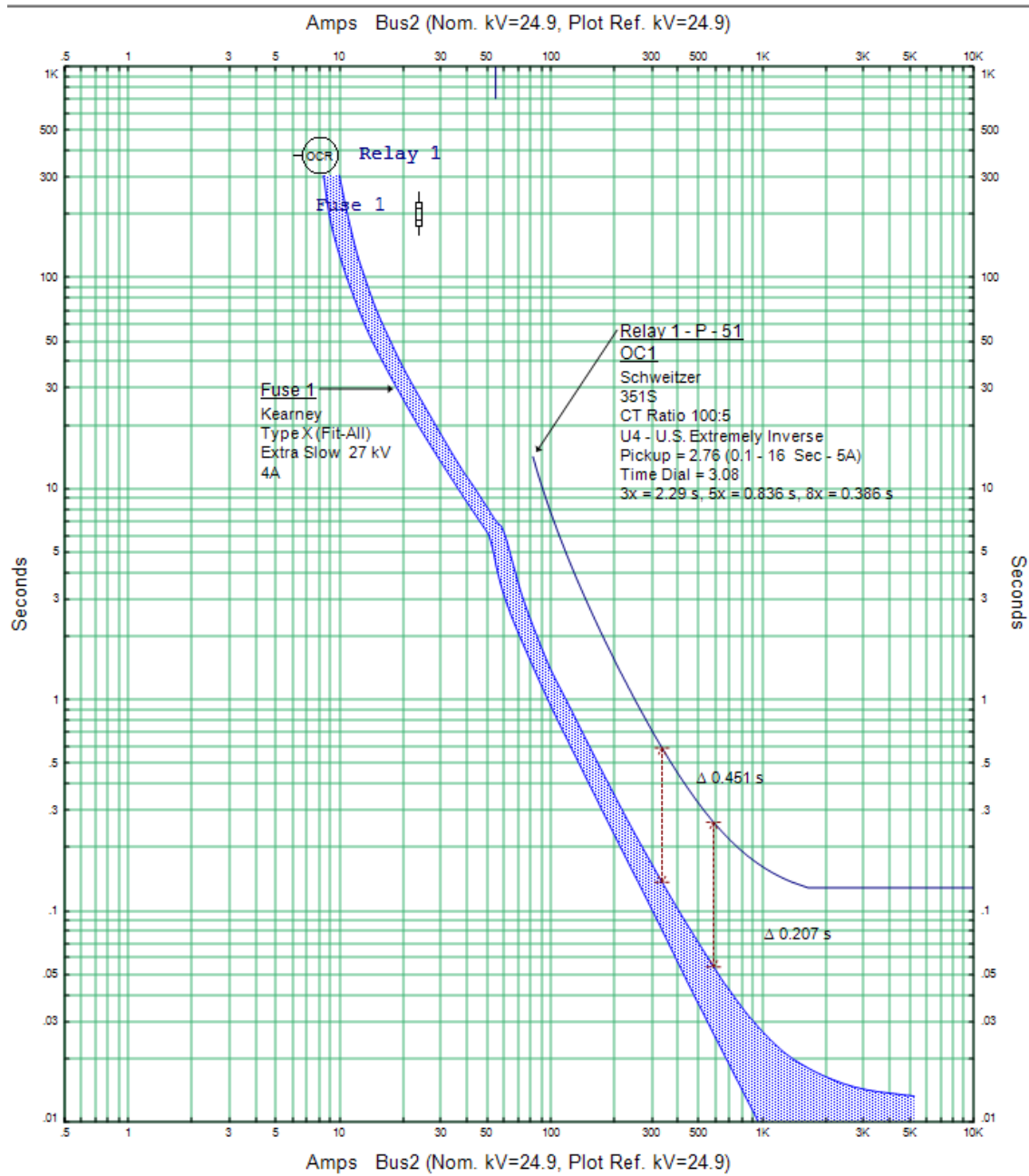
45. Javadian, S.A.M., R. Tamizkar, and M.R. Haghifam. *A protection and reconfiguration scheme for distribution networks with DG*. in *2009 IEEE Bucharest PowerTech*. 2009.
46. Ma, J., et al., *A New Adaptive Voltage Protection Scheme for Distribution Network With Distributed Generations*. *Canadian Journal of Electrical and Computer Engineering*, 2013. **36**(4): p. 142-151.
47. Schaefer, N., et al. *Adaptive protection system for distribution networks with distributed energy resources*. in *10th IET International Conference on Developments in Power System Protection (DPSP 2010). Managing the Change*. 2010.
48. Yu, C., et al. *The Study on Fault Directional Relay in Protection System for Distribution System under High DG Penetration Level*. in *2009 Asia-Pacific Power and Energy Engineering Conference*. 2009.
49. Tian, J., et al. *A fast current protection scheme for distribution network with distributed generation*. in *10th IET International Conference on Developments in Power System Protection (DPSP 2010). Managing the Change*. 2010.
50. Ituzaro, F.A., *A Technique to Utilize Smart Meters Load Information for Adapting Overcurrent Protection for Radial Distribution Systems with Distributed Generations*. *Master of Science Thesis, Texas A&M University*, 2012.
51. Kersting, W.H. *Radial distribution test feeders*. in *2001 IEEE Power Engineering Society Winter Meeting. Conference Proceedings (Cat. No.01CH37194)*. 2001.
52. Kersting, W.H. and G. Shirek. *Short circuit analysis of IEEE test feeders*. in *PES T&D 2012*. 2012.
53. *ETAP Star Tool*. [cited 2017; Available from: <https://etap.com/product///star-protective-device-coordination-software>].

54. Wheeler, K.A., S.O. Faried, and M. Elsamahy, *Modeling and Coordination of Distribution Network Fuses Using PSCAD*, in *2015 CIGRE Canada Conference*. 2015: Canada.

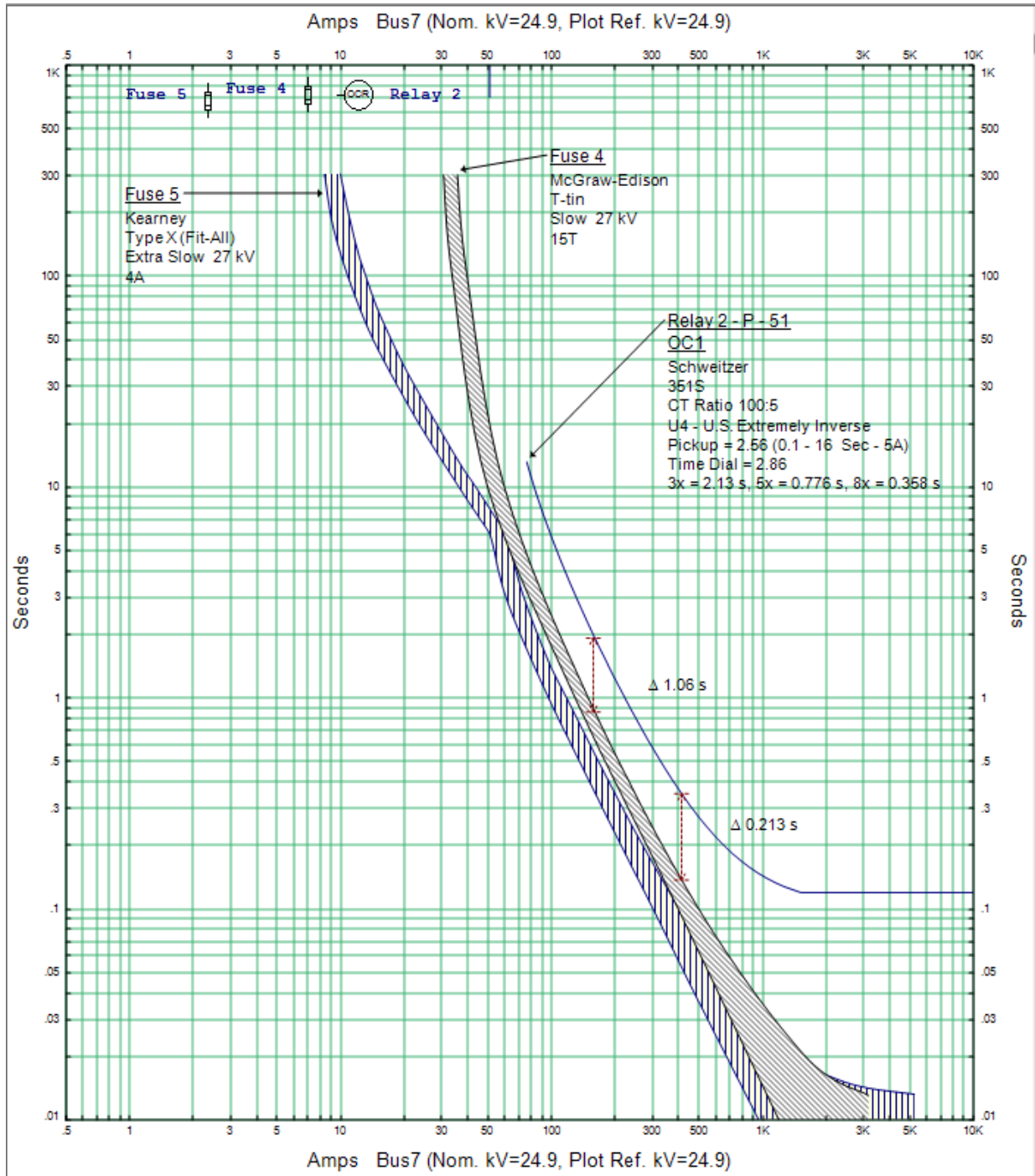
APPENDIX A

ETAP Star Tool Coordination Curves for Fuse-Recloser

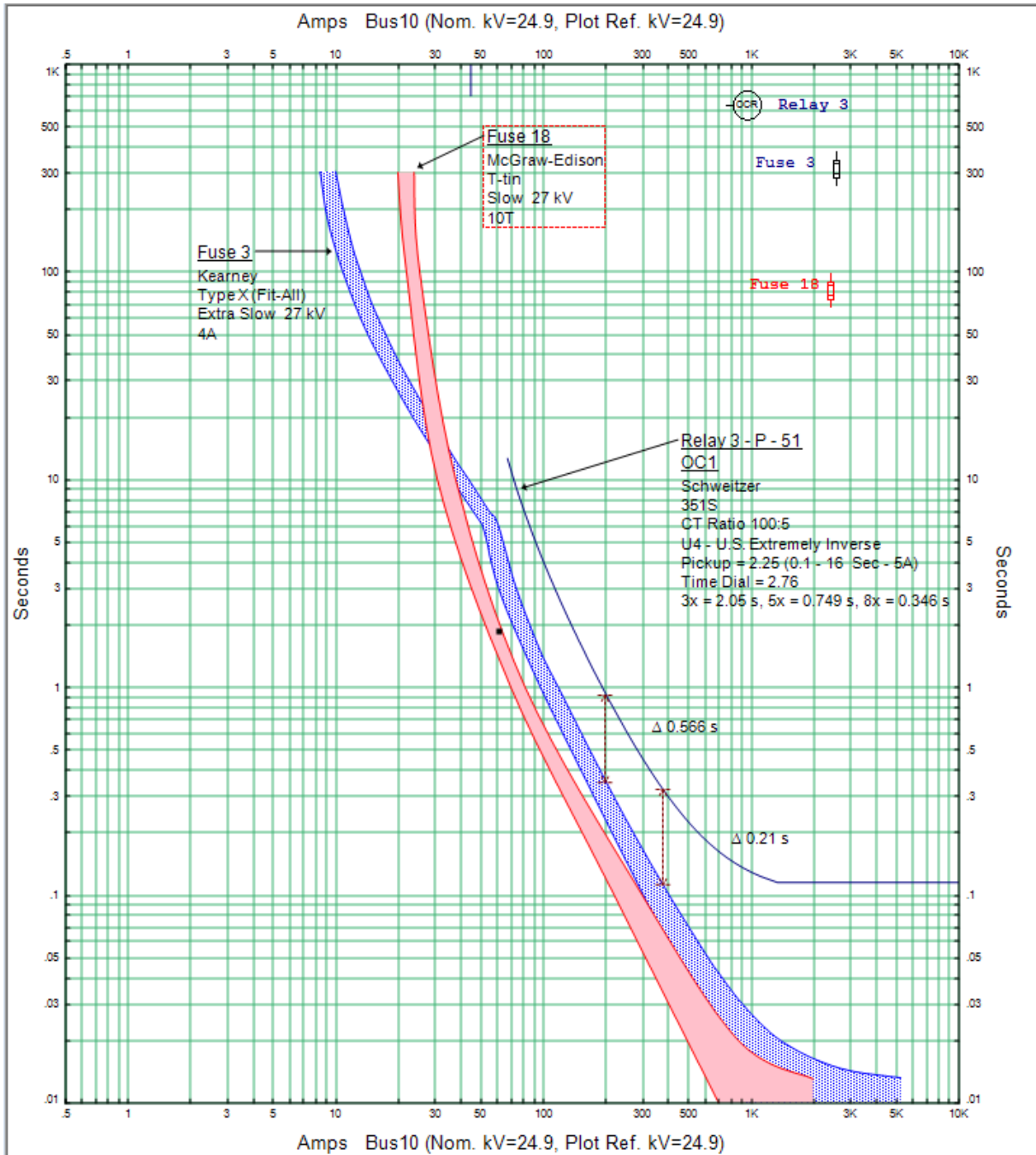
Feeder	A	Fuse @	808 – 810 Phase B	OC PU	2.76
Zone	1	Fuse Type:	KEARNEY X4	OC TDS	3.08
Nodes:	800 to 814			SC Max	590
				SC Min	360



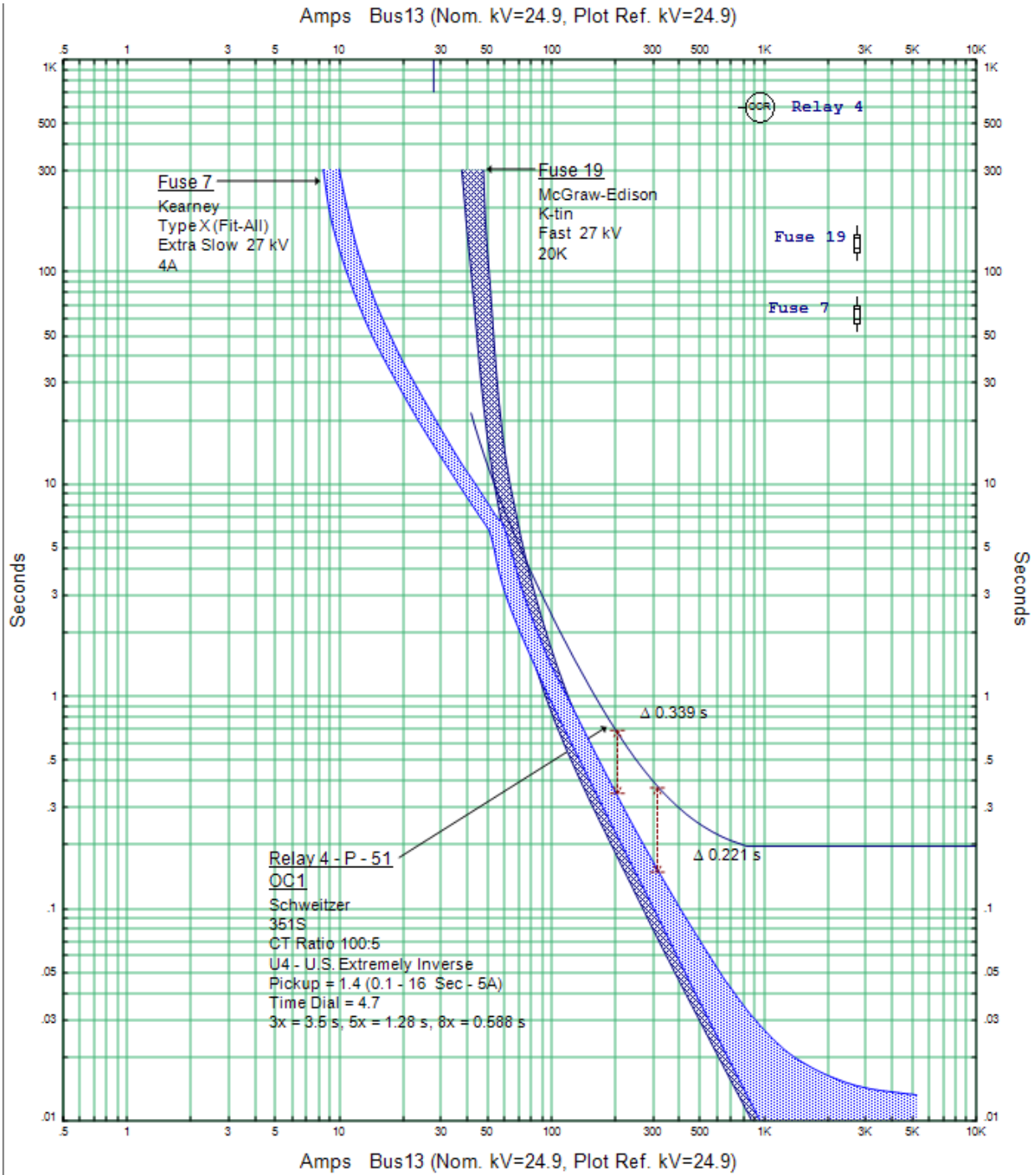
Feeder	A	Fuse @	816 - 818 Phase A	OC PU	2.56
Zone	2	Fuse Type:	KEARNEY T15	OC TDS	2.86
Nodes:	814 to 830	Fuse @	824 - 826 Phase B	SC Max	410
		Fuse Type:	KEARNEY X4	SC Min	170



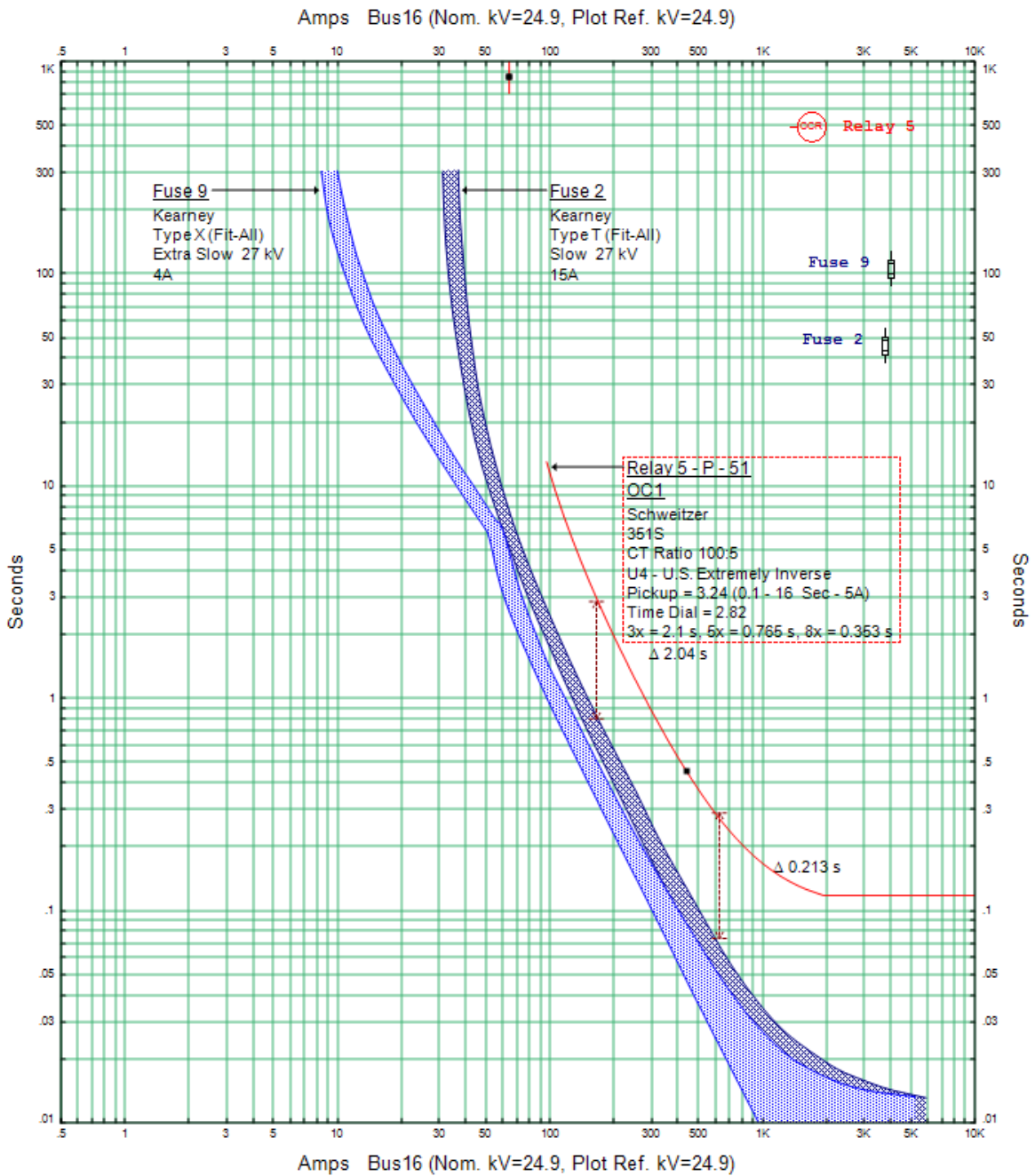
Feeder	A	Fuse @	832 3Phase	OC PU	2.25
Zone	3	Fuse Type:	TIN 10T	OC TDS	2.76
Nodes:	854 to 858	Fuse @	854 & 858	SC Max	365
		Fuse Type:	KEARNEY X4	SC Min	215



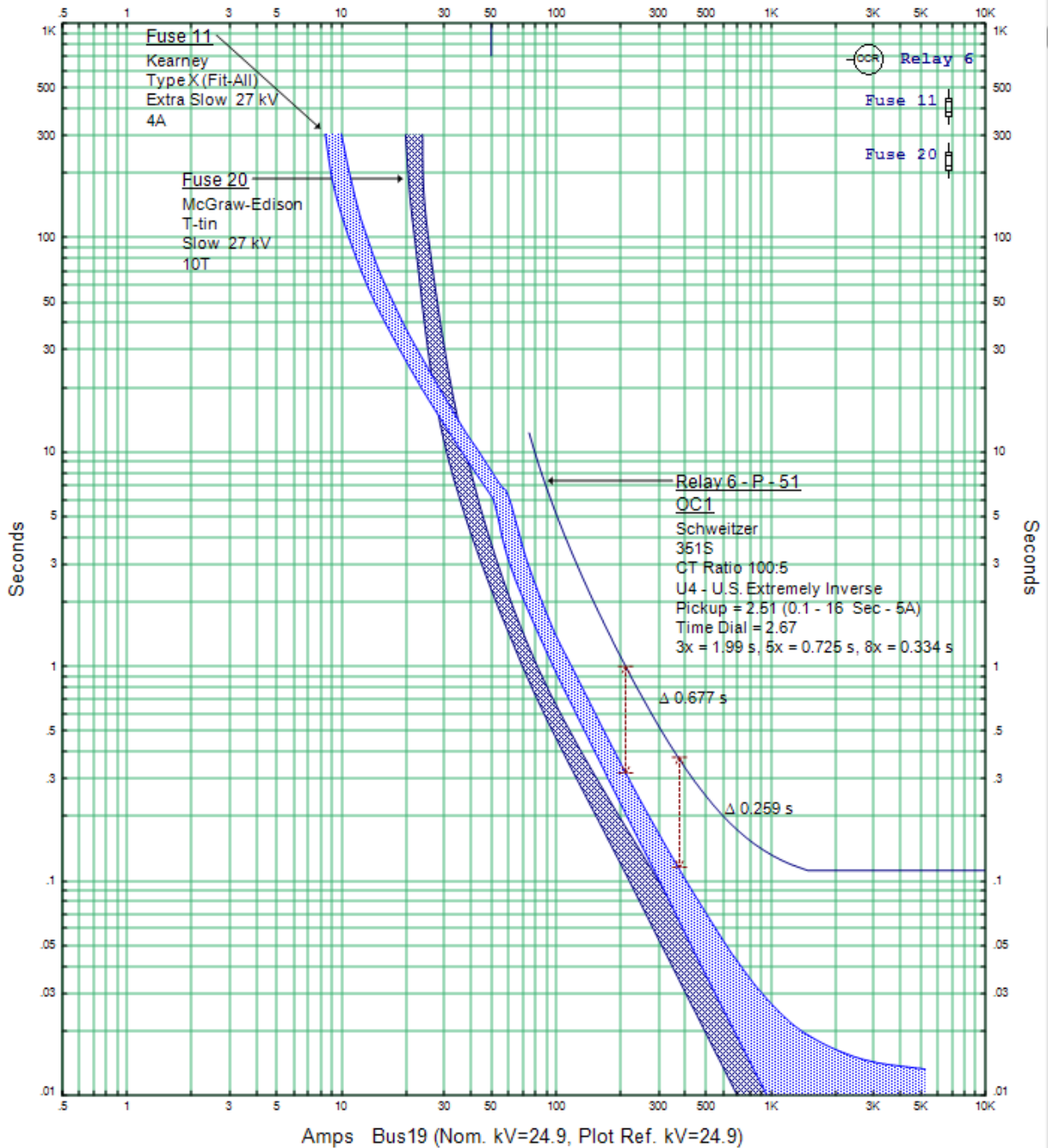
Feeder	A	Fuse @	836- 840 3Phase	OC PU	1.4
Zone	4	Fuse Type:	KEARNEY X4	OC TDS	4.7
Nodes:	834 - 840	Fuse @	834 3Phase	SC Max	310
		Fuse Type:	TIN 20K	SC Min	210



Feeder	B	Fuse @	808 B	OC PU	3.24
Zone	1	Fuse Type:	KEARNEY X4	OC TDS	2.82
Nodes:	800 - 828	Fuse @	816 A	SC Max	590
		Fuse Type:	KEARNEY T15	SC Min	170
		Fuse @	824 B		
		Fuse Type:	KEARNEY X4		



Feeder	B	Fuse @	832 3Phase	OC PU	2.51
Zone	2	Fuse Type:	Tin-10T	OC TDS	2.67
Nodes:	830 to 858	Fuse @	854 Phase B	SC Max	365
		Fuse Type:	KEARNEY X4	SC Min	215
		Fuse @	858 Phase A		
		Fuse Type:	KEARNEY X4		



Feeder	B	Fuse @	836 B	OC PU	0.46
Zone	4	Fuse Type:	KEARNEY X4	OC TDS	11.98
Nodes:	860 - 840			SC Max	288
				SC Min	220

